

**UNIVERSITY OF NAPLES “FEDERICO II”**

**PhD Program in  
Molecular Pathology and Physiopathology**



**School of Molecular Medicine  
XXVIII cycle**

***Innovative therapies based on the use of  
non-coding RNAs for non-small cell lung  
cancer (NSCLC)***

**SUPERVISOR:**  
Prof. Gerolama Condorelli

**CANDIDATE:**  
Dr. Valentina Russo

**PhD COORDINATOR:**  
Prof. Vittorio Enrico Avvedimento

**Academic Year 2015/2016**

**“Innovative therapies based  
on the use of non-coding  
RNAs for non-small cell lung  
cancer (NSCLC)”**

# TABLE OF CONTENTS

<b>LIST OF PUBLICATIONS</b>	4
<b>LIST OF ABBREVIATIONS</b>	5
<b>ABSTRACT</b>	7
<b>1. BACKGROUND</b>	8
<b>1.1 Lung cancer</b>	8
1.1.1 Risk factors	9
1.1.2 Classification and treatment	9
<b>1.2 MicroRNAs</b>	12
1.2.1 miRNAs biogenesis	12
1.2.2 Role of miRNAs	14
1.2.3 Alteration of miRNAs in cancer	15
1.2.4 miRNAs and NSCLC	16
1.2.5 MiRNAs en route to the clinic	17
<b>1.3 Aptamers</b>	18
1.3.1 Aptamers production: SELEX method	20
1.3.2 Post-SELEX modifications of aptamers	22
1.3.3 Aptamers as therapeutics	23
1.3.4 Aptamers as delivery agents	24
1.3.5 Aptamers in diagnosis	25
1.3.6 Molecular chimeras	26
<b>2. AIM OF THE STUDY</b>	29
<b>3. MATERIALS AND METHODS</b>	30
<b>3.1 TCGA miRNA dataset and patients' information</b>	30
<b>3.2 Cell lines</b>	30
<b>3.3 Isolation of primary cell cultures from human lung biopsies</b>	30
<b>3.4 Cell transfection</b>	31
<b>3.5 Aptamer-miRNA chimera</b>	31
<b>3.6 RNA extraction and Real-time PCR</b>	32
<b>3.7 Protein isolation and Western blotting</b>	32
<b>3.8 <i>In vitro</i> proliferation assay</b>	33
<b>3.9 Colony formation assay</b>	33
<b>3.10 Luciferase reporter assay</b>	33
<b>3.11 Rescue experiments</b>	34
<b>3.12 <i>In vitro</i> Dicer assay</b>	34

<b>3.13</b>	Chimera stability in human serum	34
<b>3.14</b>	Transwell migration assay	35
<b>3.15</b>	Clonogenic cell survival assay	35
<b>3.16</b>	Statistical analysis	35
<b>4.</b>	<b>RESULTS</b>	36
<b>4.1</b>	miR-34c is downregulated in NSCLC tissues and cell lines	36
<b>4.2</b>	Overexpression of miR-34c inhibits <i>in vitro</i> growth of NSCLC cells by arresting cell cycle progression	38
<b>4.3</b>	AXL as direct target of miR-34c	41
<b>4.4</b>	Design and folding of aptamer-miRNA conjugate	43
<b>4.5</b>	GL21.T as selective delivery of functional miR-34c	45
<b>4.6</b>	Functional aspects of GL21.T/miR-34c chimera	48
4.6.1	GL21.T/miR-34c effects on cell proliferation	48
4.6.2	GL21.T/miR-34c effects on cell migration	51
4.6.3	GL21.T/miR-34c effects on cell sensitivity to ionizing radiation	52
<b>5.</b>	<b>DISCUSSION</b>	53
<b>6.</b>	<b>CONCLUSIONS</b>	58
<b>7.</b>	<b>ACKNOWLEDGEMENTS</b>	59
<b>8.</b>	<b>REFERENCES</b>	60
	<b>PUBLICATIONS</b>	69

## LIST OF PUBLICATIONS

- 1 Roscigno G, Quintavalle C, Donnarumma E, Puoti I, Diaz-Lagares A, Iaboni M, Fiore D, **Russo V**, Todaro M, Romano G, Thomas R, Cortino G, Gaggianesi M, Esteller M, Croce CM, Condorelli G. *MiR-221 promotes stemness of breast cancer cells by targeting DNMT3b*. Oncotarget. 2016 Jan 5. doi:10.18632/oncotarget.5979.
- 2 Fiore D, Donnarumma E, Roscigno G, Iaboni M, **Russo V**, Affinito A, Adamo A, De Martino F, Quintavalle C, Romano G, Greco A, Ylermi S, Brunetti A, Croce CM, Condorelli G. *miR-340 predicts glioblastoma survival and modulates key cancer hallmarks through down-regulation of NRAS*. Oncotarget. 2016 Jan 21. doi:10.18632/oncotarget.6968.
- 3 Iaboni M, **Russo V**, Fontanella R, Roscigno G, Fiore D, Donnarumma E, Esposito CL, Quintavalle C, Giangrande P, de Franciscis V, Condorelli G. *Aptamer-miRNA-212 conjugate sensitizes NSCLC cells to TRAIL*. Molecular Therapy - Nucleic Acids, 2016. doi:10.1038/mtna.2016.5.

## LIST OF ABBREVIATIONS

3' UTR: 3' Untranslated region  
ATCC: American Type Culture Collection  
BSA: Bovine serum albumin  
CLL: Chronic lymphocytic leukemia  
DMEM: Dulbecco's Modified Eagle's Medium  
DMEM-F12: Dulbecco's Modified Eagle's Medium/Nutrient F12-Ham  
dsRBD: Double-stranded RNA-binding domain  
EGFR: Epidermal growth factor receptor  
EXP5: Exportin 5  
FBS: Fetal Bovine Serum  
FDA: Food and Drug Administration  
Gas6: Growth-arrest-specific gene 6  
H&E: Hematoxylin and eosin  
miRNA/miR: MicroRNA  
miR-NC: pre-miR-Negative Control  
MUC1: Mucin 1  
ncRNAs: Non-coding RNAs  
NSCLC: Non-small cell lung cancer  
PEG: polyethylene glycol  
PSMA: prostate specific membrane antigen  
PTK7: protein tyrosine kinase 7  
RISC: RNA Induced Silencing Complex  
RTK: Receptor Tyrosine Kinase  
RT-PCR: Real-Time Polymerase Chain Reaction  
SCLC: Small cell lung cancer

SELEX: Systematic Evolution of Ligands by Exponential enrichment

siRNA: Short interfering RNA

snoRNA: Small nucleolar RNA

snRNA: Small nuclear RNA

TBS: Tris Buffered Saline

TCGA: The Cancer Genome Atlas

Unt: Untreated cells

VEGF: Vascular endothelial growth factor

WHO: World Health Organization

## ABSTRACT

Recent studies have shown the importance of microRNAs (miRNAs) as key regulators in several human disease, and also their great potential as new class of therapeutics cancer therapeutics. However, a major obstacle to their translation to clinic is actually represented by the lack of a robust and reliable way to selectively deliver them to the target malignant tumor cells.

Today, nucleic-acid aptamers represent an expanding new class of biomolecules which is revealing as an interesting and highly promising for the specific delivery of RNA-based therapeutics.

In this study, I intend to validate the use of aptamers as cell-specific delivery molecules for “therapeutic” miRNAs. I identified a tumor-suppressive miRNA in non-small cell lung cancer (NSCLC), miR-34c. I validated that the expression of miR-34c is low in NSCLC and when transfected into cell lines is able to impact on cell survival.

By applying methods successfully used in our laboratory, I conjugated the tumor-suppressor miR-34c to a nucleic acid aptamer, that selectively recognize the AXL receptor and is rapidly internalized (GL21.T), generating a “molecular chimera”. With stick-end annealing, the aptamer and a single chain anti-miRNA (or the passenger strand of the miRNA) are annealed by the mean of complementary sticky ends elongated at the 3’ end of the aptamer and at the 5’ end of the single chain of the miRNA, respectively.

I demonstrated that the GL21.T/miR-34c chimera is able to bind and to carry the miRNA within the NSCLC cells. Interestingly, I demonstrated that a miR-34c target is the AXL receptor. Thus, the GL21.T/miR-34c chimera is able to exert a dual inhibition of AXL, either at functional or at transcriptional level.

Finally, I evaluated the functional effects of the chimera NSCLC cells that selectively express AXL receptor.

# 1. BACKGROUND

## 1.1 Lung cancer

The term lung cancer refers to a group of diseases characterized by uncontrolled cellular growth arising from the respiratory epithelium (bronchi, bronchioles, and alveoli).

Lung cancer, which was a rare disease before 1900, is now considered one of the most frequently types of diagnosed malignancies worldwide (Figure 1). It has been estimated a strong increase of new lung cancer cases in developing countries [Siegel et al. 2015].

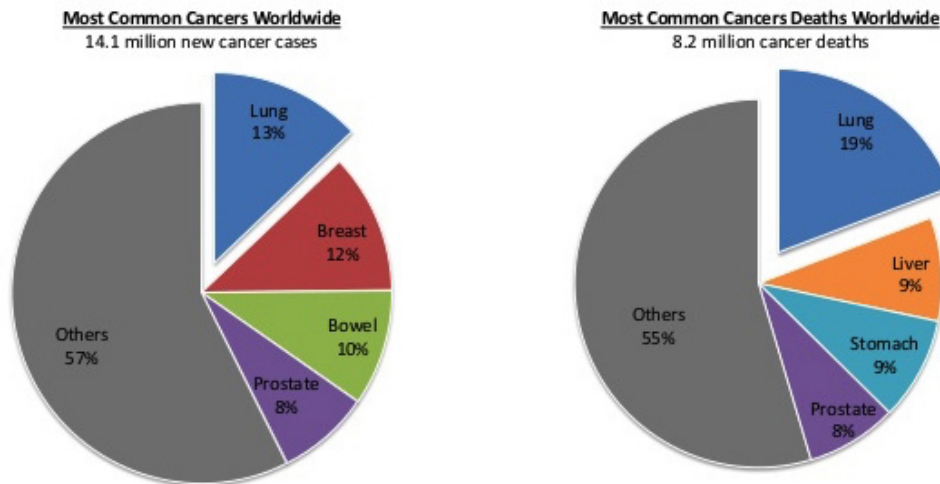


**Figure 1.** The perspectives of most common cancers and causes of cancer death worldwide (for both sexes).

Every year, in Italy, are diagnosed more than 38,000 new cases of lung cancer. The peak incidence is recorded between the fifth and sixth decade of life. The mortality rate is unfortunately very high, about 90%.

Following onset, lung cancer has immediate and very serious consequences on the correct and healthy functioning of the organism. In fact cancer cells can easily make metastasis, circulating into the body, by the circulatory system or through the lymphatic system [Schuchert and Luketich 2003].

### 1.1.1 Risk factors

The primary cause of lung cancer is tobacco smoking; approximately 80% of new lung cancers occur in smokers. The risk of lung cancer increases with the length of time and the number of cigarettes smoked. Unfortunately, the risk for an ex-smoker is still significantly higher than the risk for those who have never smoked, although the chances of developing lung cancer may significantly reduce.

A lifetime smoker has a 10- to 20-fold increased risk of developing lung cancer compared to a nonsmoker. Moreover, one in five women and one in 12 men diagnosed with lung cancer have never smoked, because the smoke inhaled and other tobacco products contains many potential carcinogens, as well as agents that cause inflammation [Dela Cruz et al. 2011].

In addition to cigarette smoke, also some industrial exposures increase the risk of lung cancer development. The important role of specific occupational exposures (asbestos, crystalline silica, radon, and heavy metals) in lung cancer etiology has been well described [Field and Withers 2012].

It is also reported that the risk of lung cancer is higher among people exposed to ionizing radiation, for working reasons or diagnostic use [Shilnikova et al. 2003] (Figure 2).

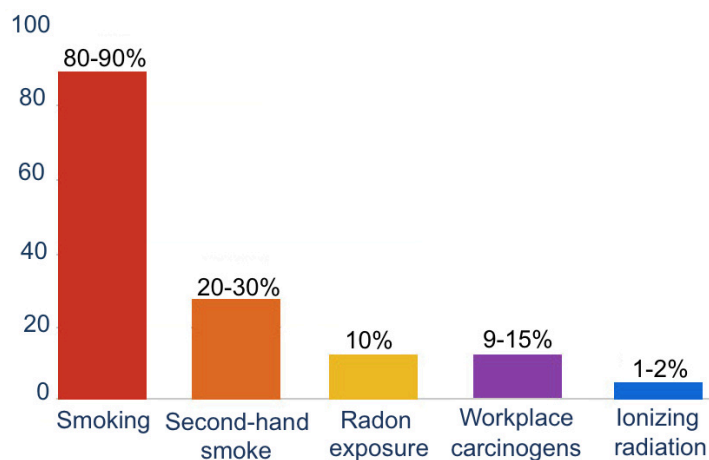


**Figure 2.** The leading factors in the development of lung cancer.

### 1.1.2 Classification and treatment

The most recent classification of lung cancers is the World Health Organization (WHO) classification, which was firstly published in 1967 and updated lately in 2015 [Travis et al. 2015].

The first WHO classifications were based mainly on light microscopy, using routine hematoxylin and eosin (H&E), then immunohistochemistry was

introduced, which is still the best staining method used in diagnosis. Moreover, molecular biology has strongly increased the knowledge of lung tumors, highlighting further differences among tumor types (Figure 3).

According to histology and molecular biology, the WHO classification divides lung cancers in two main groups, based on the size and the type of tumor cells:

- a) Small cell lung cancer (SCLC), which constitutes about 20% of malignant cases;
- b) Non-small cell lung cancer (NSCLC), which account for approximately 80% of all primary lung cancers.

SCLC is a kind of tumor more aggressive than NSCLCs and often it spreads quite early.

NSCLC includes three common types of tumors:

- Squamous (or epidermoid) carcinoma
- Adenocarcinoma
- Large cell carcinoma.

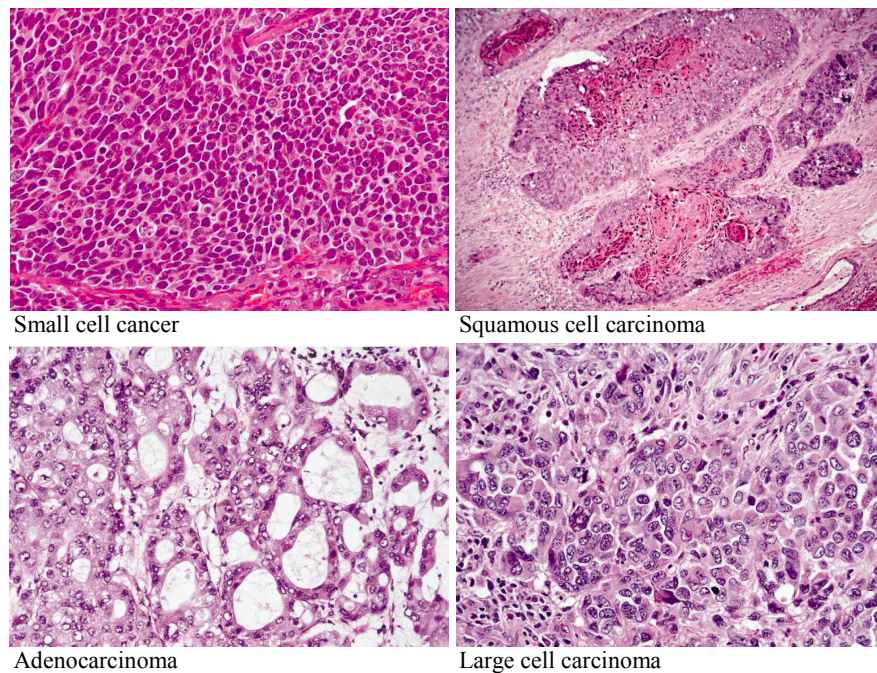


**Figure 3.** Current World Health Organization classification for lung cancer [H&E].

While the WHO classification emphasizes morphologic aspects of tumor, staging of cancer at the time of diagnosis is important for prognosis and treatments planning. The TNM system is the most commonly used method for classifying tumors, but it should be used just for NSCLC (Table 1). The system is based on the spread of the primary tumor (T), the extent of lymph node

involvement (N), and the presence or absence of metastases (M). The T, N, and M combination determines the appropriate stage, numbered I through IV.

Primary Tumor	Lymph Node			
	N0	N1	N2	N3
T1	Stage IA	Stage IIA	Stage IIIA	Stage IIIB
T2	Stage IB	Stage IIB		
T3	Stage IIB	Stage IIIA		
T4	Stage IIIA			
Stage IV	M1 (any T, any N)			

**Table 1.** NSCLC staging based on TNM system classification.

These tumors, unfortunately, spread throughout the entire body at an early stage. Frequently, metastasis may be the first manifestation of a still occult primary lung cancer. No organ or tissue is safe from the tumor spread, but more frequent sites of metastasis are liver (30-50%), brain (20%) and bones (20%).

Symptoms related to disseminated disease include weight loss, abdominal pain due to involvement of the liver, adrenals and pancreas, and pain due to bone marrow metastases.

Basically, there are three possible treatments for lung cancer, depending on the stage:

1. *Surgery*
2. *Radiotherapy*
3. *Chemotherapy*.

When the diagnosis is early (I or II stages), the best results are obtained with the first method, but radiotherapy could be an alternative treatment option for patients who refuse surgery or are not eligible for a standard lobectomy.

Chemotherapy provides only modest survival benefits (1 to 2 months) when the patients are diagnosed with an incurable advanced/metastatic stage disease. One of the features that most affects the survival rate is the resistance to chemotherapeutic drugs. In fact, the treatment has a successful clinical response only in 20-30% of cases; it is therefore necessary to develop new therapies [Travis 2011].

During the last decade a novel treatment approach has been generated, the *targeted therapy*, a type of treatment that blocks tumor cell proliferation and the spread of cancer cells, by interfering with specific molecules ("molecular targets") that play a key role in the cancer progression, and in metastases development. The fundamental aim of targeted therapies is the identification of

good targets, that are present, or at least more abundant in cancer cells, compared to normal cells.

Many different targeted therapies have already been approved by Food and Drug Administration (FDA) for lung cancer treatment, such as Bevacizumab (Avastin®), a monoclonal antibody that targets vascular endothelial growth factor (VEGF), Erlotinib (Tarceva®) and Gefitinib (Iressa®), both EGFR inhibitors used in NSCLC with epidermal growth factor receptor (EGFR) gene mutations. As for chemotherapy, also in this kind of therapies cancer cells can acquire resistance within 1 or 2 years, so it is necessary to develop new therapeutic strategies [Chan and Hughes 2015].

Finally, there are also palliative treatment approaches that improve the survival and the quality of life of these patients, especially looking to reduce the symptoms of the disease in the lungs [Travis 2011].

## **1.2 MicroRNAs**

In the last two decades, many non-coding RNAs (ncRNAs) were found to regulate a wide variety of biological processes. Among these, microRNAs (miRNAs) are the most investigated and best characterized.

MiRNAs are members of a family of small RNAs, which includes small nuclear RNA (snRNA) involved in mRNA splicing, small nucleolar RNA (snoRNA) which directs modification of ribosomal RNA and short interfering RNA (siRNA) produced from long double-stranded RNA precursors. Similar to miRNA, siRNA also functions to regulate gene expression.

MiRNAs are small non-protein-coding molecules (19-24 nucleotides), highly conserved through the evolution, that negatively regulate gene expression by a post-translational repression mechanism. They bind to a specific site of a target mRNA in the 3'UTR allowing the degradation of the messenger if there is a perfect complementarity between the miRNA and its 3'UTR, or translational repression in case of a not perfect complementarity [Bartel 2004].

Since their discovery, thousands of microRNAs have been cloned and characterized from different organisms, including arthropods, nematodes, vertebrates and plants. Currently there are over 1800 human microRNAs listed in the miRBase database, accounting for about 1% of the human transcriptome, although it is predicted that the true figure is likely to be closer to one thousand [Griffiths-Jones et al. 2006].

### **1.2.1 miRNAs biogenesis**

Despite some differences in miRNA biogenesis between animals and plants, the most important events in miRNA biogenesis remain similar.

The biogenesis of miRNAs starts with the transcription of genomic regions located within or between protein-coding genes, resulting in the synthesis of a long precursor molecules (pri-miRNAs), over 1 kb in size, which have a stem-loop structure, are capped at the 5'-end and have a 3'-poly (A) tail. Pri-miRNAs are currently thought to be transcribed primarily by RNA polymerase II and, less frequently by RNA polymerase III [Lee et al. 2002].

A single pri-miRNA may contain a "cluster" of different miRNAs or a single miRNA and can contain from 200 to several thousands of nucleotides.

Subsequently, pri-miRNA transcripts undergo to a two steps maturation process involving RNase III enzymes and companion double-stranded RNA-binding domain (dsRBD) proteins.

In the nucleus, the RNase III enzyme, Drosha, cleaves both strands of the pri-miRNA transcript in a staggered manner, producing a stem-loop precursor molecule (pre-miRNA), a 60-70 nt long hairpin RNA with 2-nt overhangs at the 3' end.

These pre-miRNA molecules are transported into the cytoplasm for further processing to become mature miRNAs. The transport occurs through a nuclear pore complex and is mediated by the RanGTP-dependent nuclear transport receptor, exportin-5 (EXP5). EXP5 exports the pre-miRNA out of the nucleus, where hydrolysis of the GTP results in the release of pre-miRNA. In the cytoplasm the pre-miRNA is subsequently processed by Dicer, an endonuclease RNase III enzyme, which cuts both strands of the pre-miRNA at the base of the stem-loop, producing a duplex molecule 21-25 nt long.

The duplex molecule contains the single-stranded mature miRNA and a fragment termed miRNA\*, which is derived from the opposite complementary arm of the pre-miRNA. The mature miRNA is then incorporated into a large protein-effector complex, called RISC (RNA-induced silencing complex), while the miRNA\* strand is subsequently degraded.

RISC complex facilitates the interaction between miRNA and its target mRNA and function as an endonuclease that cuts the target mRNA, or, for steric hindrance, can block the binding of mRNA with the complex of protein synthesis (Figure 4) [Bartel 2004, Lee et al. 2002, Gregory and Shiekhattar 2005].

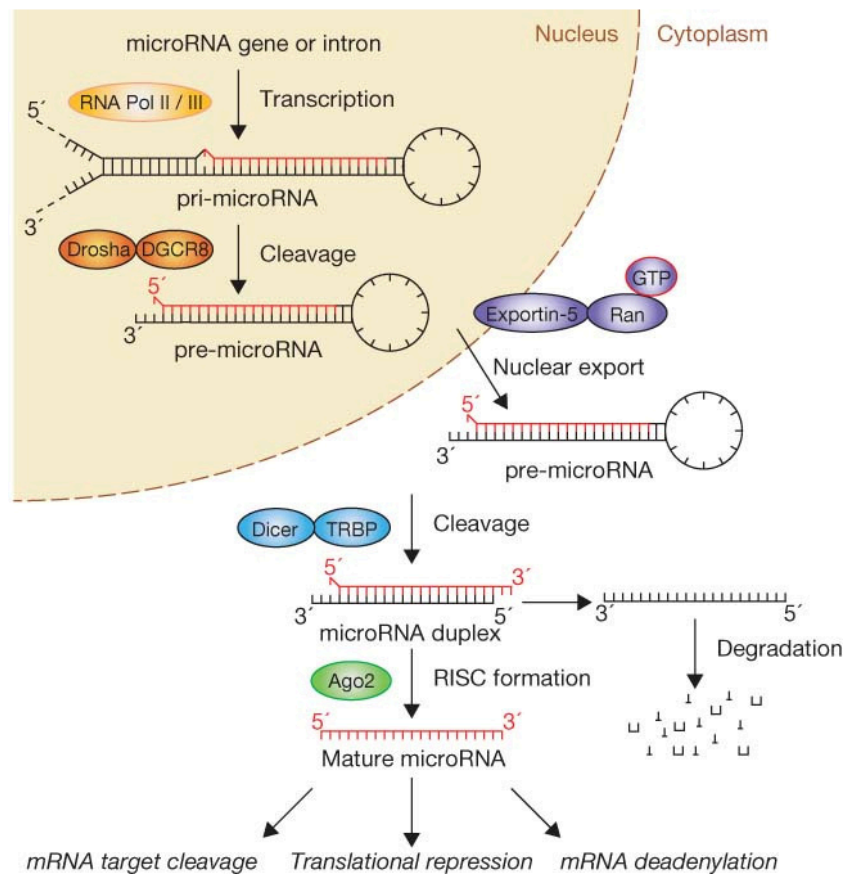


**Figure 4.** Model of miRNA biogenesis and mechanisms of gene expression regulation.

### 1.2.2 Role of miRNAs

With the finding of the first miRNA, lin-4, in 1993 [Lee et al. 1993] and later, let-7, in 2000 [Pasquinelli et al. 2000], the information on miRNAs has grown exponentially and suggested them as one of the crucial players of gene expression regulation. As master gene regulators, miRNAs are able to impact a variety of cellular pathways and functions. Early studies have shown that miRNAs are critical to developmental timing, cell death, cell proliferation, immunity and patterning of the nervous system [Ambros 2004].

MiRNAs are expressed in a tissue-specific manner and a deregulation of miRNAs expression within a tissue type can lead to a variety of human diseases. Thus, it is critical to understand how miRNAs are regulated in normal cellular processes as well as during disease processes.

The identified mechanisms for this observed alteration include impaired miRNA processing, chromosomal alterations, effects of environmental factors

(e.g., cigarette smoke and infection), transcriptional enhancers or repressors, epigenetic regulation, and polymorphisms.

### 1.2.3 Alteration of miRNAs in cancer

Cancer is characterized by aberrantly proliferative cells that are subject to a rapid and uncoordinated cell growth. Malignant cancers are able to invade adjacent tissues and/or metastasize to more distant, and sometimes specific, tissues. Genes involved in cancer are generally classified into oncogenes or tumor suppressor genes (Figure 5).

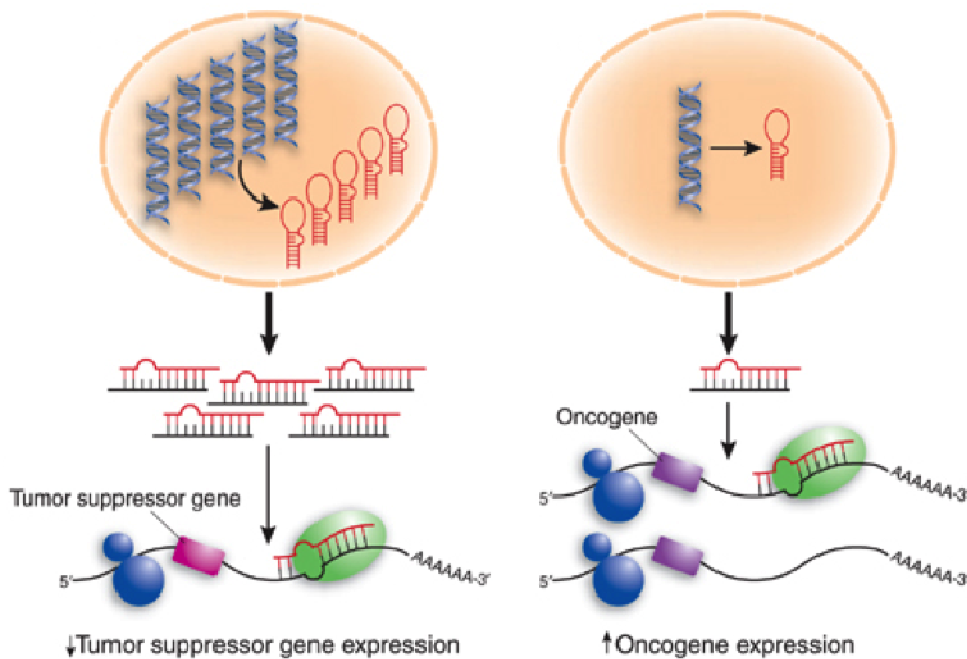


**Figure 5.** miRNAs can act as oncogenes or tumor suppressors.

The first evidence for miRNAs involvement in human cancer comes from a study by Calin et al. [Calin et al. 2002], examining a recurring deletion at chromosome 13q14 to search for a tumor suppressor gene involved in chronic lymphocytic leukemia (CLL). To date, a lot of miRNAs have been characterized for their function in cancer.

Several experiments and clinic analysis suggest that some miRNAs are recurrently deregulated in human cancer. In most case, miRNAs are upregulated or down-regulated in all tumors, suggesting a crucial role for these miRNAs in tumorigenesis. Oncogenic miRNAs, called “oncomirs”, may promote tumor development by negatively inhibiting tumor suppressor genes

and/or genes that control cell differentiation or apoptosis. On the other hand, some tumor suppressor miRNAs may prevent tumor development by negatively inhibiting oncogenes and/or genes that control cell differentiation or apoptosis. Their expression is decreased in cancerous cells [Zhang et al. 2007].

For example, it has been demonstrated that let-7 family contains miRNAs regulating the RAS family of oncogenes in different type of cancer including breast, prostate, glioma and non-small cell lung cancers (NSCLCs) [Johnson et al. 2005]. Costinean reported, for the first time, that a miRNA by itself could induce a neoplastic disease. In fact, by using a transgenic mouse model, they demonstrated that overexpression of miR-155 in B cells was able to induce a pre-B leukemia [Costinean et al. 2006].

MiRNAs play a key role also in tumor metastasis. Indeed, for example miR-139 suppresses metastasis of hepatocellular carcinoma [Tavazoie et al. 2008], while miR10-b was found highly expressed in metastatic breast cancer cells [Ma et al. 2007] even if its clinical utility is still questioned [Gee et al. 2008].

Evidence now indicates that the involvement of miRNAs in cancer is much more extensive than initially expected. Studies that investigated the expression of the entire microRNAome in various human solid tumors and hematologic malignancies have revealed differences in miRNAs expression between neoplastic and normal tissues [Calin et al. 2005; Ciafrè et al. 2005; Pallante et al. 2006; Weber et al. 2006]. These studies show that each neoplasia has a distinct miRNAs signature that differs from that of other neoplasms and that of the normal tissue counterpart.

More recently, many evidences are emerging that tumor-derived miRNAs are present and detectable in serum, plasma, urine and other human body fluids. Because of their abundance, tissue specificity and relative stability, circulating miRNAs hold a great promise as not invasive or minimally invasive biomarkers in cancer [Kosaka et al. 2010].

#### **1.2.4 miRNAs and NSCLC**

The aberrant expression of miRNAs has been texted in various human cancers including lung cancer. There are significant differential expressions of miRNAs between lung cancer and normal lung tissues.

miRNAs status in lung cancer, as in other types of cancer, can be classified into two categories: down-regulation of tumor suppressive miRNAs that target oncogenes, and up-regulation of oncogenic miRNAs that target tumor suppressors.

By increasing our knowledge of cancer, it is evident that besides involvement of miRNA in cancer development, they can also be used in the diagnosis and treatment.

Several studies have recognized a number of miRNA associated with NSCLC [Lin et al. 2010; Markou et al. 2013], among them miR-34c holds tumor suppressor activity.

miR-34c is a member of the miR-34 family, consisting of three homologous miRNAs that are encoded by two different genes: miR-34a is encoded by its specific transcript, whereas miR-34b and miR-34c share a common primary transcript. Several reports have highlighted a decreased expression of miR-34s in numerous malignancies, such as miR-34c in lung cancer [Garofalo et al. 2013].

### **1.2.5 MiRNAs en route to the clinic**

In light of recent advances in the field, it is likely that I will see the transition of therapeutics that are based on miRNAs into the clinic in the not-so-distant future.

They are similar to protein-coding genes in that they regulate many survival-signaling pathways, are themselves subject to mutagenesis and often have conflicting roles in various disease states. They differ, however, in their therapeutic potential. In essence, miRNA replacement therapies may do what protein-coding gene replacement therapies have tried to do, but with fewer obstacles to overcome. MiRNA are much smaller and less antigenic than their protein-coding counterparts and, as such, cellular delivery is possible without the use of potentially harmful viral-based delivery mechanisms that are needed for the cellular uptake of larger protein-coding genes.

Likewise, effective tools for systemically silencing miRNAs have been developed, that specifically and safely target miRNAs. These antagomirs act as small sponges that soak-up miRNAs, resulting in subsequent miRNA degradation and, thus, the upregulation of predicted targets with an in vivo effect that can be sustained for over 3 weeks. This is in contrast to standard antisense miRNA targeting, which has a limited ability to suppress miRNA functions and often leads to toxicity. Thus far, antagomirs have proven to efficiently silence miRNA function with limited side effects.

Although the initial proof-of-principle studies using miRNAs as therapeutics took advantage of adenoviral-based and lentiviral-based delivery methods, translation into clinical practice requires the development of safer delivery vehicles. These include packaging mature miRNAs into lipid-based nanoparticles (neutral or charged) that can be delivered locally to the tumor tissue or systemically, in which case they have been found to accumulate and to therapeutically regulate their targets in the lung, pancreas and prostate. Expanding on this, physical and chemical moieties of the particles that facilitate the targeted distribution and the controlled and sustained release of miRNA – including liposomes, polymers and dendrimer conjugates – are under clinical investigation.

Certainly, I must be cautious of the possible side effects of these molecules in human trials, independently of the side effects that could be associated with the delivery agents. Even in situations in which the miRNA is delivered directly to the tumour, miRNA could escape from the tumor cells and become

systemic. It is plausible that miRNA overexpression could lead to the saturation of the miRNA machinery and non-specific effects. Furthermore, increasing the cellular concentration of miRNAs may suppress lower-affinity targets that might not be targeted at endogenous miRNA levels.

Similarly to current chemotherapies, concentration and dose schedules need to be evaluated for efficacy and toxicity, and the long-term effects following treatment must be assessed [Nana-Sinkam and Croce 2012].

Given all these problems, fewer studies using directed miRNA targeting have reached clinical trial.

### **1.3 Aptamers**

For a long time nucleic acids were mainly considered as linear carriers of information, whereas most cell functions were ascribed to protein molecules possessing complex three-dimensional structure.

It was found that single-stranded RNA molecules are able to form very different three-dimensional structures, which allows them to recognize specifically various molecular targets. They were called aptamers.

The term aptamer is derived from the Latin word “aptus”—which means fitting [Ellington and Szostak 1990] and the Greek word “meros” meaning particle.

Aptamers are short non-naturally occurring single stranded oligonucleotides (DNA or RNA) with a specific and complex three-dimensional shape.

Based on their three-dimensional structures, aptamers are characterized by two important properties: the ability to fold into complex tertiary structures [Hermann and Patel 2000] and to bind with high affinity and specificity to their target (Figure 6).

Antisense, ribozymes, siRNAs, miRNAs recognize the target nucleic acid by complementary base pairing and, by activating an intracellular molecular machinery, impair the expression of the corresponding protein. Instead, aptamers act by directly binding the target protein without interfering with its expression [Cerchia and de Franciscis 2006].

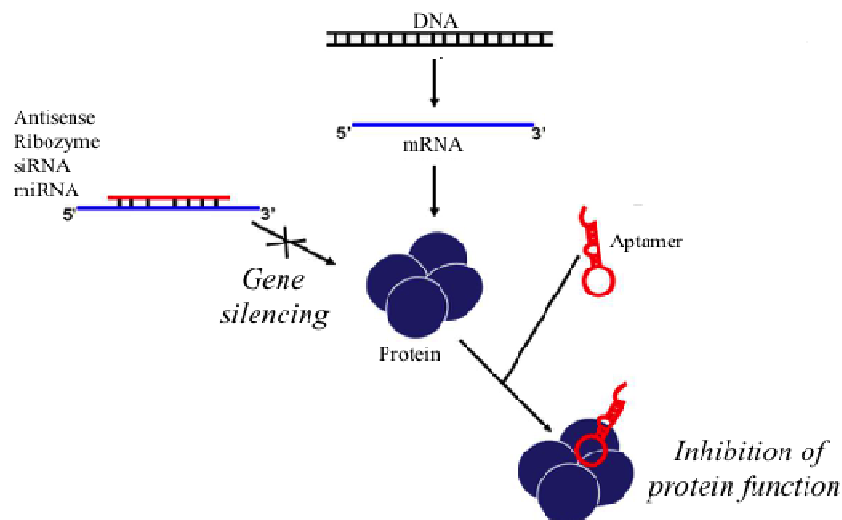


**Figure 6.** Schematic representation of the aptamer functionality.

Amongst drugs used for molecular targeting, monoclonal antibodies have made tremendous contributions in a wide range of applications. However, there are certain limitations associated with antibodies; monoclonal antibodies generally are incapable of membrane penetration due to larger size and hence are not ideal as carriers for targeted delivery of cytotoxic molecules inside the cells. Moreover, production of monoclonal antibodies is laborious, expensive, time consuming and suffers from batch-to-batch variations. They are also immunogenic, temperature sensitive, and their target binding kinetics cannot be easily modified.

Aptamers, considered being oligonucleotides analogous to antibodies, actually rival antibodies in many ways. These short molecules fold to form unique tertiary structures, allowing them to bind to target proteins with high specificity and affinity, often leading to modulation of the target protein activity. The dissociation constants of aptamers/target molecules are in the nanomolar/picomolar range.

The size of aptamers (8-25 kDa) is between that of a single chain antibody fragment and a small peptide and thanks to their structure and low molecular weight, they are not immunogenic. It is also the small size, that provides aptamer a better chance of internalization than the antibodies, although this is possible only when it is bound to a target protein that undergoes internalization or when the target is a cell surface receptor, to which it might act as a ligand [Pestourie et al. 2005]. This feature allows aptamer to be used as bifunctional ligands that, along with recognition, can also be employed as delivery vehicles.

Once identified, aptamers can be chemically synthesized and stabilized to have a consistent structure-activity with little immunogenicity. These

molecules are highly temperature-resistant and are stable over long term storage (Figure 7).

Due to these unique characteristics, aptamers showed great application prospected in different areas of biotechnology, and shortly after their introduction, a considerable number of aptamers entered clinical trials for a wide range of applications, such as diagnosis, therapy, target validation and delivery [Dua et al 2011].

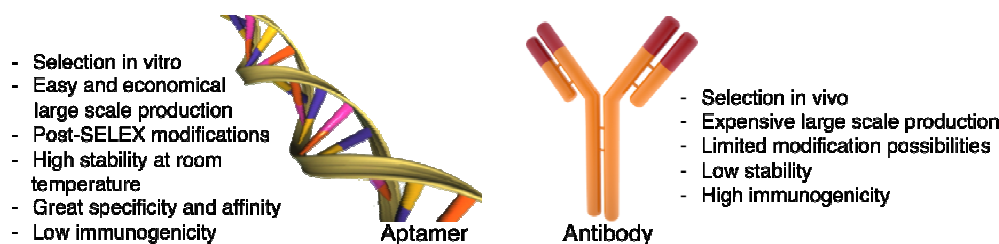


**Figure 7.** Comparison between aptamer and antibody features.

### 1.3.1 Aptamers production: SELEX method

DNA or RNA aptamers are isolated from combinatorial libraries by a selection procedure named Systematic Evolution of Ligands by Exponential enrichment (SELEX) technology. Thus, they are entirely chemically synthesized, avoiding complex manufacturing processes using cell-based (eukaryotic or prokaryotic) expression systems that are required for antibodies production.

The SELEX technology is an evolutionary, *in vitro* combinatorial chemistry process used to identify aptamers as specific ligands of a given target from large pools of diverse oligonucleotides. The starting point for the generation of an aptamer is the chemical synthesis of a single-stranded nucleic acid (RNA, DNA) library of large sequence complexity. A typical oligonucleotide library contains random sequences of 20–50 nt flanked by two constant 5' and 3' regions that include primer sites for PCR amplification. The complexity of the library and its molecular diversity is characterized by the length of the random region, providing each individual oligonucleotide with a unique sequence. Randomization is used to create possible sequences of enormous diversity. A starting complexity of  $10^{14}$ – $10^{15}$  is generally considered to be appropriate. A library containing 25 nt randomized nucleotides ( $4^{25} = 10^{15}$ ) reaches the highest possible limit of sequence diversity available for screening in a SELEX experiment. Further, all known single stranded oligonucleotide motifs can be built within this length. This suggests that libraries with short randomized regions are sufficient for a successful aptamer selection. Short libraries are better manageable, cost effective in chemical synthesis and involve lesser post-SELEX optimizations. However, longer randomized regions could provide

greater structural complexity to the library and better opportunities for the identification of aptamers.

As illustrated in Figure 8, the SELEX method includes four main steps:

- 1) Binding, incubating the library with the target molecule under favorable binding conditions;
- 2) Partition, separating molecules that, under the employed conditions, adopt conformations that permit binding to a specific target from other sequences;
- 3) Elution, dissociating the nucleic acid-target complexes and
- 4) Amplification, amplifying the nucleic acids pool, through PCR/RT-PCR.

The pool obtained from the first cycle will be then used as starting pool for the next rounds of selection, thus reiterating these steps a library of reduced complexity enriched in sequences that bind to the target, is generated.

After the final round, the resulting oligonucleotides are subjected to DNA sequencing. The sequences corresponding to the initially variable region of the library are screened for conserved sequences and structural elements indicative of potential binding sites and subsequently tested for their ability to bind specifically to the target molecule.

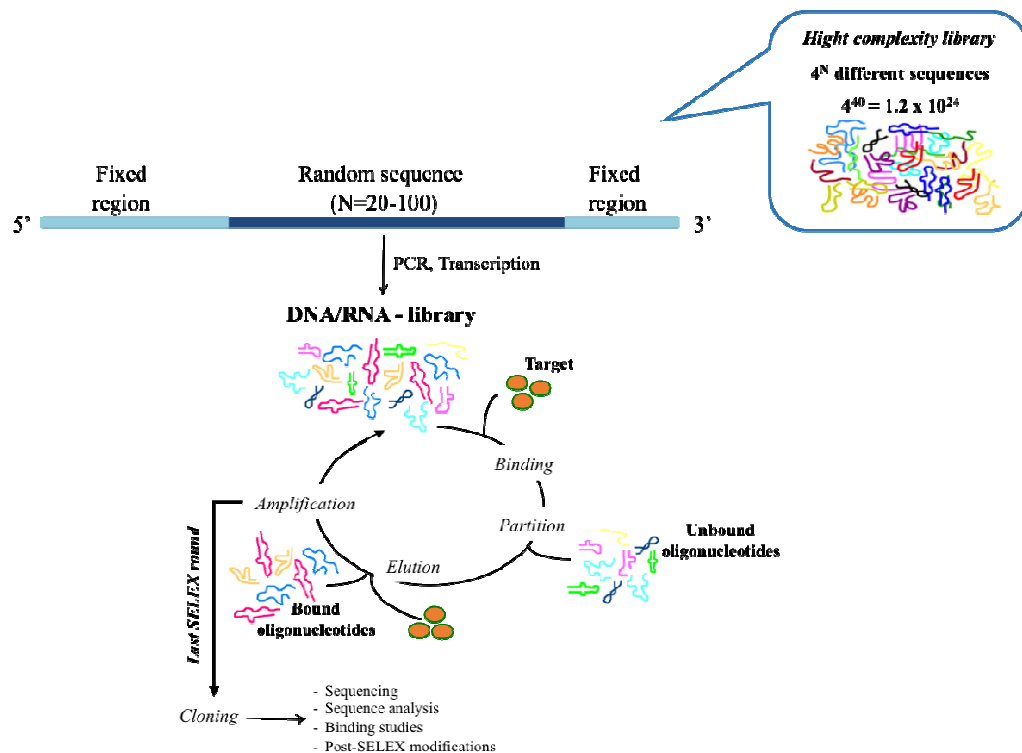


**Figure 8.** A schematic representation of the SELEX process.

Even if many aptamers are still selected by the traditional *in vitro* methodology, over the last few years considerable efforts have focused on

automating *in vitro* selection procedures [Eulberg et al. 2005], thereby accelerating aptamers generation.

### 1.3.2 Post-SELEX modifications of aptamers

Aptamers generated by SELEX method have many limitations for direct use in downstream applications. Natural, unmodified oligonucleotides, especially RNA-based aptamers, are unstable in biological fluids. In order to protect them from digestion by nucleases, and to optimize their pharmacokinetic and pharmacodynamic profiles, chemically modified nucleotides are incorporated into the oligonucleotide backbone [Klein et al. 1990].

The endonucleases that target RNA in biological fluids are generally specific for pyrimidines; therefore, the introduction of modified pyrimidine residues is sufficient to stabilize it towards nucleases. The most commonly employed functional group modifications are 2'-fluoro (2'-F), 2'-methoxy (2'-OMe), or 2'-amino (2'-NH<sub>2</sub>) modifications of the pyrimidine nucleotides, all of which can be introduced at either the pre- or post-SELEX step (Figure 9).

Even with extensive nucleotide modifications to hinder nuclease attack, aptamers can be cleared from the circulation within minutes (Hicke et al. 2006). The short circulating half-life due to the small size of RNA and DNA aptamers is a serious obstacle to administering of aptamers to patients for therapeutic applications. While a low molecular weight can be an advantage as it allows economical chemical synthesis and better target accessibility of aptamers, it promotes rapid clearance by the renal system [Rusconi et al. 2002; Willis et al. 1998]. The most common method to increase the size of aptamers is to add a polyethylene glycol (PEG) moiety [Farokhzad et al. 2004].

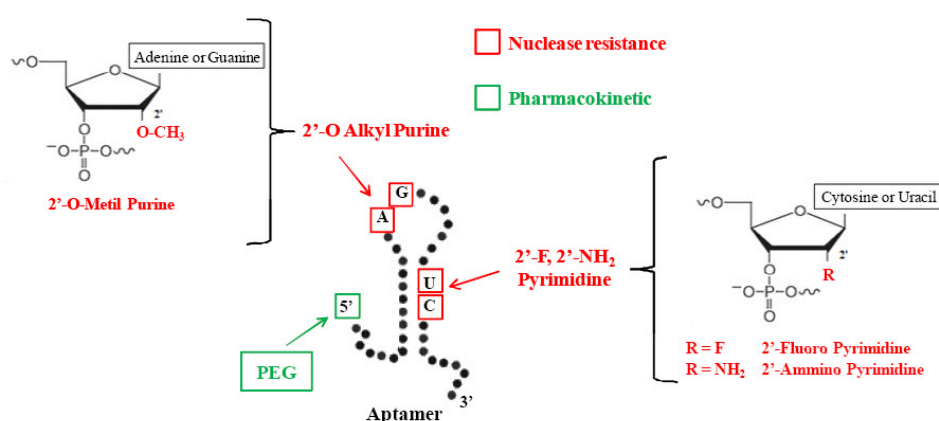


**Figure 9.** Scheme of the most typical modifications used to improve aptamer nuclease resistance (red) or its pharmacokinetic profile (green).

### 1.3.3 Aptamers as therapeutics

The development of aptamers as therapeutics has principally involved aptamers that bind and inhibit the activity of their protein targets.

The list of aptamers against important therapeutic targets is growing rapidly and some aptamers is now in clinical trials as therapeutic agents (Table 2).

Aptamer name	Target	Disease indication	Clinical status
Macugen	VEGF-165	AMD Diabetic retinopathy	Approved
AS1411	Nucleolin	AML	Phase II
E10030	PDGF-B	AMD	Phase II
ARC1905	C5	AMD	Phase I
ARC1779	vWF	TMA	Phase II
NU172	Thrombin	Acute coronary artery bypass	Phase II
NOX-A12	SDF-1 $\alpha$	Lymphoma	Phase I
NOX-E36	CCL2	Type 2 diabetes	Phase I

**Table 2.** Aptamers in the clinical trials. (Abbreviations: AMD, age-related macular degeneration; AML, acute myeloid leukemia; TMA, thrombotic microangiopathie)

To date, the most successful therapeutic application of an aptamer has been an RNA molecule, known as Macugen, that binds and antagonizes the action of VEGF-165, the VEGF isoform preferentially involved in pathological ocular neovascularization.

This aptamer has been fully approved by the FDA in December 2004, for the treatment of age-related macular degeneration (AMD), characterized by the formation of a neovascular membrane leaking blood and fluid under the retina with consequent destruction of the macula and loss of vision [Ng et al. 2006].

In phase III clinical trials Macugen demonstrated to be effective for diabetic retinopathy treatment, resulting in improved vision and reduced macular edema. Furthermore, Macugen is also a potential candidate for the treatment of highly vascularized tumors, even if the effectiveness of a systemic administration is still unclear.

Many other aptamers, not yet approved by the FDA, are currently in clinical trials (see Table 2). Among them, it is very interesting for cancer therapy the DNA aptamer AS1411, directed against nucleolin, a protein often overexpressed on the surface of cancer cells [Bates et al. 2009].

Once bound to nucleolin, AS1411 moves within the cancer cell, where it triggers cellular death by apoptosis, inhibiting NF- $\kappa$ B [Girvan et al. 2006] and Bcl-2 [Soundararajan et al. 2008] pathways.

Different studies have been carried out to assess the effectiveness of AS1411 as tumor treatment for different solid human malignancies (such as AML) and it is currently in phase IIb clinical trial.

### 1.3.4 Aptamers as delivery agents

The negatively charged phosphate backbone of the nucleic acid molecule is the primary cause for its inadequate and inefficient cellular association, owing to electrostatic repulsion from the negatively charged cell surface. Moreover, oligonucleotides longer than 25 bases are difficult to import into cells because of their size and predisposition to self-hybridize [Patil et al. 2005].

Currently an increasing number of aptamers targeting cancer cell surface epitopes have been successfully used for the specific delivery of active drug substances both *in vitro* and *in vivo*, including nanoparticles [Farokhzad et al. 2006], anti-cancer therapeutics [Bagalkot et al. 2006], toxins [Chu et al. 2006], enzymes [Chen et al. 2008], radionuclides [Hicke et al. 2006], viruses [Tong et al. 2009], small interfering RNAs (siRNAs) [Wu et al. 2011] and more recently microRNAs [Liu et al. 2012].

Several cell-internalizing aptamers have been successfully used as targeting vehicles. These include aptamers against the protein tyrosine kinase 7 (PTK7) [Xiao et al. 2008], prostate specific membrane antigen (PSMA) [Lupold et al. 2002], and mucin 1 (MUC1) [Hu et al. 2012].

To date, another published internalizing RNA aptamer is GL21, which have been selected through a whole cell-SELEX on U87MG cells, a malignant human glioma cell line, using in the counter-selection step less malignant human T98G glioma cells [Cerchia et al. 2009]. GL21 aptamer is able to bind and inhibits the signaling of AXL receptor, belonging to the TAM family of tyrosine kinase receptors (RTKs), that also includes Sky (Tyro3, Dtk) and Mer. This RTKs are characterized by an extracellular domain consisting of two immunoglobulin-like domains followed by two fibronectin type 3-like domains.

AXL receptor is activated by Growth-arrest-specific gene 6 (Gas6), a member of the vitamin K-dependent protein family that resembles blood coagulation factors rather than typical growth factors (Figure 10) [Stitt et al. 1995].

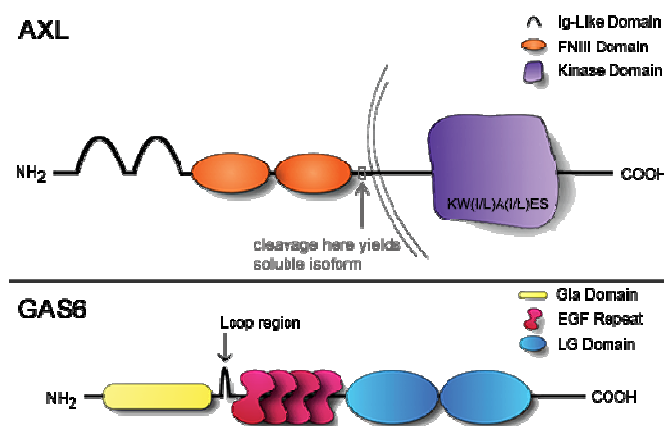


**Figure 10.** AXL receptor and Gas6 ligand structures.

AXL overexpression has been reported in many human cancers and is associated with invasiveness and/or metastasis in lung [Shieh et al. 2005], prostate [Sainaghi et al. 2005], breast [Zhang et al. 2008], gastric [Wu et al. 2002] and pancreatic cancers [Koorstra et al. 2009].

Furthermore, by a phosphoproteomic approach based on the profiling of phosphotyrosine signaling, activated AXL protein was detected in ~5% primary tumors of non-small-cell lung cancer [Rikova et al. 2007]. Using a rational approach based on its predicted secondary structure they designed a 34-mer truncated version of the 92-mer original molecule, named GL21.T, which contains the active site of GL21 and preserves high binding affinity to the U87MG cells.

Determining the cell type specificity, GL21.T cannot bind cells without AXL receptor, while it is able to bind also other human cancer cell types that present the receptor on the cellular surface. It is also capable of being endocytosed into target cells, getting ~30% of cell internalization following 15-minute incubation and reached ~60% following 2 hours of aptamer treatment [Cerchia et al. 2012].

### **1.3.5 Aptamers in diagnosis**

Aptamers have also started to play increasingly important roles in human disease diagnosis [Soontornworajit et al. 2011]. Indeed, once aptamers are selected, they can be functionalized using a wide variety of fluorophores, as well as cobalt or iron paramagnetic particles, gold nanoparticles, radio-isotopes and biotin. These characteristics render the aptamers suitable as ligands for protein detection in a great number of different methodologies.

Due to their relatively small size (8-25 kDa) in comparison to antibodies (150 kDa), aptamers should be better suited for rapid tumor penetration and blood clearance, two excellent characteristics for contrast agents in imaging (Figure 11).

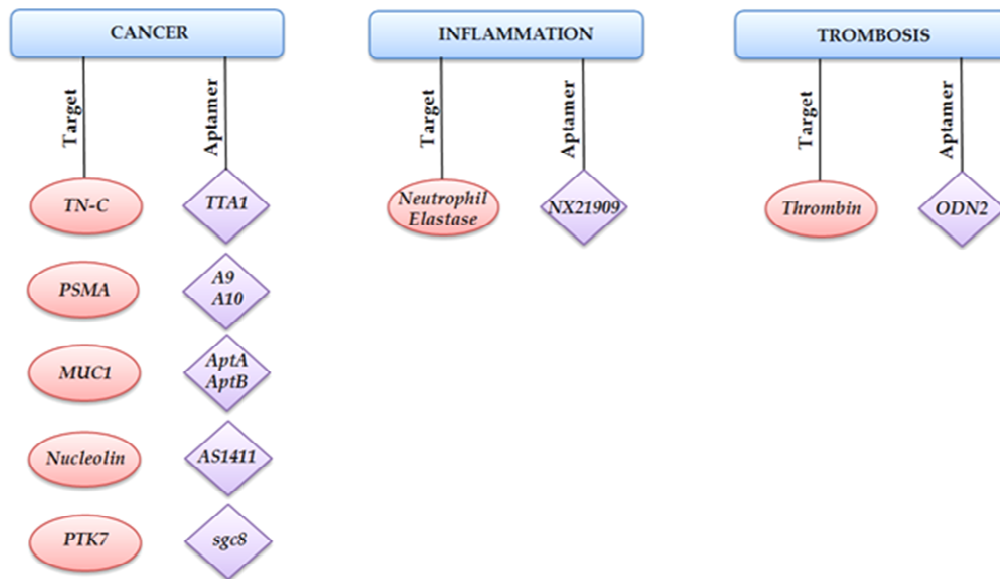


**Figure 11.** List of aptamers developed as ligands for imaging.

One such example of imaging applications is TTA1, a modified RNA aptamer targeted against tenascin-C, an extracellular matrix protein upregulated in a number of tumors such as breast, lung, colon, prostate, glioblastoma, and lymphoma [Levy-Nissenbaum et al. 2008]. The aptamer was conjugated to the Technetium-99m (99mTc) with the purpose of performing single photon emission-computed tomography (SPECT), a 3D-imaging technique that can aid in visualizing tumors [Hicke et al. 2006].

Because of their high affinity to bind specific cell markers, aptamers can also aid in clinical diagnosis of diseases. Recently, RNA aptamers have become an attractive tool in detecting diseased cells on a histological section and, most importantly, the presence of very low amounts of circulating disease cells in the bloodstream [Wan et al. 2010].

### 1.3.6 Molecular Chimeras

As mentioned, instead of directly interrupting a disease process, internalized aptamers could work as delivery agents into cells. Until now, some aptamers have been successfully used for the targeted delivery of active drug substances, both in vitro and in vivo, including anti-cancer drugs, toxins, enzymes, radionuclides, virus, siRNAs and miRNAs.

The cargos are attached to the aptamers either through their assembly with linked functionalized groups, or through direct conjugation, creating a molecular chimera, as in the case of oligonucleotides [Zhou and Rossi 2010].

Aptamer-mediated targeted delivery can enhance the therapeutic efficacy and reduce the toxic effects of drugs.

To date, different aptamers have been used for the creation of a molecular chimera (Figure 12).

The best characterized for targeted delivery is a 2'-F-Py RNA aptamer against the extracellular domain of PSMA. This aptamer has been used by independent groups to specifically deliver siRNAs to target cells [Chu et al. 2006; McNamara et al. 2006; Dassie et al. 2009; Wullner et al. 2008].

In addition to siRNAs, the anti-PSMA aptamer has been further used to deliver toxins or chemotherapeutic agents encapsulated within nanoparticles or directly intercalated into the aptamer [Dhar et al. 2008].

Another promising delivery molecule is the anti-CD4 RNA aptamer that was non-covalently joined to siRNAs via phi29 RNAs (ncRNA molecules of the bacteriophage phi29) containing complementary loop domains.

Two pRNA molecules were respectively fused with siRNAs and the anti-CD4 aptamer. Through the interaction of right and left interlocking loops, the two chimeric pRNAs could dimerize into a stable nanovector of approximately 25 nm in diameter [Guo et al. 2005].

Also, John Rossi's group used a RNA aptamer against gp120 for targeted delivery of siRNA against Human Immunodeficiency Virus (HIV) infections [Zhou et al. 2009].

27-mer Dicer substrate RNA duplex and the aptamer were attached with complementary 'sticky' sequence. After a simple annealing, they formed stable base pairs.

In this design format, one pair of complementary GC-rich sticky bridge sequences was chemically attached to the 3' end of the aptamer. The complement to this sequence was attached to one of the two siRNA strands and the aptamer and siRNA were joined by Watson-Crick base pairing. A flexible three-carbon atom hinge (C3) was added as a spacer between the adhesive (sticky) sequence and the aptamer to allow spatial and structural flexibility. Importantly, this sticky bridge-based strategy can be used to facilitate the effective interchange of different siRNAs with a single aptamer, which is required to avoid viral resistance to the siRNA component.

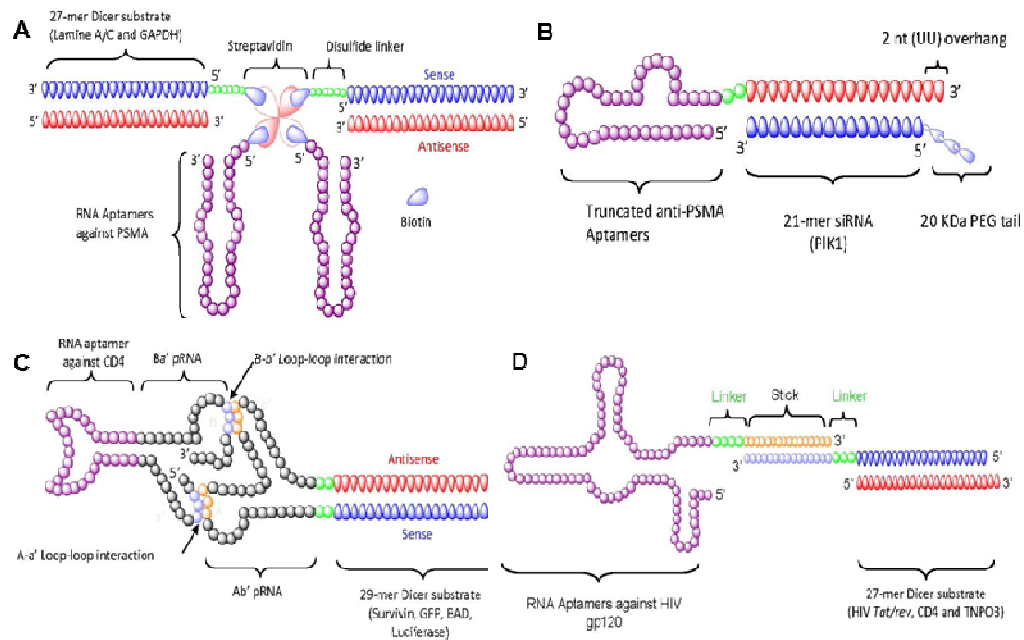


**Figure 12.** Representations of molecular chimeras: A) Anti-PSMA RNA aptamer-mediated RNAi (Chu et al.); B) Anti-PSMA RNA aptamer-mediated RNAi (Dassie et al.); C) Anti-CD4 RNA aptamer-mediated RNAi; D) Anti-gp120 RNA aptamer-mediated RNAi.

Moreover, recent papers explored the use of aptamer to deliver RNA interfering molecules (siRNAs or miRNAs) into cancer cells as cancer therapeutics. This is possible to selectively deliver by conjugating the silencing RNA moiety to an aptamer moiety with high binding affinity for cancer-specific transmembrane receptor tyrosine kinase.

As shown by de Franciscis's group, a single strand miRNA (or anti-miRNA) can, as well, be conjugated to an aptamer. Further, it is shown that the conjugates could act as a multifunctional molecule since it combines the silencing effects of miRNA (anti-miRNA) molecules with the receptor-inhibiting function of the aptamer [Esposito et al. 2014; Catuogno et al. 2015].

These recent achievements open the concrete opportunity to translate the knowledge of the mechanisms of action of the several types of non-coding RNAs into safe and more efficient therapeutics.

## **2. AIM OF THE STUDY**

Despite the great increase in the knowledge and the innovations in standard treatment, NSCLC is still one of the more aggressive and lethal malignant diseases worldwide. The lack of a complete comprehension of molecular mechanisms involved in NSCLC progression and development, and the absence of an effective targeted therapy system could be the reasons of this failure.

Recent studies have demonstrated that several miRNAs are deregulated in NSCLC, acting both as oncogenes or tumor-suppressors. They represent attractive candidates as therapeutic targets in cancer, but the main problem in their therapeutic use is the lack of a robust and reliable way to selectively deliver them within the cancer cells.

Thus, it is crucial to develop and validate cell specific delivery agents. A promising approach for the carrying is now represented by the use of aptamers.

The aim of this work is primarily to individuate a miRNA down-regulated in NSCLC patients and, then, to use the previously described RNA aptamer inhibitor of the tyrosine kinase receptor AXL (GL21.T), as a means to deliver the selected miRNA into NSCLC cells expressing AXL.

The results achieved by this project could be a good starting point to develop novel ncRNA-based therapies for NSCLC.

### **3. MATERIALS AND METHODS**

#### **3.1 TCGA miRNA dataset and patients' information**

miRNA expression data and corresponding clinical information for NSCLC datasets were downloaded from the Cancer Genome Atlas (TCGA) data portal in June 2013 (<http://tcga-data.nci.nih.gov>). The collection of the data from TCGA platform was compliant with laws and regulation for the protection of human subjects, and necessary ethical approvals were obtained.

The level 3 data for the 218 NSCLC patients were quantile normalized and log<sub>2</sub> transformed. Only patients with overall survival (OS) information were taken into account.

The association between continuous miRNA expression and OS was carried out using univariable Cox regression analysis. The difference in the survival outcome between risk groups was estimated by log-rank Mantel-Cox test and plotted by Kaplan-Meier curve. The analyses were performed with BRB-Array Tools - R/BioConductor (version 2.10). For the multivariable analysis, the Cox proportional hazard model was applied, and a backward stepwise selection procedure (Wald) was used to identify miRNAs with independent prognostic value. All reported *p*-values were two-sided. The analyses were performed using SPSS (version 2.1).

#### **3.2 Cell lines**

All the human NSCLC cell lines were purchased from American Type Culture Collection (ATCC). MRC-5, Calu-1 and MCF-7 cells were cultured under standard conditions in Dulbecco's Modified Eagle's Medium (DMEM), while A549 and H460 cells in RPMI-1640 Medium, all supplemented with 10% heat-inactivated fetal bovine serum (FBS), 2 mM L-glutamine, and 100 U/ml penicillin/streptomycin. All media and supplements were from Sigma Aldrich (Milan (MI)-Italy). Cells were maintained at 37°C in a humidified atmosphere with 5% CO<sub>2</sub>.

#### **3.3 Isolation of primary cell cultures from human lung biopsies**

For primary cell-culture experiments, human lung biopsies (samples from "Azienda Ospedaliera Universitaria Primo Policlinico", NA) were cut by mechanical fragmentation with sterile scissors and tongs. Isolated cells were routinely seeded onto 100mm dishes and grown in Dulbecco's Modified Eagle's Medium/Nutrient F12-Ham (DMEM-F12). Media were supplemented with 10% heat-inactivated fetal bovine serum (FBS) and 100 U/ml

penicillin/streptomycin. All media and supplements were from Sigma Aldrich (Milan (MI)-Italy). Primary cells were maintained at 37°C in a humidified atmosphere with 5% CO<sub>2</sub>.

### 3.4 Cell transfection

For miRNAs transient transfection, cells were seeded in a 6-well plate one day ahead, grown to 50-70% confluence and then transfected with 100 nM (final concentration) of pre-miR-34c, pre-miR-Negative Control #1 (miR-NC), anti-miR-34c or anti-miR-NC (Ambion®, Life Technologies, Monza (MB)-Italy), using Oligofectamine (Invitrogen, Life Technologies, Monza (MB)-Italy), according to the manufacturer's protocol.

To transiently knockdown AXL gene expression, si-AXL or siRNA Control (Santa Cruz Biotechnologies, D.B.A. ITALIA srl, Segrate (MI)-Italy) were transfected, using Oligofectamine, at a final concentration of 50 nM (Santa Cruz Biotechnologies, D.B.A. ITALIA s.r.l., Segrate (MI)-Italy).

For transient overexpression of AXL (4 µg, final concentration), cells were transfected using Lipofectamine 2000 (Invitrogen, Life Technologies, Monza (MB)-Italy), according to the manufacturer's protocol.

### 3.5 Aptamer-miRNA chimera

The following sequence were used for the chimera production:

- GL21.T sticky:

5' AUGAUCAAUCGCCUCAAUUCGACAGGAGGCUCACXXXXGUAC  
AUUCUAGAUAGCC

- miR-34c guide: 5' AAUCACUAACCACACGGCCAGG

- miR-34c passenger sticky:

5' ACUAGGCAGUGUAGUUAGCUGAUUGC/GGCUAUCUAGAAUGU  
AC

All RNA were modified with 2'-F pyrimidines, and synthesized by TriLink Biotechnologies (San Diego (CA)-USA). Stick sequences, consisting of 2'-F-Py and 2'-OMe purines, are underlined. The italic X indicates a covalent spacer, a three-carbon linker ((CH<sub>2</sub>)<sub>3</sub>).

Before each treatment, aptamer was subjected to a short denaturation-renaturation step (5 min 85°C, 2 min on ice, 10 min at 37°C). To prepare GL21.T/miR34c, 5 µM of miR-34c strands (miR-34c guide and miR-34c passenger sticky) were incubated at 95°C for 15 min, 55°C for 10 min, and RT for 20 min, in Binding Buffer 10X (200 mM HEPES, pH 7.4, 1.5 M NaCl, 20 mM CaCl<sub>2</sub>). 5µM of sticky aptamer was then annealed by incubating together at 37 °C for 30 min.

For all the experiments, treatments with GL21.T aptamer or GL21.T/miR34c chimera were performed at 400 nM (final concentration).

### 3.6 RNA extraction and Real-time PCR

Total RNAs (microRNA and mRNA) were extracted using Trizol reagent (Invitrogen, Life Technologies, Monza (MB)-Italy), according to protocols recommended by the manufacturer.

Reverse transcription of total miRNA was performed starting from equal amounts of total RNA/sample (500 ng), using miScript reverse Transcription Kit (Qiagen, D.B.A. ITALIA s.r.l., Segrate (MI)-Italy). Quantitative analysis of miR-34c and RNU6B (as internal reference) was performed by Real-Time PCR using specific primers (Qiagen, D.B.A. ITALIA s.r.l., Segrate (MI)-Italy)) and miScript SYBR Green PCR Kit (Qiagen, D.B.A. ITALIA s.r.l., Segrate (MI)-Italy)). The reaction for detection of miRNAs was performed as follow: 95°C for 15', 40 cycles of 94°C for 15'', 55°C for 30'' and 70°C for 30''.

For reverse transcription of mRNA was used SuperScript® III Reverse Transcriptase (Invitrogen, Life Technologies, Monza (MB)-Italy). Quantitative analysis of AXL and  $\beta$ -actin (as internal reference), was performed by Real-time PCR using specific primers and iQ™ SYBR Green Supermix (Bio-Rad, Segrate (MI)-Italy)). The reaction for detection of mRNAs was performed as follow: 95°C for 15', 40 cycles of 94°C for 15'', 57°C for 30'' and 72°C for 30''. All reactions, for detection of mRNAs or miRNAs, were run in a final 25  $\mu$ l volume.

The threshold cycle (CT) is defined as the fractional cycle number at which the fluorescence passes the fixed threshold. For quantization, the  $2^{(-\Delta\Delta CT)}$  method was used [Livak and Schmittgen 2001]. Experiments were carried out in triplicate for each data point, and data analysis was performed by using Applied Biosystems StepOne Plus™ Real-Time PCR Systems.

### 3.6 Protein isolation and Western blotting

Cells were washed twice in ice-cold PBS, and lysed in Lysis buffer (containing 50 mM HEPES pH 7.5, 150 mM NaCl, 1% Glycerol, 1% Triton X100, 1.5 mM MgCl<sub>2</sub>, 5 mM EGTA, 1 mM Na<sub>3</sub>VO<sub>4</sub>, and 1X protease inhibitor cocktail).

Protein concentration was determined by the Bradford assay (BioRad, Segrate (MI)-Italy)) using bovine serum albumin (BSA) as the standard, considering that 5  $\mu$ g of BSA show a value of absorbance of 0.333 at a wavelength of 595 nm. Equal amounts of proteins were denatured in Sample Buffer (containing 10% SDS, 87% glycerol, 5%  $\beta$ -mercaptoethanol and 0,1% Bromophenol Blue) for 5min at 100°C, and then analyzed by SDS-PAGE (10% acrylamide).

Gels were electroblotted into nitrocellulose membranes (G&E Healthcare, Milan (MI)-Italy) and, after the transfer, membranes were blocked for 1 hour with a solution of 5% non-fat dry milk in Tris Buffered Saline (TBS) containing 0.1% Tween-20.

Filters were probed with the primary antibodies shaking over night at 4°C.

Detection was performed by peroxidase-conjugated secondary antibodies, using the enhanced chemiluminescence system (ThermoFisher, Life Technologies, Monza (MB)-Italy).

Primary antibodies used were: anti-AXL (R&D systems, Milan (MI)-Italy), and anti- $\beta$ Actin (Sigma Aldrich, Milan (MI)-Italy).

### **3.7 *In vitro* proliferation assay**

Cell viability was evaluated with the CellTiter 96® AQueous One Solution Cell Proliferation Assay (Promega, Milan (MI)-Italy), according to the manufacturer's protocol. The assay is based on reduction of 3-(4,5-dimethylthiazol-2-yl)-5-(3-carboxymethoxyphenyl)-2-(4-sulfophenyl)-2H-tetrazolium, inner salt (MTS) to a colored product that is measured spectrophotometrically, as optical density.

Cells were transfected with miRNAs (or anti-miRNAs) or treated with chimera or aptamer alone, for 24hrs. Subsequently cells were trypsinized, and plated in 96-well plates in triplicate, and incubated at 37°C in a 5% CO<sub>2</sub> incubator.

Metabolically active cells were detected by adding 20  $\mu$ l of MTS reagent to each well. After 30 min of incubation, the plates were analyzed on a Multilabel Counter (Bio-Rad, Segrate (MI)-Italy). The optical density is related to the percentage of viable cells.

### **3.8 Colony formation assay**

Colony formation assay was performed for studying the ability of a single cell to grow into a colony.

Cells were firstly transfected with miRNAs (or anti-miRNAs) or treated with chimera or aptamer alone, for 24hrs, then they were plated in duplicate in 6-well plates. After the incubation at 37°C in humidified 5% CO<sub>2</sub>, colonies composed of at least 50 cells were visualized by staining with 0.1% crystal violet in 25% methanol solution for 30 min at 4°C. Dishes were washed with water and then let dry on bench.

### **3.9 Luciferase reporter assay**

A549 cells (120.000 cells per well) were seeded in a 6-well plate and co-transfected with 1  $\mu$ g of 3'UTR AXL plasmid (and miR-34c or miR-NC), using Lipofectamine 2000.

Both firefly and Renilla luciferase expression was measured 48 hrs post-transfection, using the Dual Luciferase Assay (Promega, Milan (MI)-Italy), according to the manufacturer's instructions.

Three independent experiments were performed in triplicate. 3'UTR AXL plasmid is a kind gift of Konrad E. Huppi (National Cancer Institute, Bethesda, USA).

### **3.10 Rescue experiments**

To determine whether AXL mediate the effects of miR-34c, rescue experiments were performed in which the effects of miR-34c were measured in the setting of overexpression of a deletion mutant of AXL lacking the 3'UTR.

A549 cells were transfected with miR-34c and with the mutant AXL lacking the 3'UTR using X-tremeGENE 9 DNA Transfection Reagent (Roche), as described. Protein levels were then analyzed by Western blotting, as illustrated above.

### **3.11 *In vitro* Dicer assay**

GL21.T or GL21.T/miR34c (1 µg) were left undigested or digested using Recombinant Human Turbo Dicer Kit (Genlantis, San Diego, CA) according to the supplier's instructions. RNAs were then loaded on a 15% non-denaturing polyacrylamide gel electrophoresis gel, stained with ethidium bromide and visualized with GEL.DOC XR (BioRad) gel camera.

### **3.12 Chimera stability in human serum**

GL21.T/miR34c chimera was incubated 4 µM in 80% human serum from 1 to 8 hrs. Type AB Human Serum provided by Euroclone (Cat. ECS0219D) was used. At each time point 4 µl (16 pmol RNA) was withdrawn and incubated for 1 h at 37 °C with 5 µl of proteinase K solution (600 mAU/ml) in order to remove serum proteins that interfere with electrophoretic migration. Following proteinase K treatment, 9 µl TBE1X and 2 µl gel loading buffer (Invitrogen, Waltham, MA, USA) were added to samples that were then stored at -80 °C. All time point samples were separated by electrophoresis into 10% non-denaturing polyacrylamide gel. The gel was stained with ethidium bromide and visualized GEL.DOC XR (BioRad) gel camera.

### **3.13 Transwell migration assay**

Transwell Permeable Supports, 6.5 mm diameter inserts, 8.0  $\mu\text{M}$  pore size, polycarbonate membrane (Corning Incorporated, Euroclone Spa, Pero (MI)-Italy) were used to perform migration assay.

Cells were transfected or treated for 24 hrs, re-suspended in serum free medium, and plated into the upper chamber of a 24-well transwell (Corning Incorporated, Euroclone Spa, Pero (MI)-Italy). Lower chamber of the transwell was filled with 600  $\mu\text{l}$  of culture medium containing 10% FBS.

Cells were incubated at 37°C for 20-24 hrs. The transwell were then removed from the 24-well plates and stained with 0.1% Crystal Violet in 25% methanol. Percentage of migrated cells was evaluated by eluting crystal violet solution with 1% sodium dodecyl sulfate and reading the absorbance at 570 nm wavelength.

### **3.14 Clonogenic cell survival assay**

The clonogenic assay was performed on Calu-1 cells, transfected or treated, seeded in six-well plates and incubated for 12 days after irradiation at different doses (0, 2, 4 and 6 Gy). Following the incubation, media were removed and colonies with at least 50 cells were washed with PBS, and stained with 0.1% of crystal violet solution. Plate efficiency (PE) was calculated by dividing the number of colonies formed by the number of cells plated. The survival factor (SF) was calculated by dividing the PE of irradiated samples by the PE of the respective non-irradiated samples. SF values were plotted as a function of radiation dose.

### **3.15 Statistical analysis**

All experiments were performed at least three times. Continuous variables are given as mean  $\pm$  standard deviation. For comparisons between two groups, the Student's t test was used to determine differences between mean values for normally distributed. Comparisons among more than three groups were determined by one-way ANOVA followed by Bonferroni's *post hoc* testing.

NSCLC patient survival was illustrated by Kaplan-Meier curves; survival differences between groups were examined with log-rank test. Analyses were conducted with GraphPadPrism 6 software. P values < 0.05 were considered statistically significant.

## 4. RESULTS

### 4.1 miR-34c is downregulated in NSCLC tissues and cell lines

Among oncosuppressor miRNAs reported for NSCLC, I focused my attention on miR-34c since its oncosuppressive role has been already well demonstrated in NSCLC [Garofalo et al. 2013], as well as in other types of cancer [Gallardo et al. 2009; Cai et al. 2010; Corney et al. 2007; Ji et al. 2009; Corney et al. 2010; Hagman et al. 2013].

I analyzed miR-34c expression in a large cohort of NSCLC patients in data collected from TCGA database (515 NSCLC and 46 normal lung samples) by bioinformatic analysis. MiR-34c levels resulted significantly downregulated in NSCLC tissues compared with normal lung tissues (Figure 13).

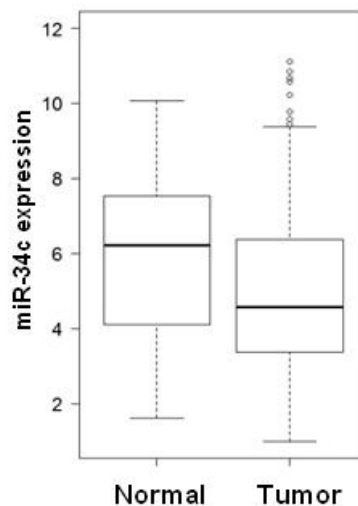


**Figure 13. miR-34c is down-regulated in NSCLC.** Significant increase of miR-34c expression was identified in normal lung vs adenocarcinoma tissues collected from the TCGA database.

Furthermore, Log-Rank Mantel-Cox test showed that patients with higher levels of miR-34c had a longer overall survival, suggestive of a prognostic role of miR-34c ( $p$ -value $<0.05$ ). The correlation of miRNA-34c expression profiles with NSCLC patient survival are represented by a Kaplan–Meier curve (Figure 14).

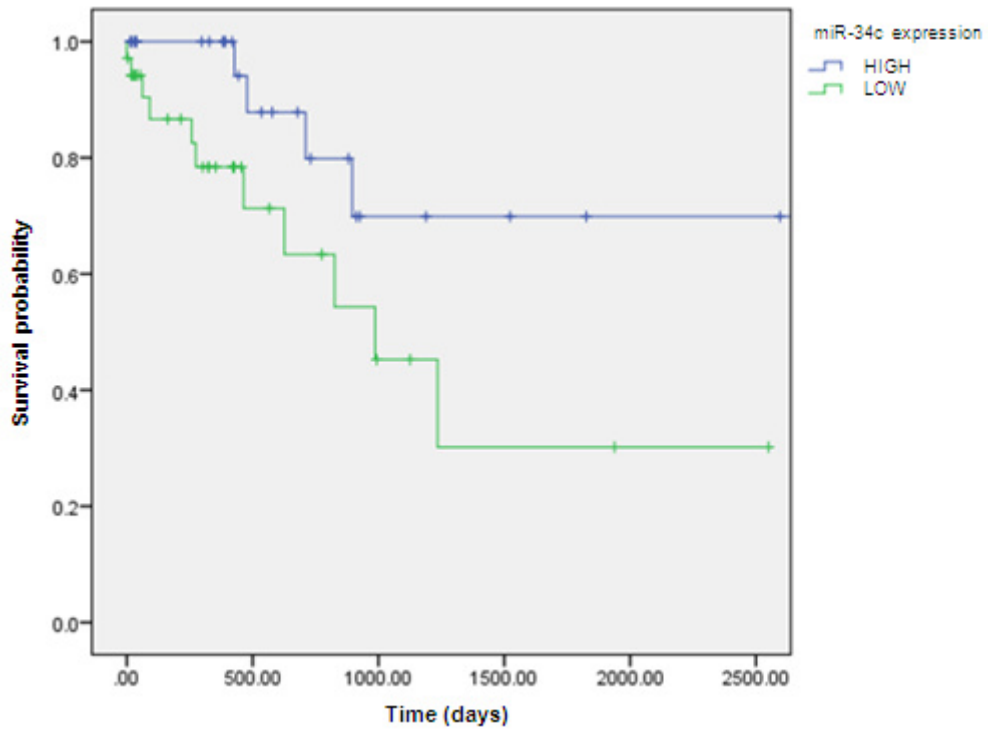


**Figure 14. High miR-34c expression predicted a better prognosis in NSCLC.** Kaplan-Meier survival analysis for TCGA NSCLC patients with -high and -low miR-34c expression.

I then analyzed by Real-time PCR miR-34c expression levels in different NSCLC (A549, Calu-1, H460 and Calu-3) and normal (MRC-5) cell lines.

As shown in Figure 15, the endogenous levels of miR-34c in all NSCLC cell lines examined were significantly lower compared to MRC-5.

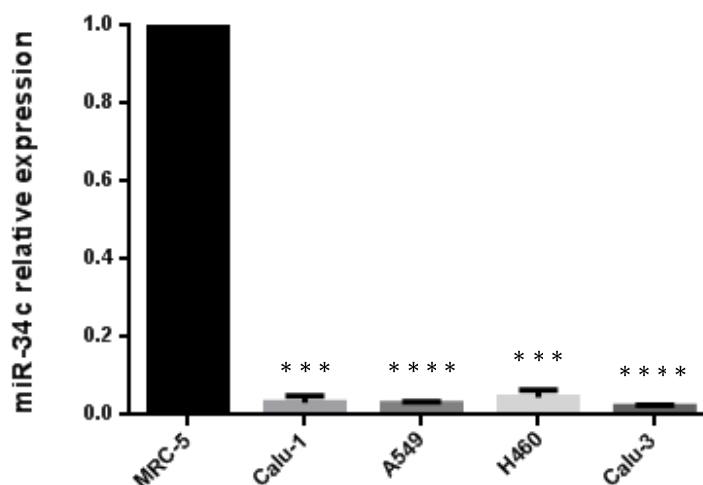


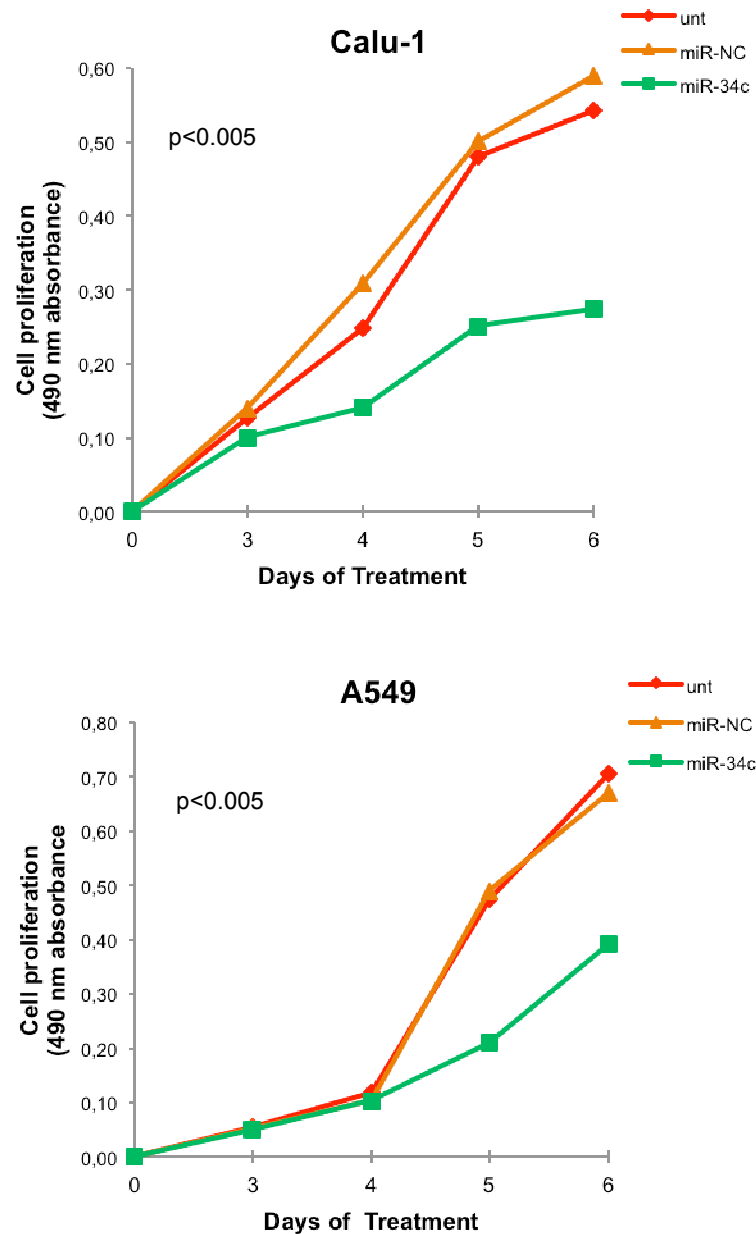
**Figure 15. miR-34c downregulation in NSCLC cell lines.** The expression level of miR-34c in NSCLC cell lines (Calu-1, A549, Calu-3 and H460) was lower than in normal lung cell line (MRC-5). miR-34c expression level was assessed by Real-Time PCR. The transcript level was normalized over RNU6B expression, used as an internal reference. \*\*\* P-value<0.005; \*\*\*\* P-value<0.001, compared with MRC-5 cells.

These results indicated a strong down-regulation of miR-34c in NSCLC, and reveal the potential role of this miRNA as a biomarker for NSCLC prognosis.

#### 4.2 Overexpression of miR-34c inhibits *in vitro* growth of NSCLC cells

To better understand the tumor suppressive role of miR-34c in NSCLC, I selected two NSCLC cell lines, Calu-1 and A549, among those evaluated, for their low expression of miR-34c.

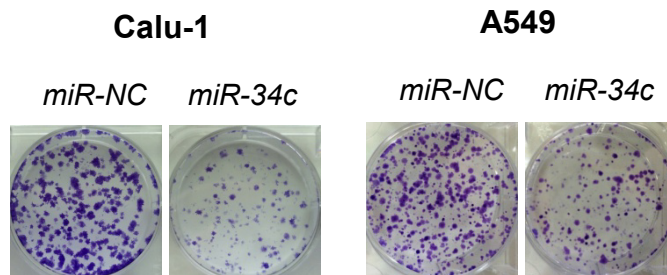
Calu-1 and A549 cells were transfected with miR-34c (or miR-NC), and miR-34c effects on cell proliferation were analyzed. As shown in Figure 16, the growth rate, measured by MTS assay, of miR-34c overexpressing cells was reduced, compared to the negative control (untreated cells or transfected with miR-NC).



**Figure 16. MiR-34c decreases proliferation in NSCLC.** Calu-1 and A549 cells were transfected with miR-NC or miR-34c and cell proliferation was analyzed by MTS assay 3, 4, 5 and 6 days upon transfection. P-value<0.005 compared with the non-transfected cells (Unt).

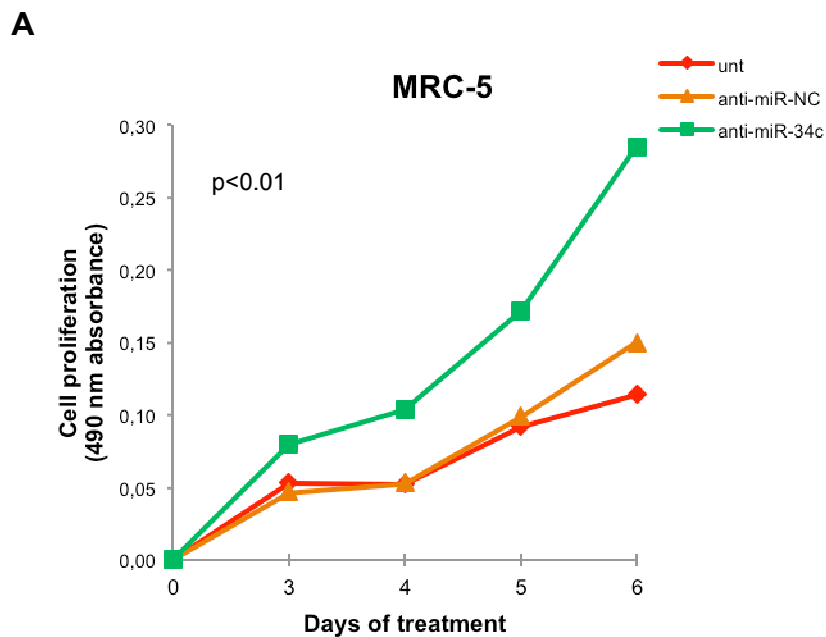
I also evaluated a long term effect on proliferation, performing a colony formation assay. The colony number of Calu-1 and A549 cells transfected with miR-NC was significantly higher compared to the cells transfected with miR-

34c mimic (Figure 17). Thus, upregulation of miR-34c induces long-term growth inhibition in NSCLC cells.



**Figure 17. MiR-34c decreases long-term proliferation in NSCLC.** Calu-1 and A549 cells were transfected with miR-NC or miR-34c. Overexpression of miR-34c significantly inhibited colony formation.

To confirm the data, I evaluated the effect of miR-34c knockdown in MRC-5 cells, which express high levels of miR-34c. This resulted in an increase of cell proliferation and colony formation capability compared with control cells (untreated or transfected with anti-miR-NC) (Figure 18).



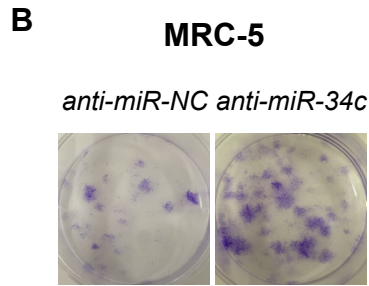


**Figure 18. Anti-miR-34c increases proliferation in normal lung cells.** (A) MTS assay determined cell proliferation in MRC5 cells following downregulation of miR-34c. P-value<0.01, compared with non-transfected cells (Unt). (B) Colony formation assay determined the effect of downregulated miR-34c on colony forming ability in MRC5 cell lines. Downregulation of miR-34c in normal lung cells promotes cell proliferation and allows colony formation.

Thus, these results indicated that miR-34c upregulation induces growth inhibition in NSCLC cells.

### 4.3 AXL as direct target of miR-34c

To identify the molecular mechanisms by which miR-34c affects post-transcriptional regulatory functions, I used miRNA target prediction algorithms (TargetsScan, Miranda, Pictar), that revealed a putative miR-34c binding site within the 3'-UTR of AXL (Figure 19).

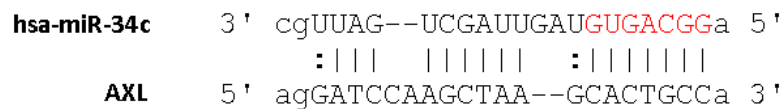


**Figure 19. miR-34c directly targets AXL.** The predicted miR-34c binding sites in the 3'-UTR of AXL mRNA (predicted by the MiRanda program).

To determine whether the binding of miR-34c to AXL 3'UTR resulted in mRNA degradation, I examined the expression of AXL in Calu-1 cells 72 hrs upon transfection with pre-miR-34c. As shown in Figure 20, the exogenous expression of miR-34c induced a significant reduction of AXL protein level, compared with controls.

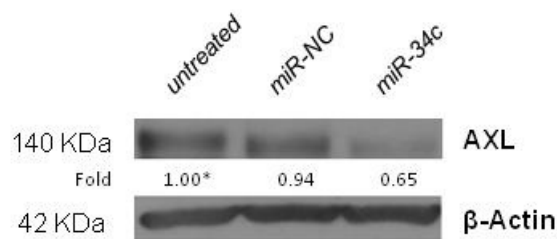


**Figure 20. MiR-34c overexpression decreased AXL protein levels.** The expression was analyzed in Calu-1 cells untreated or transfected with miR-NC or miR-34c for 72 hrs, by Western blot analysis.  $\beta$ -Actin was used as internal control.

In addition, to validate if miR-34c directly binds the putative region of the 3'UTR of AXL mRNA, I conducted a dual luciferase reporter assay. When I transiently co-transfected A549 cells with AXL-3'UTR in the presence of miR-34c, I observed a significant and consistent reduction in the luciferase activity (>50%) after 48 hrs, if compared to cells transfected with AXL-3'UTR in the presence of miR-NC, used as negative control (Figure 21).

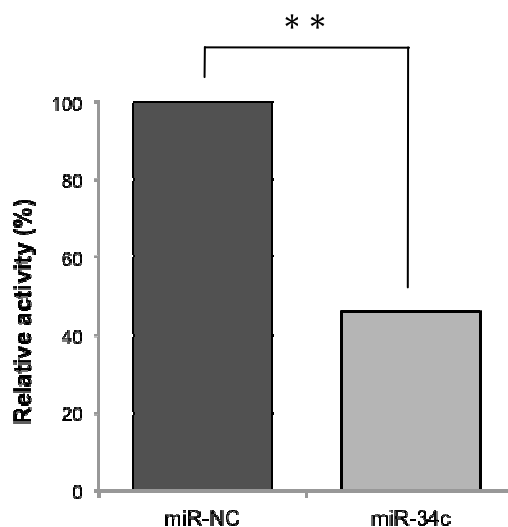


**Figure 21. MiR-34c directly targets AXL.** A549 cells were transiently transfected with the AXL-3'UTR in the presence of miR-34c or miR-NC. Luciferase activity was evaluated 48 hrs upon transfection. \*\* P-value<0.01.

In order to demonstrate a relationship between miR-34c and AXL, I employed a rescue experiment transfecting A549 cells with miR-34c and an AXL plasmid lacking the 3'UTR region. AXL protein levels were detected by Western Blot. Interestingly, the transfection of AXL plasmid, in presence of

miR-34c, was able to rescue AXL protein levels to a situation similar to AXL overexpressing cells (Figure 22).

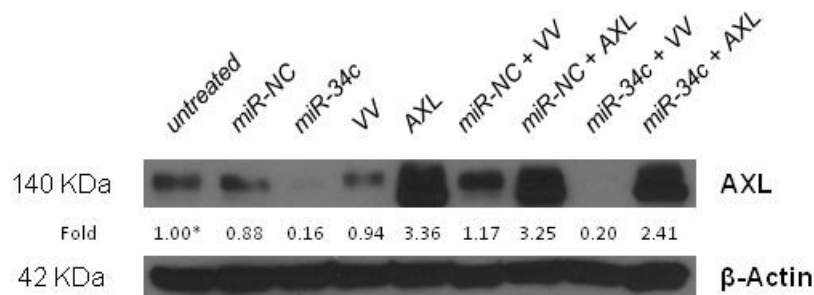


**Figure 22. Rescue of AXL expression levels.** Western blot analysis of AXL protein expression in A549 cells co-transfected with vector control (VV) or AXL plasmid lacking the 3'UTR region, and miR-34c or miR-NC. β-Actin was used as internal control.

These data suggest that miR-34c regulates proliferation of NSCLC cells through AXL direct targeting.

#### 4.4 Design and folding of an aptamer-miRNA conjugate

I generated, via stick-end annealing, a molecular chimera (termed GL21.T/miR-34c), consisting of a duplex miRNA cargo and a nucleic acid aptamer, used as delivery carrier. I fused the passenger strand of miR-34c and the aptamer GL21.T, that selectively recognizes the AXL receptor, by the mean of complementary sticky ends elongated at the 3' end of the aptamer and at the 5' end of the miRNA single chain, respectively. Finally, I annealed the guide strand of miRNA to the template (Figure 23).

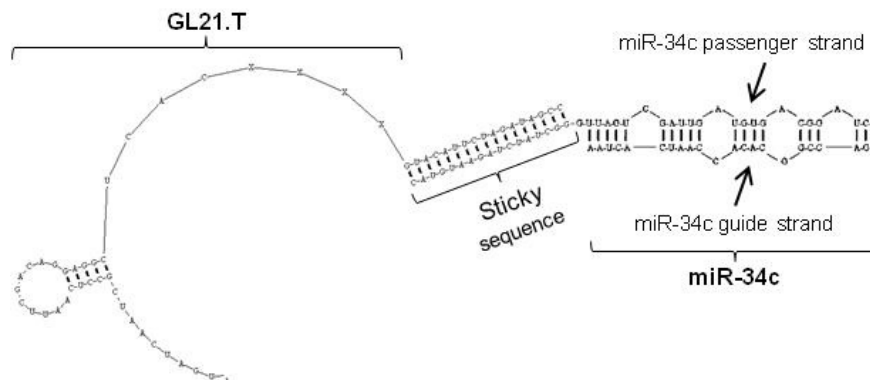


**Figure 23. GL21.T/miR-34c design.** Secondary structure prediction of GL21.T/miR-34c conjugate, using RNA structure 5.3 program.

I verified the correct annealing of the conjugate by a non-denaturing gel electrophoresis analysis. In Figure 24, the annealed GL21.T/miR-34c conjugate is clearly visible as a shift of band migration (lane 4).

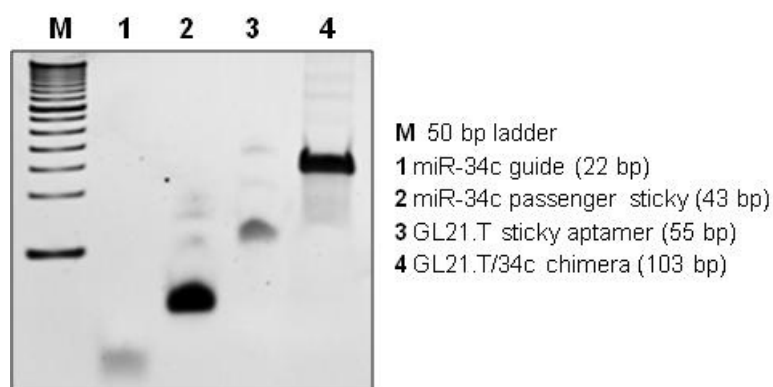


**Figure 24. GL21.T/miR-34c conjugate folding.** To confirm the annealing efficiency, all RNA sequences and annealed GL21.T/miR-34c conjugate were loaded on a 10% non denaturing polyacrilamide gel visualized after staining with ethidium bromide.

To test whether the miR-34c, when conjugated to the aptamer, is still recognized as a Dicer substrate, I incubated GL21.T/miR-34c in the presence or absence of recombinant human Dicer enzyme, for 1 hour at 37°C. As showed in Figure 25, the conjugate, but not the GL21.T aptamer, was digested by Dicer enzyme, resulting in three cleaved products corresponding to the bands of the expected size. I observed the Dicer cleavage products by a non-denaturing gel electrophoresis analysis.

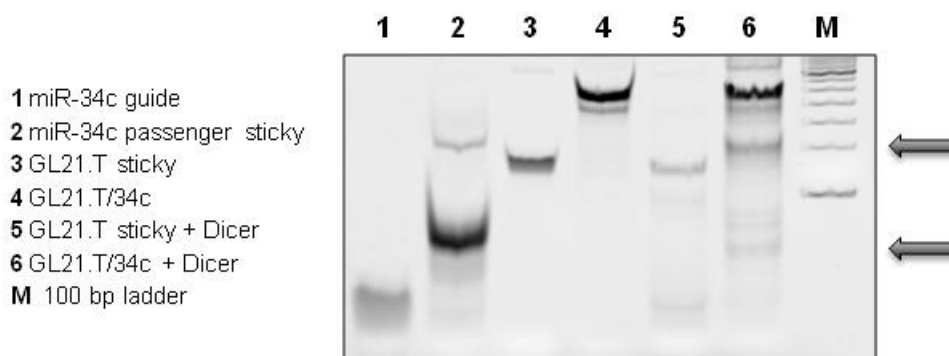


**Figure 25. GL21.T/miR-34c conjugate processing.** The indicated RNA sequences, treated or untreated with recombinant Dicer, were loaded on a 12% non-denaturing polyacrilamide gel and visualized after staining with ethidium bromide. The arrows indicate bands corresponding to the Dicer cleavage products.

An important feature for the potential clinical translation of new therapeutics is represented by their *in vivo* stability. Therefore, to evaluate the GL21.T/34c stability, I incubated the conjugate in human serum for increasing times up to one week. Serum-RNA samples were recovered at the indicated time-points (0, 1, 2, 4, 8 hrs) and analyzed by non-denaturing polyacrylamide gel electrophoresis (Figure 26). As shown, the conjugate was stable up to approximately 2 hrs and then gradually degraded.

The multiple RNA bands observed at longer times likely reflect different stabilities of the two components of the conjugate.

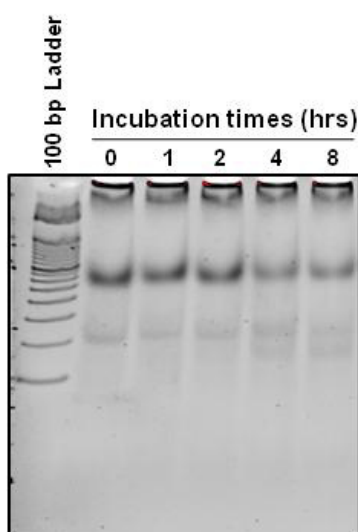


**Figure 26. GL21.T/miR-34c serum stability.** GL21.T/34c chimera was incubated 4  $\mu$ M in 80% human serum for indicated times. Loss of correct folding and RNA degradation was evaluated by electrophoresis into 12% non-denaturing polyacrylamide gel stained with ethidium bromide.

#### 4.5 GL21.T as selective delivery of functional miR-34c

In order to understand whether GL21.T aptamer may act as a selective carrier for delivering the conjugated miRNA, I performed *in vitro* experiments in two different cell lines, expressing different AXL levels, Calu-1 and MCF7. In fact, by a preliminary analysis of AXL protein levels in different cell lines, Calu-1 and MCF7 express high and low levels of AXL protein, respectively (Figure 27).

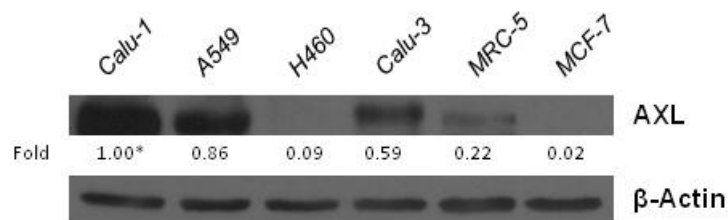


**Figure 27. Differential expression of AXL.** AXL protein expression in different cell lines (Calu-1, A549, Calu-3, H460, MRC-5, and MCF-7) was evaluated by Western blot analysis.  $\beta$ -Actin was used as internal control.

I treated Calu-1 and MCF-7 cells with GL21.T/miR-34c for 72 hours and then I evaluated miR-34c levels by RT-PCR. As shown, GL21.T/miR-34c conjugate increased miR-34c level in Calu-1 cells (AXL<sup>+</sup>), compared to the GL21.T aptamer alone (Figure 28; left panel).

On the contrary, the treatment of MCF-7 cells (AXL<sup>-</sup>) with the conjugate did not result in alterations of miR-34c levels (Figure 28; right panel).

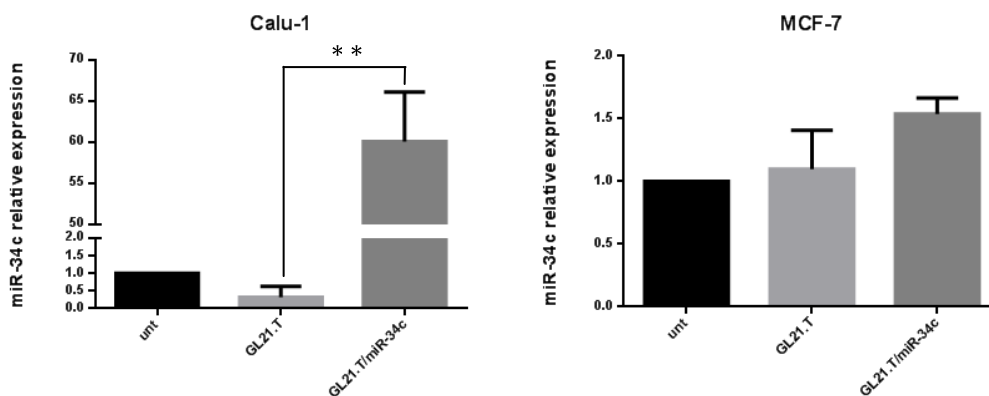


**Figure 28. GL21.T aptamer-mediated delivery of miR-34c.** Calu-1 and MRC-5 cells were treated with GL21.T or GL21.T/miR-34c 400nM. After 72 hrs, miR-34c was quantified by RT-PCR (\*\* P-value<0.01).

To confirm the receptor-dependent delivering of miR34c, I silenced AXL levels in Calu-1 cells (AXL<sup>+</sup>), and, 48 hours after si-AXL transfection, I treated cells with GL21.T/miR-34c for 72 hours. I evaluated the miR-34c levels by RT-PCR. As expected, I did not observe an increase of miR-34c levels in Calu-1 (siAXL)-treated cells (Figure 29). The efficiency of si-AXL transfection was determined by immunoblotting (data not shown).

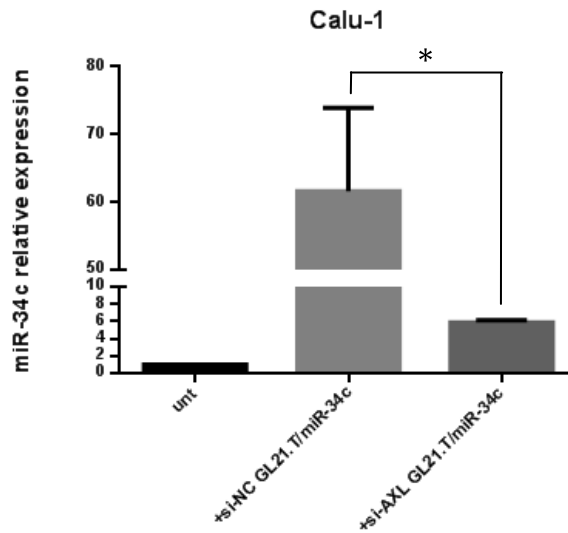


**Figure 29. Receptor-dependent internalization of GL21.T-miR34c chimera.** Calu-1 cells were transfected with si-AXL or siRNA control (si-NC) for 48 hrs and treated with GL21.T/miR-34c for 72 hrs. miR-34c levels were quantified by RT-PCR (\* P-value<0.05).

Otherwise, I transiently upregulated AXL in MCF7 cells (AXL<sup>+</sup>), transfecting AXL cDNA. Following treatment with the conjugate, I assessed miR-34c levels by RT-PCR. Interestingly, the forced expression of AXL in AXL<sup>+</sup> cells induced an increase of miR-34c level mediated by the chimera (Figure 30).

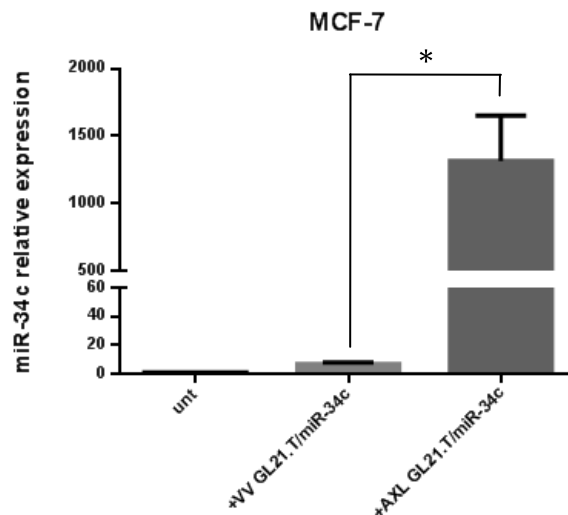


**Figure 30. Receptor-dependent internalization of GL21.T-miR34c chimera.** MCF7 cells were transfected with AXL or control vector (VV) for 24 hrs and treated

with GL21.T/miR-34c for 72 hrs. miR-34c levels were quantified by RT-PCR (\* P-value<0.05).

These results indicate that GL21.T is able to deliver miR-34c inside the cells, in a specific way mediated by AXL receptor.

As previously demonstrated, miR-34c targets the AXL 3'-UTR. Accordingly, I observed that GL21.T/miR-34c treatment, but not the aptamer alone, was able to suppress the expression of AXL protein (Figure 31).

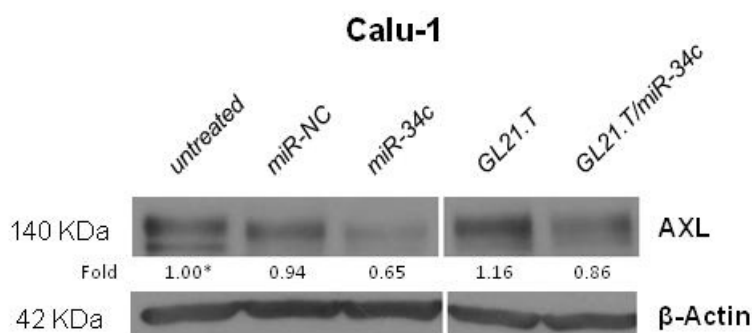


**Figure 31. GL21.T/miR-34c treatment decreased AXL protein levels.** Calu-1 cells were transfected or treated as indicated, and AXL protein expression was analyzed by Western blot after 72 hrs. β-Actin was used as internal control.

## 4.6 Functional aspects of GL21.T/miR-34c chimera

### 4.6.1 GL21.T/miR-34c effects on cell proliferation

To further support the efficacy of the conjugate treatment I investigated whether, in the GL21.T/miR-34c conjugate contest, miR-34c and the AXL inhibitor aptamer cooperate to produce synergistic effects on cell growth. To this aim, I treated Calu-1 cells with GL21.T/miR-34c conjugate and then analyzed antiproliferative effects by the MTS assay, and colony formation assay.

MTS assay showed that cell proliferation of Calu-1 cells was inhibited by GL21.T/miR-34c treatment to almost the same extent as observed with miR-34c transfection (Figure 32A).

Furthermore, I observed in Calu-1 cells treated with GL21.T/miR-34c a decreased ability to form colonies (Figure 32B).

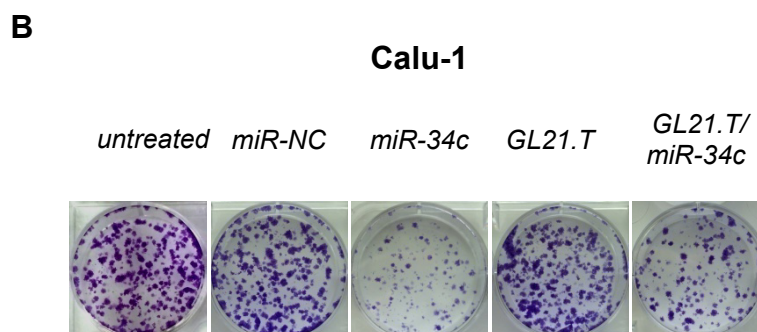
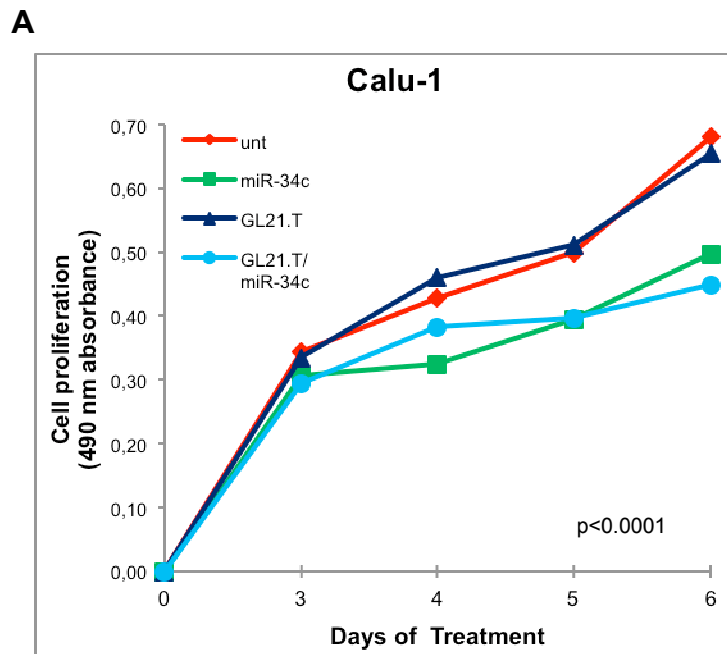


**Figure 32. Antiproliferative effects of GL21.T/miR-34c in NSCLC cells.** (A) Calu-1 cells were transfected with miR-34c or treated with GL21.T/miR-34c and GL21.T aptamer alone. Cell proliferation was analyzed by MTS assay 3, 4, 5 and 6 days upon transfection. P-value<0.0001, compared with the non-transfected cells (Unt). (B) Colony formation of Calu-1 cells. Cells were transfected with miR-NC and miR-34c or treated with GL21.T/miR-34c and GL21.T aptamer alone.

I also determined the effects of GL21.T/miR-34c conjugate on cell growth in primary cells obtained by surgical specimens of lung cancer patients. Preliminarily, I analyzed AXL protein levels in different primary lung cancer cells, to discriminate patients with high and low levels of AXL (Figure 33A).

Then, I performed preliminary proliferation assays on #5T and #9T patients cells, with high and low AXL levels, respectively. As shown, #5T cells treated with the conjugate have reduced viability, compared to control cells (Figure

33B). While, treatment of #9T cells did not display a reduction in cell growth (Figure 33C).

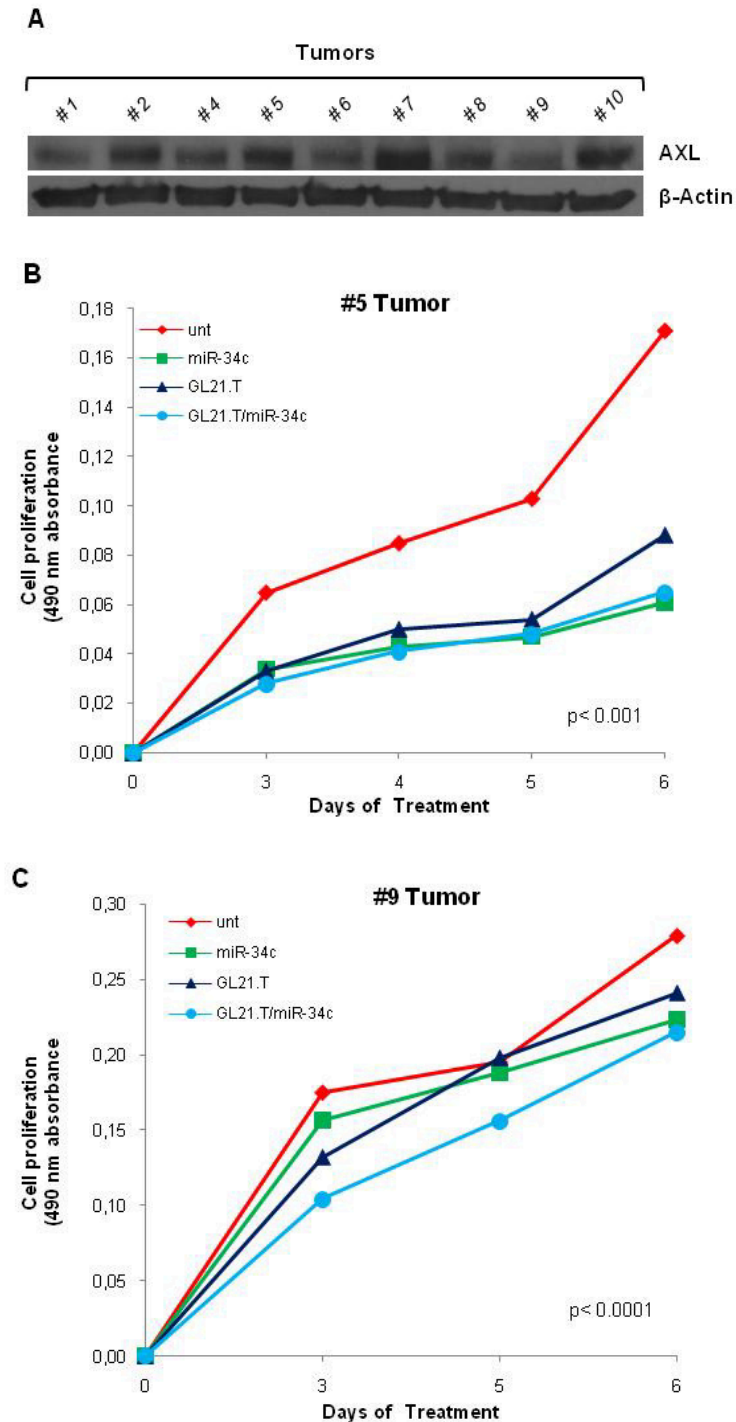


**Figure 33. Antiproliferative effects of GL21.T/miR-34c in primary lung cancer cells.** (A) AXL protein expression in different primary lung cancer cells was evaluated by Western blot analysis.  $\beta$ -Actin was used as internal control. (B) #5T cells (AXL<sup>+</sup>)

were transfected with miR-34c or treated with GL21.T/miR-34c and GL21.T aptamer alone. Cell proliferation was analyzed by MTS assay 3, 4, 5 and 6 days upon transfection. P-value<0.001, compared with the non-transfected cells (Unt). (C) #9T cells (AXL) were transfected with miR-34c or treated with GL21.T/miR-34c and GL21.T aptamer alone. Cell proliferation was analyzed by MTS assay 3, 5 and 6 days upon transfection. P-value<0.0001, compared with the non-transfected cells (Unt).

#### 4.6.2 GL21.T/miR-34c effects on cell migration

Then, I assessed the ability of the conjugate to affect cell migration.

As shown in Figure 34, the migration of Calu-1 cells treated with aptamer alone was similar to that of untreated cells. However, miR-34c transfection and GL21.T/miR-34c treatment inhibited Calu-1 migration to approximately 40% and 20%, respectively, compared to untreated cells.

The results of transwell migration assay showed that high levels of miR-34c could significantly suppress the migration abilities of Calu-1 cells, as a consequence of its inhibitory activity on AXL gene expression, also when delivered by GL21.T aptamer.

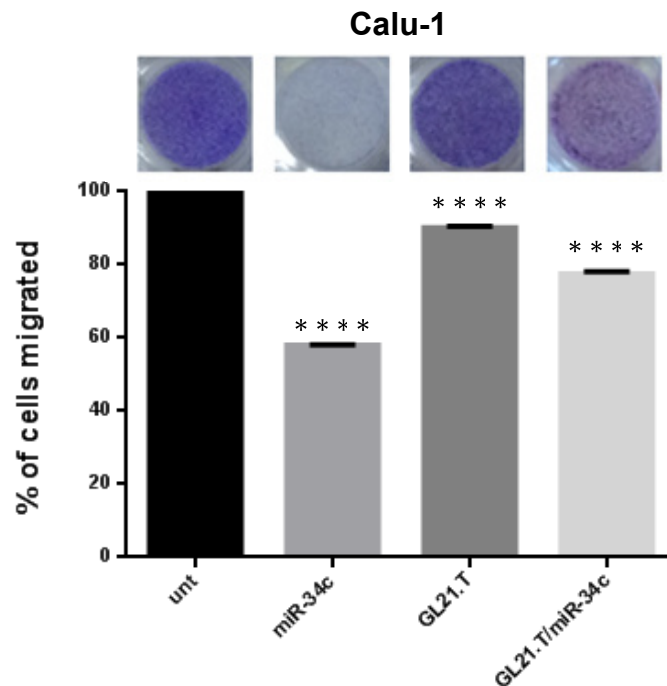


**Figure 34. GL21.T/miR-34c reduce cell migration motility.** Calu-1 cells were transfected with miR-34c or treated with GL21.T aptamer or GL21.T/miR-34c conjugate. The cell migration capability was analyzed by Transwell Migration Assay using 10% FBS as migration inducer. Migrated cells were stained with crystal violet

and photographed. \*\*\*\* P-value<0.0001, compared with the non-transfected cells (Unt).

#### 4.6.3 GL21.T/miR-34c effects on cell sensitivity to ionizing radiation

Finally, I evaluated the long-term irradiation effects on cell survival. In the Calu-1 cell line, overexpression of miR-34c increased the sensitivity of cells to all ionizing radiation doses, when compared to control cells. Moreover, GL21.T/miR-34c conjugate was able to increase this sensitivity to low exposure doses (Figure 35).

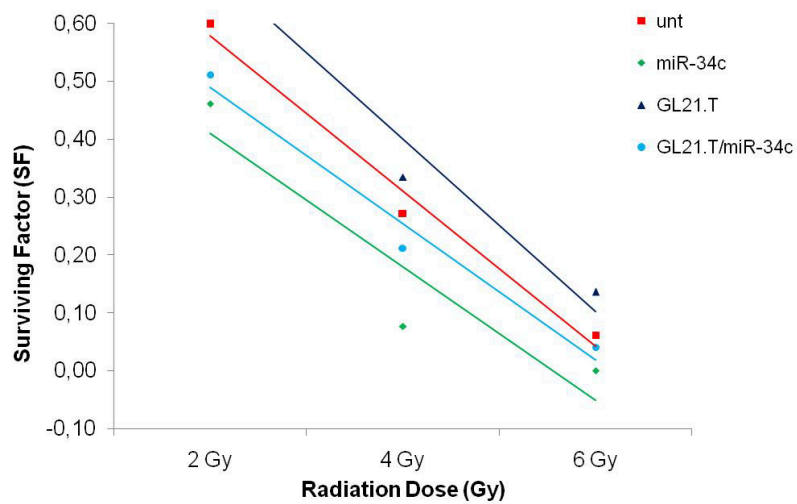


**Figure 35. GL21.T/miR-34c enhances cell sensitivity to ionizing radiation.** Effect of GL21.T/miR-34c conjugate on Calu-1 long-term cell survival after irradiation at different doses.

## 5. DISCUSSION

According to the World Health Organization, lung cancer is the leading cause of cancer death in both men and women worldwide, accounting around 19% of all deaths and this percentage is expected to further increase in the next years. Thus, the high mortality rate associated with lung cancer has encouraged numerous efforts to identify novel therapeutic targets and treatment [Travis et al. 2015].

For the identification of new therapies it is critical to specifically target cancer cells with the aim to reduce the frequency of side effects.

Non-coding RNAs (ncRNAs) represent a structurally and functionally heterogeneous class of molecules recently implicated in multiple biological processes. Due to their altered expression in many tumors, ncRNAs have attracted increasing attention as highly promising therapeutics in cancer.

As discussed, among the most promising ncRNAs in cancer treatment are miRNAs. MicroRNAs have been frequently indicated to be deregulated in different human cancers, acting both as oncogenes or tumor-suppressors. There is growing evidence that they play substantial roles in basic cellular functions. In addition, they have the capacity to target tens to hundreds of genes simultaneously. Thus, they are attractive candidates as prognostic biomarkers and therapeutic targets in cancer.

Accumulating evidences have demonstrated direct connections between deregulation of microRNAs and NSCLC carcinogenesis and prognosis. One of the first miRNAs to be associated with lung cancer pathogenesis was let-7. Takamizawa et al. found that reduced let-7 expression is significantly associated with the short survival of lung cancer patients [Takamizawa et al. 2004].

Furthermore, it appears that miRNAs can be used to differentiate histological subtypes and predict survival of cancer patients. For example, it has been shown that expression levels of miR-34 is strongly correlated with squamous cell carcinomas (SQ) and adenocarcinomas (AD) differentiation [Landi et al. 2010]. This difference in miRNA levels is most significant in the earlier stages of disease.

It has been shown that NSCLC presents a distinctive miRNA expression profile and recent studies have linked some microRNAs alterations to key hallmarks of cancer, including proliferation, survival, invasion, and angiogenesis. Among these studies, Vösa et al. analyzed the expression profile of 858 miRNAs in 38 early-stage NSCLC and 27 adjacent normal lung tissue samples. Their findings revealed a large list of altered miRNAs involved in tumor gene expression. Among the deregulated miRNAs, there are miR-126, crucial for angiogenesis and vascular maintenance, and miR-21, implicated in modulation of the K-Ras pathway. Other significantly deregulated miRNAs are miR-9, miR-30d, miR-106a, and miR-451. Moreover, they reported that low

expression of miR-374a is associated with a poor survival prognosis, but its function is currently unknown [Võsa et al. 2012]

Yu et al. conducted another interesting analysis about miRNAs that predicts cancer relapse and survival of patients with lung cancer. They reported a five-miRNA signature, identifying two miRs that correlate with survival (miR-221 and let-7a), and three miRs associated with poor clinical outcome (miR-137, miR-372, and miR-182\*) [Yu et al. 2008]. Also Landi et al. performed an interesting study on 440 miRNAs in 107 male smokers obtaining a different signature. They found that a decreased expression of miR-25, miR-34, miR-191, and let-7 was associated with significantly poorer survival in SCC patients [Landi et al. 2010].

Because of the lack of a robust moiety to selectively drive miRNAs to malignant tumor cells, the main problem remains their translation to the clinic.

In this regards, nucleic acid-based aptamers represent a very promising approach for delivering of therapeutic cargos in diseased cells.

Several studies have demonstrated new applications for aptamers in anti-cancer targeted therapies, both as tools for cancer cell-targeted therapy and as possible molecular vehicles [Dassie et al. 2009; Zhou and Rossi 2010; Wu et al. 2011; Liu et al. 2012]. Aptamers have been successfully used for the delivery of active molecules, both *in vitro* and *in vivo*, including anticancer drugs, toxins, siRNAs, and, more recently, miRNAs. In fact, some evidences confirm that either siRNAs or miRNAs, appropriately conjugated to aptamers, are functionally delivered and processed into target cells in a receptor dependent manner [Esposito et al. 2014; Catuogno et al. 2015; Iaboni et al. 2016].

Also in this study, I demonstrate that cell-targeted aptamers can be used to deliver a miRNA into specific NSCLC cell types. I designed and characterized an aptamer-miRNA conjugate (GL21.T/miR-34c), covalently joining GL21.T, an anti-AXL aptamer, to the tumor suppressor miRNA, miR-34c.

Among all down-regulated miRNAs reported for NSCLC, I focused my attention on miR-34c, a tumor suppressor miRNA largely investigated in cancers. Its oncosuppressive role has been well defined in various tumor types, including lung cancer [Gallardo et al. 2009; Cai et al. 2010; Ji et al. 2009; Corney et al. 2010; Hagman et al. 2013].

This miRNA was first reported to play an oncosuppressive role by Corney et al. They found that miR-34c is a transcriptional target of p53 and represents a novel effector mediating its suppression of neoplastic growth. It was able to inhibit proliferation and adhesion-independent growth by targeting different genes, such as Cyclin D1, Notch1, Met, and Ezh2 [Corney et al. 2007].

Another work reported mechanisms and implications of miR-34c deregulation in prostate cancer. In a prostate cohort of 47 patients with PCa, miR-34c was found down-regulated compared to adjacent prostate tissue, and MET was identified as its target gene. miR-34c overexpression was correlated with MET down-regulation, leading to the inhibition of cell migration [Hagman et al. 2013]. Further, it was reported that miR-34c and MET are

connected by a positive feedback loop. MET triggers the activation of PI3K/AKT pathway, that inhibits p53, which in turn activates the expression of miR-34c.

Recently, Garofalo et al. demonstrated that miR-34a and miR-34c are downregulated in NSCLC cell lines and described as the miR-34a/c replacement antagonizes tumorigenicity and increases sensitivity to TRAIL-induced cell death, suggesting an important therapeutic application for lung cancer [Garofalo et al. 2013]. The therapeutic utility of miR-34 is further confirmed by Kasinski et al., who investigated the effects of miR-34 re-expression on tumor formation and progression in a mouse lung cancer model [Kasinski et al. 2012]. In fact, they found that, using a systemic nano-delivery, the combination of two tumor-suppressive miRNAs, miR-34 and let-7, controls tumor growth leading to a survival advantage.

In this study, I investigated miR-34c expression and functional role *in vitro*. Firstly, I evaluated miR-34c expression in NSCLC tissues compared with non-tumor lung tissues, in data collected from “The Cancer Genome Atlas” (TCGA) database. MiR-34c resulted significantly lower in NSCLC samples compared to normal lung. More importantly, in a cohort of NSCLC patients (64 primary specimens from TCGA), statistical analysis revealed that patients with higher expression of miR-34c showed a significant longer survival and a better prognosis. Taken together, these data confirm that miR-34c down-regulation is implicated in cancer processes that disclose a worse outcome.

Zhou et al. and Liu et al. showed that the over expression of miR-34c suppressed proliferation of NSCLC cells, partially by inhibiting PAC1/MAPK pathway and eIF4E [Zhou et al. 2015; Liu et al. 2015]. Also my *in vitro* functional studies prove that the increase of miR-34c in NSCLC cells determined a long-term inhibition of cell proliferation. In fact, the analysis of cell proliferation in Calu-1 cells transiently transfected with miR-34c demonstrated that this miRNA up-regulation reduces cell growth. The same result was obtained performing a colony formation assay in the same cells. Conversely, the expression of anti-miR-34c was able to induce cell proliferation of MRC-5 normal lung cells.

Further, I provide evidence for the first time that miR-34c is able to directly bind a 3'UTR region of AXL, thus strongly inhibiting AXL at protein level. By luciferase assay, I also identified the 3'UTR region of the AXL gene that represents the miRNA binding site. AXL is a member of TAM receptors, a receptor tyrosine kinase (RTK) family, comprising Tyro3, AXL, and MerTK. These receptors have attracted great interest as potential therapeutic targets in a wide range of cancers, since they are important in many physiological processes. Particularly, AXL overexpression has been reported in a number of solid tumors as strongly associated with metastatic capacity, invasiveness *in vitro*, and resistance to targeted therapies [Gjerdrum et al. 2010; Holland et al. 2010; Hutterer et al. 2008; Thomson et al. 2011; Zhang et al. 2008; Zhang et al. 2012].

The development of my aptamer-miRNA conjugate is an important example

of targeted miRNA delivery, using an RNA aptamer. Indeed, the aptamer-miRNA conjugate generated combines the multifunctional properties of the miRNA moiety with those of the GL21.T aptamer, producing a multifunctional molecule.

Because the major restriction to the use of RNA-based drugs *in vivo* is the rapid degradation of natural RNAs in serum, in order to protect the GL21.T/miR-34c molecule from this degradation the pyrimidines at all positions of aptamer and miRNA sequences were substituted with 2'-fluoropyrimidines. This modification is well characterized and well tolerated in humans, with low toxicity [Behlke 2008]. RNA oligonucleotides with this modification have already been approved for use in humans (Macugen), with many more quickly moving through the clinical pipeline [Katz and Goldbaum 2006].

The GL21.T/miR-34c chimera was further characterized, demonstrating its *in vitro* targeting and processing. GL21.T/miR-34c conjugate was efficiently processed, once delivered into target cells, to produce the mature miR-34c duplex, indicating the effective functionality of the miRNA moiety.

Given that an essential property to clinical translation of new therapeutics is related to their ability to resist degradation in human serum due to endogenous ribonucleases, I evaluated the serum stability of my chimera. Results revealed that GL21.T/miR-34c conjugate was stable up to approximately 8hrs, but its slow degradation seemed to start after an incubation for 2hrs.

Following treatment with GL21.T/miR-34c conjugate, I observed miRNA uptake into target tumor cells (Calu-1) but not in cells that do not express AXL (MCF-7). Furthermore, miRNA enhance, resulted in the downregulation of AXL target gene and in decreased cell proliferation, almost comparable to miRNA transfected effects. Same results on cell proliferation, were observed in preliminary experiments performed in primary lung cancer cells, obtained from human lung specimens.

I also demonstrated that the conjugate acts in a cell-specific manner. Indeed, I show that both the amounts of intracellular miR-34c and the extent of target downregulation depend on the level of expression of AXL on the cell surface.

Previous studies have showed that miR-34c is also involved in NSCLC migration and invasion, through targeting multiple signaling pathway [Zhou et al. 2015; Liu et al. 2015]. For this reason I performed an *in vitro* migration assay which confirm that the over-expression of miR-34c, even mediated to GL21.T aptamer, inhibited the migration ability of NSCLC cells.

Since the radiation resistance is a common phenomenon in NSCLC patients, it is crucial to identify molecules capable of increasing the radiosensitivity, for a better prognosis of such patients. Because there is already evidence in the literature on the involvement of the miR-34b as radiosensitizers, I studied a possible effect of miR-34c in promoting cancer cell death as a result of radiotherapy [Balça-Silva et al. 2012]. Interestingly, my data illustrated that miR-34c, even in the contest of chimera, is able of increasing the sensitivity of NSCLC to ionizing radiation, even at low exposure doses. This is extremely

important because the dosage diminution, results in an increase of treatment efficiency and in a reduction of side effects.

## **6. CONCLUSIONS**

In conclusion, I observed a direct correlation between miR-34c expression and survival in NSCLC patients, and demonstrated that miR-34c has a powerful oncosuppressive role in this tumor. Moreover, I found AXL receptor as a new target of this miRNA. Taken together, these results may suggest the use of miR-34c as a novel potential therapeutic tool for NSCLC treatment.

More important, I explored the new applications of aptamers in targeted anti-cancer therapies, as means for the selective delivery of miRNAs. Obtained results reveal that GL21.T/miR-34c is a multifunctional molecule.

## 7. ACKNOWLEDGEMENT

First, I would like to express my special thanks to my supervisor Professor Dr. Gerolama Condorelli, for supporting my PhD study and for allowing me to grow as a research scientist. Many thanks for the opportunity of this experience, for your encouragement and assistance during these pleasant three years.

I thank Dr. Vittorio de Franciscis and all his lab members for the continuous suggestions and scientific assistances.

I wish to thank my desk mates, Giusy and Alessandra, and all my lab colleagues, Elvira, Assunta, Ilaria, Fabio, Claudia and Susy, because I gained a lot from all of them, through personal and academic interactions, and their advices.

A special acknowledgement goes to my students, Alessia and Francesco, for all the help given. Thanks to you I grew up and I hope to have provided to your scientific growth, at least a little bit.

Special thank are also given to Dr. Margherita Iaboni, for her scientific guidance and knowledge, and many stimulating discussions. She is my primary resource for answering my scientific (and not) questions and contributed to my research project. But above all, she is a true friend.

I am also grateful to my “companion in adventure”, Raffaella Fontanella, for all the fun we have had in the last three years, for having often worked together, and because she was able to be more anxious than me in many situations.

No acknowledgments would be complete without giving thanks to my family. Words cannot express my grateful to my parents for supporting me throughout my life and for all of the sacrifices that they have made on my behalf, and to my sister for always believing in me and encouraging me to follow my dreams.

Last, but certainly not least, I would like to thank Antonio, who is constantly by my side, in my greatest moments, but even in the worst. Through his love, support and belief in me, he encourages me to achieve always my goals. He is really a treasure for me.

Finally, I would like to thank the Department of Molecular Medicine and Medical Biotechnology. It has provided the support and equipment I have needed to produce and complete my PhD thesis.

## 8. REFERENCES

- Ambros V. The functions of animal microRNAs. *Nature* 2004;431:350-5.
- Bagalkot V, Farokhzad OC, Langer R, Jon S. An aptamer-doxorubicin physical conjugate as a novel targeted drug-delivery platform. *Angew Chem Int Ed Engl* 2006;45:8149-52.
- Balca-Silva J, Sousa Neves S, Goncalves AC et al. Effect of miR-34b overexpression on the radiosensitivity of non-small cell lung cancer cell lines. *Anticancer research* 2012;32:1603-9.
- Bartel DP. MicroRNAs: genomics, biogenesis, mechanism, and function. *Cell* 2004;116:281-97.
- Bates PJ, Laber DA, Miller DM, Thomas SD, Trent JO. Discovery and development of the G-rich oligonucleotide AS1411 as a novel treatment for cancer. *Exp Mol Pathol* 2009;86:151-64.
- Behlke MA. Chemical modification of siRNAs for in vivo use. *Oligonucleotides* 2008;18:305-19.
- Cai KM, Bao XL, Kong XH et al. Hsa-miR-34c suppresses growth and invasion of human laryngeal carcinoma cells via targeting c-Met. *International journal of molecular medicine* 2010;25:565-71.
- Calin GA, Dumitru CD, Shimizu M et al. Frequent deletions and down-regulation of micro- RNA genes miR15 and miR16 at 13q14 in chronic lymphocytic leukemia. *Proceedings of the National Academy of Sciences of the United States of America* 2002;99:15524-9.
- Calin GA, Ferracin M, Cimmino A et al. A MicroRNA signature associated with prognosis and progression in chronic lymphocytic leukemia. *N Engl J Med* 2005;353:1793-801.
- Catuogno S, Rienzo A, Di Vito A, Esposito CL, de Franciscis V. Selective delivery of therapeutic single strand anti-miRs by aptamer-based conjugates. *Journal of controlled release : official journal of the Controlled Release Society* 2015;210:147-59.
- Cerchia L, De Franciscis V. Noncoding RNAs in cancer medicine. *J Biomed Biotechnol* 2006;2006:73104.

Cerchia L, Esposito CL, Camorani S et al. Targeting AXL with an high-affinity inhibitory aptamer. *Molecular therapy : the journal of the American Society of Gene Therapy* 2012;20:2291-303.

Cerchia L, Esposito CL, Jacobs AH, Tavitian B, de Franciscis V. Differential SELEX in human glioma cell lines. *PloS one* 2009;4:e7971.

Chan BA, Hughes BG. Targeted therapy for non-small cell lung cancer: current standards and the promise of the future. *Transl Lung Cancer Res* 2015;4:36-54.

Chen CH, Dellamaggiore KR, Ouellette CP et al. Aptamer-based endocytosis of a lysosomal enzyme. *Proceedings of the National Academy of Sciences of the United States of America* 2008;105:15908-13.

Chu TC, Marks JW, 3rd, Lavery LA et al. Aptamer:toxin conjugates that specifically target prostate tumor cells. *Cancer research* 2006;66:5989-92.

Chu TC, Twu KY, Ellington AD, Levy M. Aptamer mediated siRNA delivery. *Nucleic Acids Res* 2006;34:e73.

Ciafre SA, Galardi S, Mangiola A et al. Extensive modulation of a set of microRNAs in primary glioblastoma. *Biochem Biophys Res Commun* 2005;334:1351-8.

Corney DC, Flesken-Nikitin A, Godwin AK, Wang W, Nikitin AY. MicroRNA-34b and MicroRNA-34c are targets of p53 and cooperate in control of cell proliferation and adhesion-independent growth. *Cancer research* 2007;67:8433-8.

Corney DC, Hwang CI, Matoso A et al. Frequent downregulation of miR-34 family in human ovarian cancers. *Clinical cancer research : an official journal of the American Association for Cancer Research* 2010;16:1119-28.

Costinean S, Zanesi N, Pekarsky Y et al. Pre-B cell proliferation and lymphoblastic leukemia/high-grade lymphoma in E(mu)-miR155 transgenic mice. *Proceedings of the National Academy of Sciences of the United States of America* 2006;103:7024-9.

Dassie JP, Liu XY, Thomas GS et al. Systemic administration of optimized aptamer-siRNA chimeras promotes regression of PSMA-expressing tumors. *Nature biotechnology* 2009;27:839-49.

Dela Cruz CS, Tanoue LT, Matthay RA. Lung cancer: epidemiology, etiology, and prevention. *Clin Chest Med* 2011;32:605-44.

Dhar S, Gu FX, Langer R, Farokhzad OC, Lippard SJ. Targeted delivery of cisplatin to prostate cancer cells by aptamer functionalized Pt(IV) prodrug-PLGA-PEG nanoparticles. *Proceedings of the National Academy of Sciences of the United States of America* 2008;105:17356-61.

Dua P, Kim S, Lee DK. Nucleic acid aptamers targeting cell-surface proteins. *Methods* 2011;54:215-25.

Ellington AD, Szostak JW. In vitro selection of RNA molecules that bind specific ligands. *Nature* 1990;346:818-22.

Esposito CL, Cerchia L, Catuogno S et al. Multifunctional aptamer-miRNA conjugates for targeted cancer therapy. *Molecular therapy : the journal of the American Society of Gene Therapy* 2014;22:1151-63.

Eulberg D, Buchner K, Maasch C, Klussmann S. Development of an automated in vitro selection protocol to obtain RNA-based aptamers: identification of a biostable substance P antagonist. *Nucleic Acids Res* 2005;33:e45.

Farokhzad OC, Cheng J, Teply BA et al. Targeted nanoparticle-aptamer bioconjugates for cancer chemotherapy in vivo. *Proceedings of the National Academy of Sciences of the United States of America* 2006;103:6315-20.

Farokhzad OC, Jon S, Khademhosseini A, Tran TN, Lavan DA, Langer R. Nanoparticle-aptamer bioconjugates: a new approach for targeting prostate cancer cells. *Cancer research* 2004;64:7668-72.

Field RW, Withers BL. Occupational and environmental causes of lung cancer. *Clin Chest Med* 2012;33:681-703.

Gallardo E, Navarro A, Vinolas N et al. miR-34a as a prognostic marker of relapse in surgically resected non-small-cell lung cancer. *Carcinogenesis* 2009;30:1903-9.

Garofalo M, Jeon YJ, Nuovo GJ et al. MiR-34a/c-Dependent PDGFR-alpha/beta Downregulation Inhibits Tumorigenesis and Enhances TRAIL-Induced Apoptosis in Lung Cancer. *PloS one* 2013;8:e67581.

Gee HE, Camps C, Buffa FM et al. MicroRNA-10b and breast cancer metastasis. *Nature* 2008;455:E8-9; author reply E9.

Girvan AC, Teng Y, Casson LK et al. AGRO100 inhibits activation of nuclear factor-kappaB (NF-kappaB) by forming a complex with NF-kappaB essential modulator (NEMO) and nucleolin. *Mol Cancer Ther* 2006;5:1790-9.

Gjerdrum C, Tiron C, Hoiby T et al. AXL is an essential epithelial-to-mesenchymal transition-induced regulator of breast cancer metastasis and patient survival. *Proceedings of the National Academy of Sciences of the United States of America* 2010;107:1124-9.

Gregory RI, Shiekhattar R. MicroRNA biogenesis and cancer. *Cancer research* 2005;65:3509-12.

Griffiths-Jones S. miRBase: the microRNA sequence database. *Methods Mol Biol* 2006;342:129-38.

Guo K, Wendel HP, Scheideler L, Ziemer G, Scheule AM. Aptamer-based capture molecules as a novel coating strategy to promote cell adhesion. *J Cell Mol Med* 2005;9:731-6.

Hagman Z, Haflidadottir BS, Ansari M et al. The tumour suppressor miR-34c targets MET in prostate cancer cells. *British journal of cancer* 2013;109:1271-8.

Hermann T, Patel DJ. Adaptive recognition by nucleic acid aptamers. *Science* 2000;287:820-5.

Hicke BJ, Stephens AW, Gould T et al. Tumor targeting by an aptamer. *J Nucl Med* 2006;47:668-78.

Holland SJ, Pan A, Franci C et al. R428, a selective small molecule inhibitor of AXL kinase, blocks tumor spread and prolongs survival in models of metastatic breast cancer. *Cancer research* 2010;70:1544-54.

Hu Y, Duan J, Zhan Q, Wang F, Lu X, Yang XD. Novel MUC1 aptamer selectively delivers cytotoxic agent to cancer cells in vitro. *PloS one* 2012;7:e31970.

Hutterer M, Knyazev P, Abate A et al. AXL and growth arrest-specific gene 6 are frequently overexpressed in human gliomas and predict poor prognosis in patients with glioblastoma multiforme. *Clinical cancer research : an official journal of the American Association for Cancer Research* 2008;14:130-8.

Iaboni M, Russo V, Fontanella R, Roscigno G, Fiore D, Donnarumma E, Esposito CL, Quintavalle C, Giangrande P, de Franciscis V, Condorelli G. Aptamer-miRNA-212 conjugate sensitizes NSCLC cells to TRAIL. *Molecular Therapy - Nucleic Acids* 2016. (in press)

- Ji Q, Hao X, Zhang M et al. MicroRNA miR-34 inhibits human pancreatic cancer tumor-initiating cells. *PLoS one* 2009;4:e6816.
- Johnson SM, Grosshans H, Shingara J et al. RAS is regulated by the let-7 microRNA family. *Cell* 2005;120:635-47.
- Kasinski AL, Slack FJ. miRNA-34 prevents cancer initiation and progression in a therapeutically resistant K-ras and p53-induced mouse model of lung adenocarcinoma. *Cancer research* 2012;72:5576-87.
- Katz B, Goldbaum M. Macugen (pegaptanib sodium), a novel ocular therapeutic that targets vascular endothelial growth factor (VEGF). *International ophthalmology clinics* 2006;46:141-54.
- Klein R, Conway D, Parada LF, Barbacid M. The trkB tyrosine protein kinase gene codes for a second neurogenic receptor that lacks the catalytic kinase domain. *Cell* 1990;61:647-56.
- Koorstra JB, Karikari CA, Feldmann G et al. The AXL receptor tyrosine kinase confers an adverse prognostic influence in pancreatic cancer and represents a new therapeutic target. *Cancer Biol Ther* 2009;8:618-26.
- Kosaka N, Iguchi H, Ochiya T. Circulating microRNA in body fluid: a new potential biomarker for cancer diagnosis and prognosis. *Cancer Sci* 2010;101:2087-92.
- Landi MT, Zhao Y, Rotunno M et al. MicroRNA expression differentiates histology and predicts survival of lung cancer. *Clinical cancer research : an official journal of the American Association for Cancer Research* 2010;16:430-41.
- Lee RC, Feinbaum RL, Ambros V. The *C. elegans* heterochronic gene *lin-4* encodes small RNAs with antisense complementarity to *lin-14*. *Cell* 1993;75:843-54.
- Lee Y, Jeon K, Lee JT, Kim S, Kim VN. MicroRNA maturation: stepwise processing and subcellular localization. *EMBO J* 2002;21:4663-70.
- Levy-Nissenbaum E, Radovic-Moreno AF, Wang AZ, Langer R, Farokhzad OC. Nanotechnology and aptamers: applications in drug delivery. *Trends Biotechnol* 2008;26:442-9.
- Lin PY, Yu SL, Yang PC. MicroRNA in lung cancer. *British journal of cancer* 2010;103:1144-8.

Liu F, Wang X, Li J et al. miR-34c-3p functions as a tumour suppressor by inhibiting eIF4E expression in non-small cell lung cancer. *Cell proliferation* 2015;48:582-92.

Liu N, Zhou C, Zhao J, Chen Y. Reversal of paclitaxel resistance in epithelial ovarian carcinoma cells by a MUC1 aptamer-let-7i chimera. *Cancer investigation* 2012;30:577-82.

Livak KJ, Schmittgen TD. Analysis of relative gene expression data using real-time quantitative PCR and the 2(-Delta Delta C(T)) Method. *Methods* 2001;25:402-8.

Ma L, Teruya-Feldstein J, Weinberg RA. Tumour invasion and metastasis initiated by microRNA-10b in breast cancer. *Nature* 2007;449:682-8.

Markou A, Sourvinou I, Vorkas PA, Yousef GM, Lianidou E. Clinical evaluation of microRNA expression profiling in non small cell lung cancer. *Lung Cancer* 2013;81:388-96.

McNamara JO, 2nd, Andrechek ER, Wang Y et al. Cell type-specific delivery of siRNAs with aptamer-siRNA chimeras. *Nature biotechnology* 2006;24:1005-15.

Nana-Sinkam SP, Croce CM. Clinical applications for microRNAs in cancer. *Clin Pharmacol Ther* 2013;93:98-104.

Ng EW, Shima DT, Calias P, Cunningham ET, Jr., Guyer DR, Adamis AP. Pegaptanib, a targeted anti-VEGF aptamer for ocular vascular disease. *Nat Rev Drug Discov* 2006;5:123-32.

Pallante P, Visone R, Ferracin M et al. MicroRNA deregulation in human thyroid papillary carcinomas. *Endocr Relat Cancer* 2006;13:497-508.

Pasquinelli AE, Reinhart BJ, Slack F et al. Conservation of the sequence and temporal expression of let-7 heterochronic regulatory RNA. *Nature* 2000;408:86-9.

Patil SD, Rhodes DG, Burgess DJ. DNA-based therapeutics and DNA delivery systems: a comprehensive review. *AAPS J* 2005;7:E61-77.

Pestourie C, Tavitian B, Duconge F. Aptamers against extracellular targets for in vivo applications. *Biochimie* 2005;87:921-30.

Rikova K, Guo A, Zeng Q et al. Global survey of phosphotyrosine signaling identifies oncogenic kinases in lung cancer. *Cell* 2007;131:1190-203.

Rusconi CP, Scardino E, Layzer J et al. RNA aptamers as reversible antagonists of coagulation factor IXa. *Nature* 2002;419:90-4.

Sainaghi PP, Castello L, Bergamasco L, Galletti M, Bellosta P, Avanzi GC. Gas6 induces proliferation in prostate carcinoma cell lines expressing the AXL receptor. *J Cell Physiol* 2005;204:36-44.

Schuchert MJ, Luketich JD. Solitary sites of metastatic disease in non-small cell lung cancer. *Curr Treat Options Oncol* 2003;4:65-79.

Shieh YS, Lai CY, Kao YR et al. Expression of AXL in lung adenocarcinoma and correlation with tumor progression. *Neoplasia* 2005;7:1058-64.

Shilnikova NS, Preston DL, Ron E et al. Cancer mortality risk among workers at the Mayak nuclear complex. *Radiat Res* 2003;159:787-98.

Siegel RL, Sahar L, Portier KM, Ward EM, Jemal A. Cancer death rates in US congressional districts. *CA Cancer J Clin* 2015;65:339-44.

Soontornworajit B, Wang Y. Nucleic acid aptamers for clinical diagnosis: cell detection and molecular imaging. *Anal Bioanal Chem* 2011;399:1591-9.

Soundararajan S, Chen W, Spicer EK, Courtenay-Luck N, Fernandes DJ. The nucleolin targeting aptamer AS1411 destabilizes Bcl-2 messenger RNA in human breast cancer cells. *Cancer research* 2008;68:2358-65.

Stitt TN, Conn G, Gore M et al. The anticoagulation factor protein S and its relative, Gas6, are ligands for the Tyro 3/AXL family of receptor tyrosine kinases. *Cell* 1995;80:661-70.

Takamizawa J, Konishi H, Yanagisawa K et al. Reduced expression of the let-7 microRNAs in human lung cancers in association with shortened postoperative survival. *Cancer research* 2004;64:3753-6.

Tavazoie SF, Alarcon C, Oskarsson T et al. Endogenous human microRNAs that suppress breast cancer metastasis. *Nature* 2008;451:147-52.

Thomson S, Petti F, Sujka-Kwok I et al. A systems view of epithelial-mesenchymal transition signaling states. *Clinical & experimental metastasis* 2011;28:137-55.

Tong GJ, Hsiao SC, Carrico ZM, Francis MB. Viral capsid DNA aptamer conjugates as multivalent cell-targeting vehicles. *J Am Chem Soc* 2009;131:11174-8.

- Travis WD. Classification of lung cancer. *Semin Roentgenol* 2011;46:178-86.
- Travis WD, Brambilla E, Nicholson AG et al. The 2015 World Health Organization Classification of Lung Tumors: Impact of Genetic, Clinical and Radiologic Advances Since the 2004 Classification. *J Thorac Oncol* 2015;10:1243-60.
- Vosa U, Vooder T, Kolde R, Vilo J, Metspalu A, Annilo T. Meta-analysis of microRNA expression in lung cancer. *International journal of cancer* 2013;132:2884-93.
- Wan Y, Kim YT, Li N et al. Surface-immobilized aptamers for cancer cell isolation and microscopic cytology. *Cancer research* 2010;70:9371-80.
- Weber F, Teresi RE, Broelsch CE, Frilling A, Eng C. A limited set of human MicroRNA is deregulated in follicular thyroid carcinoma. *J Clin Endocrinol Metab* 2006;91:3584-91.
- Willis MC, Collins BD, Zhang T et al. Liposome-anchored vascular endothelial growth factor aptamers. *Bioconjug Chem* 1998;9:573-82.
- Wu CW, Li AF, Chi CW et al. Clinical significance of AXL kinase family in gastric cancer. *Anticancer research* 2002;22:1071-8.
- Wu X, Ding B, Gao J et al. Second-generation aptamer-conjugated PSMA-targeted delivery system for prostate cancer therapy. *Int J Nanomedicine* 2011;6:1747-56.
- Wu Y, Crawford M, Yu B, Mao Y, Nana-Sinkam SP, Lee LJ. MicroRNA delivery by cationic lipoplexes for lung cancer therapy. *Molecular pharmaceutics* 2011;8:1381-9.
- Wullner U, Neef I, Eller A, Kleines M, Tur MK, Barth S. Cell-specific induction of apoptosis by rationally designed bivalent aptamer-siRNA transcripts silencing eukaryotic elongation factor 2. *Curr Cancer Drug Targets* 2008;8:554-65.
- Xiao Z, Shanguan D, Cao Z, Fang X, Tan W. Cell-specific internalization study of an aptamer from whole cell selection. *Chemistry* 2008;14:1769-75.
- Yu SL, Chen HY, Chang GC et al. MicroRNA signature predicts survival and relapse in lung cancer. *Cancer cell* 2008;13:48-57.

Zhang B, Pan X, Cobb GP, Anderson TA. microRNAs as oncogenes and tumor suppressors. *Dev Biol* 2007;302:1-12.

Zhang YX, Knyazev PG, Cheburkin YV et al. AXL is a potential target for therapeutic intervention in breast cancer progression. *Cancer research* 2008;68:1905-15.

Zhang Z, Lee JC, Lin L et al. Activation of the AXL kinase causes resistance to EGFR-targeted therapy in lung cancer. *Nature genetics* 2012;44:852-60.

Zhou J, Rossi JJ. Aptamer-targeted cell-specific RNA interference. *Silence* 2010;1:4.

Zhou J, Satheesan S, Li H et al. Cell-specific RNA aptamer against human CCR5 specifically targets HIV-1 susceptible cells and inhibits HIV-1 infectivity. *Chem Biol* 2015;22:379-90.

Zhou YL, Xu YJ, Qiao CW. MiR-34c-3p suppresses the proliferation and invasion of non-small cell lung cancer (NSCLC) by inhibiting PAC1/MAPK pathway. *International journal of clinical and experimental pathology* 2015;8:6312-22.

## MiR-221 promotes stemness of breast cancer cells by targeting DNMT3b

Giuseppina Roscigno<sup>1,2</sup>, Cristina Quintavalle<sup>1,2</sup>, Elvira Donnarumma<sup>3</sup>, Iliaria Puoti<sup>1</sup>, Angel Diaz-Lagares<sup>4</sup>, Margherita Iaboni<sup>1</sup>, Danilo Fiore<sup>1</sup>, Valentina Russo<sup>1</sup>, Matilde Todaro<sup>5</sup>, Giulia Romano<sup>6</sup>, Renato Thomas<sup>7</sup>, Giuseppina Cortino<sup>7</sup>, Miriam Gaggianesi<sup>5</sup>, Manel Esteller<sup>4</sup>, Carlo M. Croce<sup>6</sup>, Gerolama Condorelli<sup>1,2</sup>

<sup>1</sup>Department of Molecular Medicine and Medical Biotechnology, "Federico II" University of Naples, Naples, Italy

<sup>2</sup>IEOS-CNR, Naples, Italy

<sup>3</sup>IRCCS-SDN, Naples, Italy

<sup>4</sup>Epigenetic and Cancer Biology Program (PEBC) IDIBELL, Hospital Duran I Reynals, Barcelona, Spain

<sup>5</sup>Department of Surgical and Oncological Sciences, Cellular and Molecular Pathophysiology Laboratory, University of Palermo, Palermo, Italy

<sup>6</sup>Department of Molecular Virology, Immunology and Medical Genetics, Human Cancer Genetics Program, Comprehensive Cancer Center, The Ohio State University, Columbus, OH, USA

<sup>7</sup>Department of Surgical and Oncology, Clinica Mediterranea, Naples, Italy

### Correspondence to:

Gerolama Condorelli, e-mail: gecondor@unina.it

**Keywords:** microRNAs, breast cancer, cancer stem cells, DNMT

**Received:** June 15, 2015

**Accepted:** October 09, 2015

**Published:** October 19, 2015

### ABSTRACT

**Cancer stem cells (CSCs) are a small part of the heterogeneous tumor cell population possessing self-renewal and multilineage differentiation potential as well as a great ability to sustain tumorigenesis. The molecular pathways underlying CSC phenotype are not yet well characterized. MicroRNAs (miRs) are small noncoding RNAs that play a powerful role in biological processes. Early studies have linked miRs to the control of self-renewal and differentiation in normal and cancer stem cells. We aimed to study the functional role of miRs in human breast cancer stem cells (BCSCs), also named mammospheres. We found that miR-221 was upregulated in BCSCs compared to their differentiated counterpart. Similarly, mammospheres from T47D cells had an increased level of miR-221 compared to differentiated cells. Transfection of miR-221 in T47D cells increased the number of mammospheres and the expression of stem cell markers. Among miR-221's targets, we identified DNMT3b. Furthermore, in BCSCs we found that DNMT3b repressed the expression of various stemness genes, such as *Nanog* and *Oct 3/4*, acting on the methylation of their promoters, partially reverting the effect of miR-221 on stemness. We hypothesize that miR-221 contributes to breast cancer tumorigenicity by regulating stemness, at least in part through the control of DNMT3b expression.**

### INTRODUCTION

Over the last years, evidence has accumulated on a small subclass of cancer cells with tumorigenic potential and stemness properties [1]. These so-called cancer stem cells (CSCs) have been isolated from a variety of tumor types, including those of the breast [2]. CSCs have two important characteristics: self-renewal and multipotency. These properties make CSCs able to generate new CSCs

and simultaneously to produce differentiated mature cells responsible for the cellular heterogeneity of the tumor. CSCs are now considered the driving force of the tumor. In fact, they are the only cells able to regenerate a new tumor when xenografted in to mice, even when only very few cells are injected [2]. Furthermore, CSCs are resistant to conventional chemotherapy and are considered responsible for tumor recurrence [3]. Breast cancer stem cells (BCSCs) are characterized by high CD44 and low CD24 expression,

and can be identified as cells able to grow in suspension as spherical structures called mammospheres. Mammospheres derived from tissue specimens survive in non-adherent conditions and differentiate along different mammary epithelial lineages [4]. Within a tumor, CSC enrichment correlates with the grade of the tumor [5].

MicroRNAs (miRs) belong to the non-coding RNA family. They have a size ranging from 20 to 25 nucleotides, and function as endogenous regulators of gene expression. MiRs impair mRNA translation or negatively regulate mRNA stability by recognizing complementary target sites in their 3' untranslated region (UTR). MiRs are involved in the regulation of many physiological processes, including development, proliferation, and apoptosis, as well as of pathological processes such as cancerogenesis. In breast cancer, miR-21, -155, -96, and -182 have been identified as oncogenes [6–9], whereas miR-125, -205, and -206 have been identified as tumor suppressors [10–12]. MiRs play an essential role also in self-renewal of CSCs. For instance, miR-100 inhibited the maintenance and expansion of CSCs in basal-like breast cancer, and its ectopic expression enhanced BCSC differentiation, controlling the balance between self-renewal and differentiation [13].

In the present study, we investigated whether other miRs are involved in the regulation of stemness in breast cancer. To this end, we isolated BCSCs from patients and analyzed their miR expression profile. We found that miR-221 was significantly up-regulated in BCSCs and was involved in stemness phenotyping through post-transcriptional regulation of DNMT3b, a methyltransferase involved in epigenetic regulation of gene expression.

## RESULTS

### MiRs involved in stemness

To identify miRs differentially expressed in BCSCs and involved in stemness maintenance, we performed a microarray analysis. The array was performed analyzing the miR expression profile of BCSCs, collected from three patients, compared to that of breast cancer cells growing in adherence (differentiated cells). BCSCs obtained by biopsy digestion were characterized by real time PCR for the expression of the stem cells markers *Nanog* and *Sox2* (Figure 1A) and by their ability to give rise tumors when injected into the flank of nude mice at low number (Supplementary Table S1). The microarray analysis revealed that there was a significant upregulation of miR-221, miR-24, and miR-29a in BCSCs and a down-regulation of miR-216a, miR-25, and let-7d compared to differentiated cells (Table 1). We focused our attention on miR-221, since its role in tumorigenesis has already been reported in several tumor types [14–16]. Microarray results for miR-221 were validated by real time PCR on the same samples and in one additional patient (patient #4) (Figure 1B).

### T47D mammospheres are enriched in stem progenitors and expresses high levels of miR-221

We then studied *in vitro* enrichment and propagation of mammary stem cells with the T47D breast cancer cell line.  $1 \times 10^4$  T47D cells were grown in DMEM-F12 supplemented with EGF, b-FGF, and B27. After 7 days of culture, we evaluated the stemness markers through real-time PCR and Western blot analysis, and the differentiation markers only through Western blot analysis. The stemness markers *Nanog*, *Oct 3/4*, *Slug*, and *Zeb 1* were found upregulated in the suspension cultures, whereas the differentiation markers *E-Cadherin*, *cytokeratin 18*, and *cytokeratin 8* were upregulated in adherence cultures (Figure 1C and 1D). Moreover, miR-221 expression was increased in T47D mammospheres compared to differentiated cells (Figure 1E), highlighting the correlation of this miR with the stem cell state. Similar results were obtained in additional breast cancer cell lines (MCF-7, MDA-MB-231, and BT-549) (Supplementary Figure S1).

### MiR-221 and stemness phenotype

To analyze the biological role of miR-221 for the stem cell phenotype, we overexpressed miR-221 in differentiated T47D cells and analyzed different stem cells markers. In order to obtain mammospheres, the cells were kept in stem medium for 6 days. We found that, compared to control, miR-221 overexpression induced a significant increase in the number of mammospheres (Figure 2A) and expression of stem cells markers *Nanog*, *Oct 3/4*, and  $\beta$ -Catenin (Figure 2B, 2C). Expression of anti-miR-221 induced an opposite effect (Figure 2D, 2E, 2F). Similar results were obtained in the MCF-7 cell line (Supplementary Figure S2). To further investigate the effect of miR-221 on stem cell properties, we transduced T47D cells with a lentiviral construct encoding miR-221. These stably overexpressing miR-221 cells showed enrichment of the CD44<sup>+</sup>/CD24<sup>-</sup> population thanks to an increase of CD44 (17% versus 43.7%) and to a decrease of CD24 (62.5% versus 33.8%), as assessed by FACS analysis (Figure 3A). The stable expression of miR-221 in T47D cells induced also an increase in mammosphere number. This ability was enhanced after the first and second replanting, suggesting an expansion of the stem cell compartment (Figure 3B). The increase in sphere number and the upregulation of stemness markers upon miR-221 overexpression indicated an expansion of the stemness pool. In the same manner, the stable expression of miR-221, assessed by qRT-PCR in a breast primary cell line (patient #5), was able to increase sphere formation capacity and *Nanog* expression also in a primary context (Supplementary Figure S3A, S3B, S3C).

To further verify this phenotype, we assessed the shift from asymmetric to symmetric cell division with PKH26 staining. Fast and symmetrically dividing

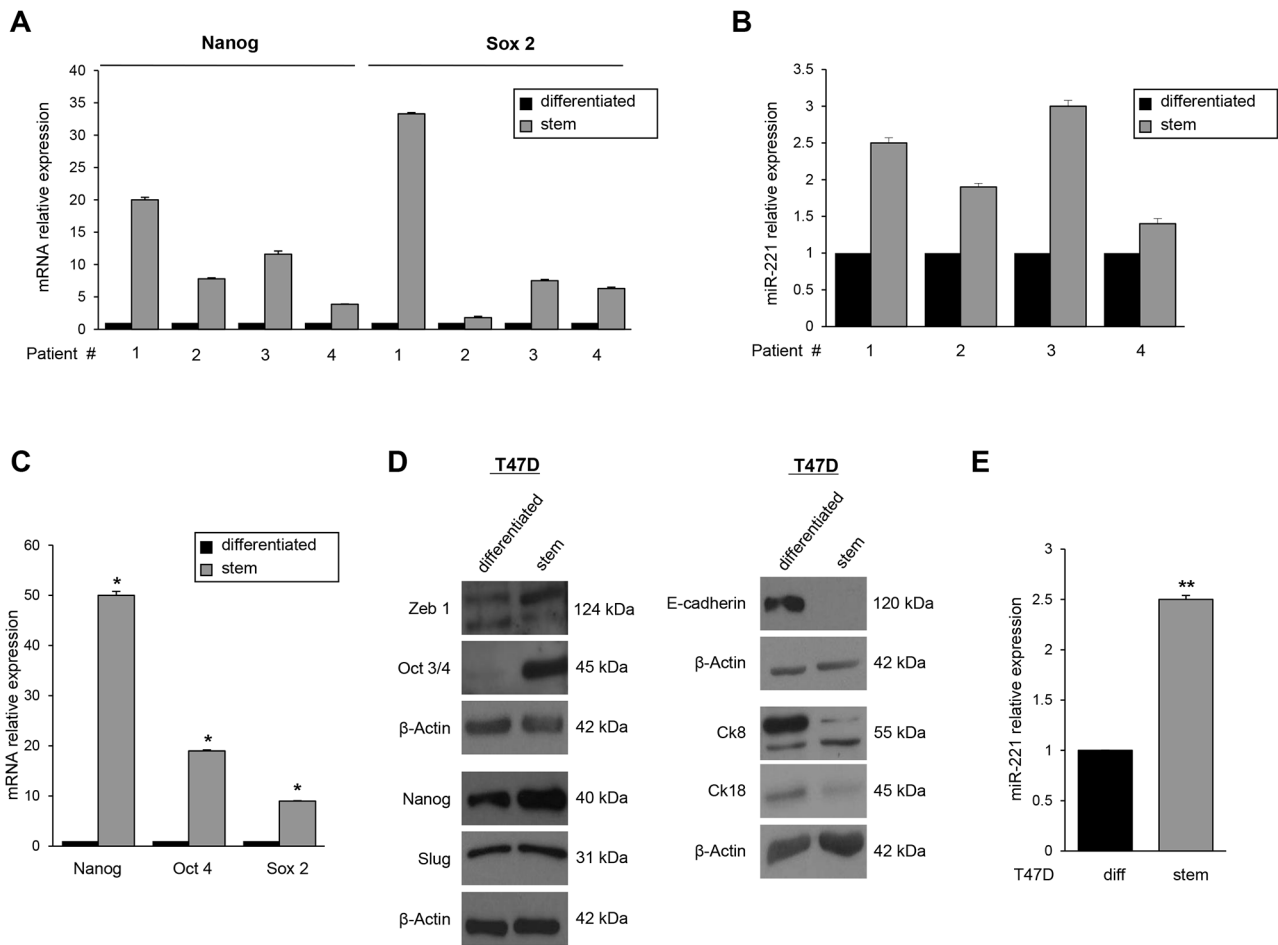


**Figure 1: MiR-221 expression in BCSCs and in T47D cell mammospheres.** A. qRT-PCR validated the increase of stem markers *Nanog* and *Sox 2* and B. of miR-221 in BCSCs. C, D. *Nanog*, *Oct 3/4*, *Sox 2*, *Zeb 1*, cytokeratin (Ck) 8 and cytokeratin (Ck) 18 were analyzed by qRT-PCR and Western blot and were found up-regulated in T47D stem cells compared to the differentiated counterpart. E. qRT-PCR revealed the upregulation of miR-221 in T47D mammospheres with respect to differentiated T47D cells. In C and E, data are mean values  $\pm$  SD of three independent experiments. Significance was calculated using Student's *t*-test. \*,  $p < 0.05$ ; \*\*,  $p < 0.01$ . Western blots are from representative experiments.

**Table 1: MiR expression in breast cancer stem cells**

Unique ID	Parametric <i>p</i> -value	Fold Change (stem vs diff)
hsa- miR-221	0.013	1.8
hsa-miR-24	0.003	2.4
hsa-miR-29a	0.012	1.4
hsa-miR-216a	0.004	2.5
hsa-miR-25	0.042	2.2
let-7d	0.034	1.3

Up- and down-regulation of miRs in breast cancer stem cells vs differentiated cells. miR screening was performed in triplicate. A two-tailed, two sample *t*-test was used ( $p < 0.05$ ). Four miRs were found significantly upregulated in breast cancer stem cells, and three were found downregulated.

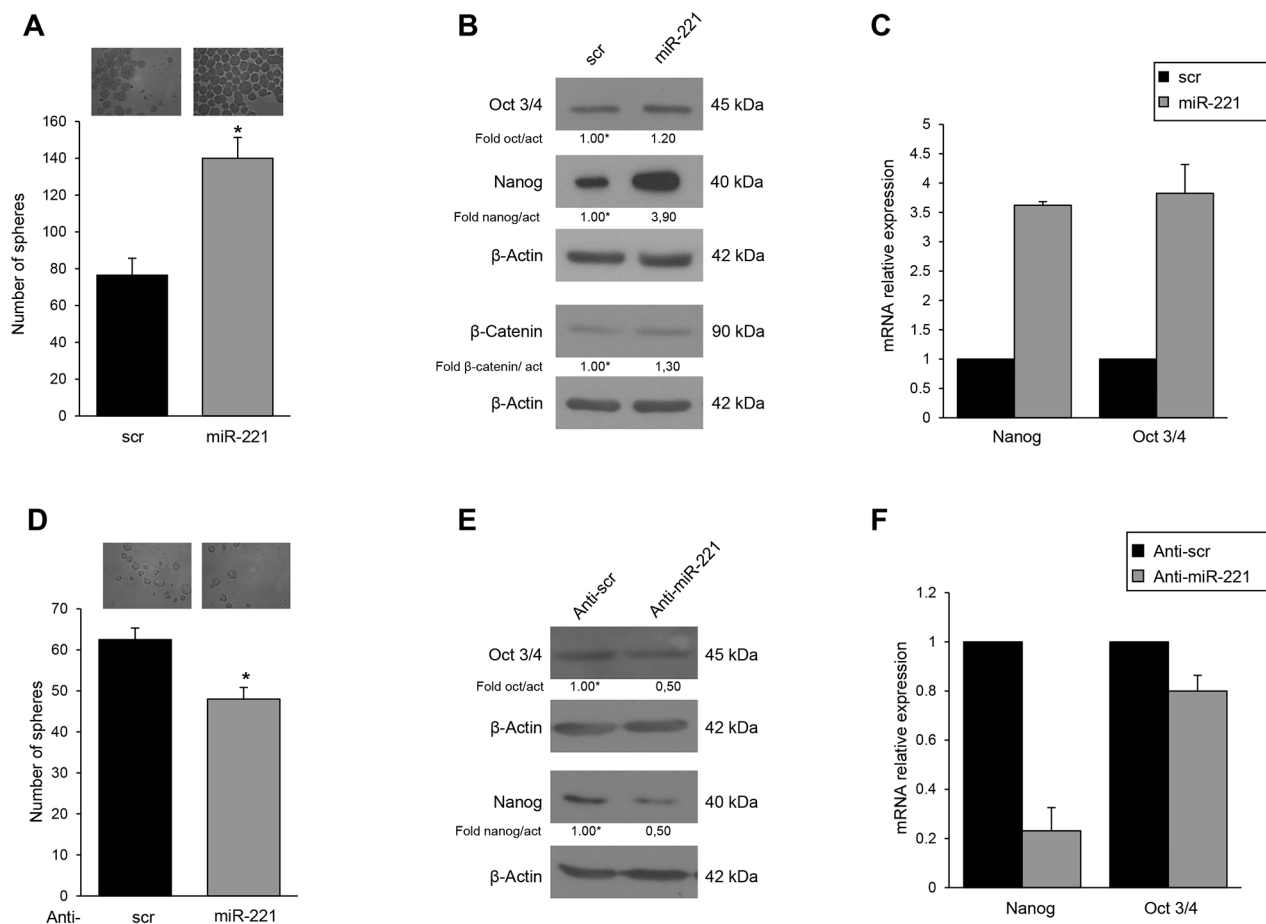


**Figure 2: MiR-221 effects on mammospheres and stemness genes expression.** **A.** T47D cells were transfected with a pre-miR, and mammospheres counted after 6 days. miR-221 induced an increase in the number of mammospheres ( $140 \pm \text{SD}$  versus  $76 \pm \text{SD}$ ). **B.** **C.** Western blot and qRT-PCR showing that pre-miR-221 transfected in T47D cells upregulates stem cell marker expression. Anti-miR-221 transfection induced a reduction of mammospheres ( $48 \pm \text{SD}$  versus  $60 \pm \text{SD}$ ) **D.** and of stem cell markers **E.**, **F.** Western blots are representative experiments. Data are mean values  $\pm$  SD of three independent experiments. In **A**, **D**, significance was calculated using Student's *t*-test. \*,  $p < 0.05$ .

CSCs tend to rapidly lose PKH26, which then results equally distributed among the daughter cells during each cell division [5, 17]. Mammospheres from T47D cells stably transduced with a Tween control or with miR-221 were labeled with PKH26 and then analyzed by fluorescence microscopy and FACS after 7 days. As shown in Figure 3C, miR-221 overexpression induced a strong decrease of PKH26 (8.6% in Tween cells versus 1.5% in miR-221 cells), suggesting that miR-221 led to an expansion in stem cell number through symmetric division. Asymmetric division was evaluated by the distribution of the cell fate determinant Numb, known to be highly present upon differentiation, and of p53, whose expression is lost in stem cells [17, 18]. Western blotting revealed lower protein expression of both markers in miR-221-overexpressing cells with respect to the Tween control (Figure 3D).

Stemness gene expression is mainly regulated by DNA methylation [19]. For this reason, we decided to evaluate the effect of miR-221 expression on DNA methylation levels of *Nanog* and *Oct3/4* promoters and consequently the regulation of their expression profile. We assessed CpG dinucleotides, which are known to be methylated during differentiation [20, 21]. The 2 CpGs analyzed of *Nanog* promoter region were -83, -36 from to the Transcription Start Site (TSS); whereas the 3 CpGs analyzed of *Oct 3/4* promoter region were +319, +346, +358 from the TSS. Through pyrosequencing analysis, we found that methylation levels at CpGs analyzed on *Nanog* and *Oct 3/4* promoters were significant decreased (17% and 8% respectively) in cells transfected with miR-221 compared to the scrambled control (Figure 3E). Similar results were obtained in additional CpGs analyzed of both promoter regions (10% for CpG at -302, -300, -296 from TSS of *Nanog* and 10% for CpG + 250, +253, +277 of *Oct 3/4*.) (Supplementary Figure S4A).

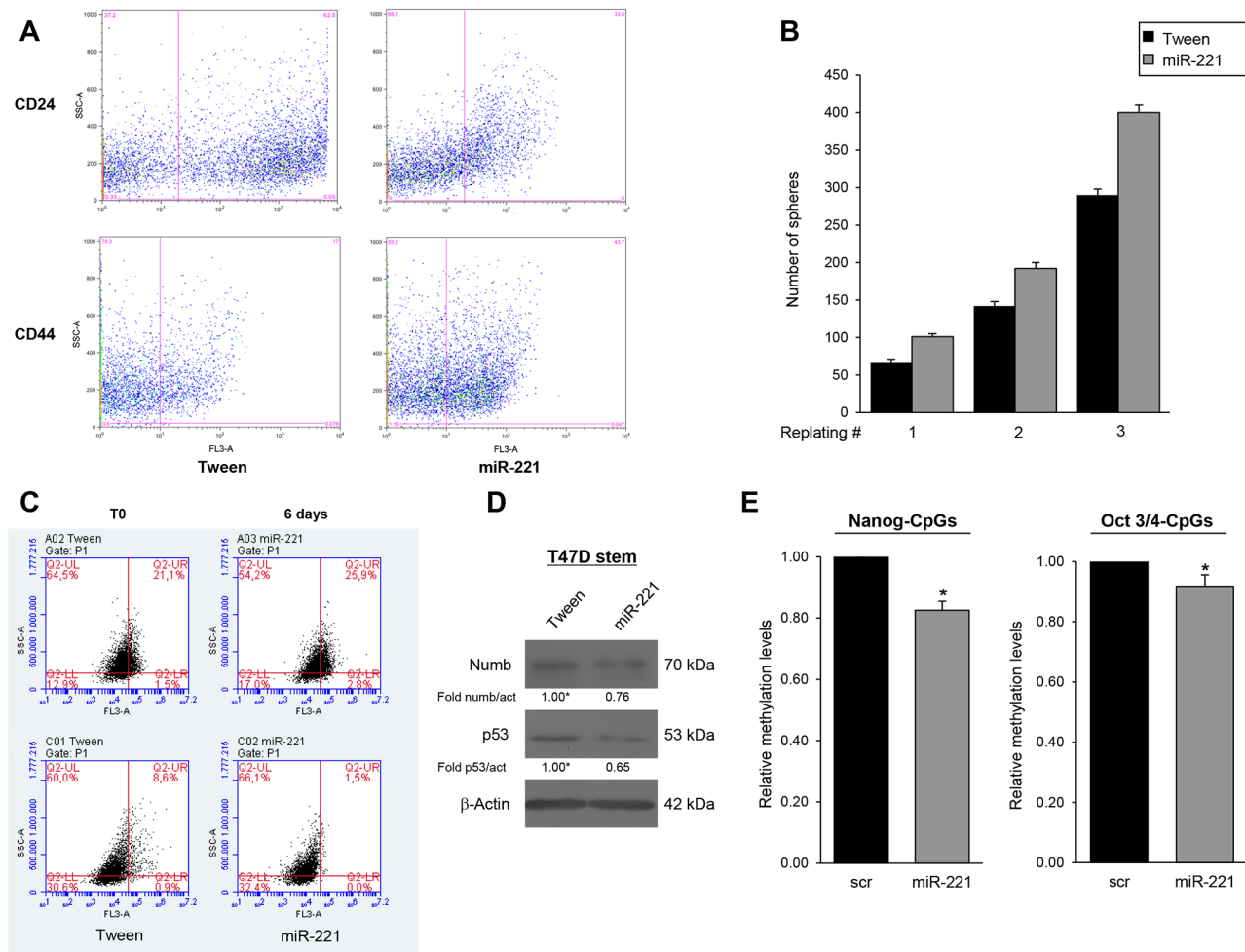


**Figure 3: MiR-221 overexpression regulates stemness properties in BCSCs.** **A.** FACS analysis of CD24/CD44 expression in T47D cells infected with miR-221 lentivirus and control Tween virus (Tw). MiR-221 stable expression induced an increase of CD44 (17% versus 43.7%) and a decrease of CD24 (62.5% versus 33.8%). **B.** Effect of lentivirally mediated overexpression of miR-221 on mammosphere number at the first plating and after dissociation and replating. The data represent the mean value  $\pm$  SD of two independent experiments. **C.** T47D mammospheres stably infected with the empty vector or miR-221 were evaluated by FACS for PKH26 staining. miR-221 infection induced a decrease of PKH26 in cells (8.6% versus 1.5%). The staining of the two populations was verified at day 0 or after 6 days, as indicated in C. **D.** Asymmetric division was evaluated by Western blotting for Numb and p53. Western blots is representative experiment. **E.** Analysis of methylation change of two consecutive CpGs of *Nanog* and 3 CpGs of *Oct 3/4* promoters (17% and 8% respectively). Methylation values: mean of consecutive CpGs. Significance was calculated using *U*-Mann Whitney test. \*,  $p < 0.05$ .

### MiR-221 specifically represses DNMT3b expression

Thereafter, we investigated miR-221 targets possibly involved in stemness. Among the potential targets predicted by bioinformatics (RNA hybrid- <http://www.microRNA.org/>, Miranda- <http://www.microRNA.org/>), we focus our attention on *DNMT3b*, which encodes a DNA methyltransferase involved in de novo DNA methylation [22–24]. To examine whether miR-221 interfered with DNMT3b expression by directly targeting the predicted 3'UTR region, we cloned this region downstream of a luciferase reporter gene in the pGL3 vector. HEK-293 cells are an easy model to use for the luciferase assay thanks to their transfection efficiency. HEK-293 cells were

transfected with the reporter plasmid in the presence of a negative control miR (scrambled miR) or miR-221. As shown in Figure 4A, DNMT3b 3'UTR luciferase reporter activity was significantly repressed by the addition of miR-221 compared to the scrambled sequence. This luciferase activity was not affected by miR-221 overexpression in the presence of a mutant construct in which the seed sequence was cloned inversely (Figure 4A). In order to find a causative effect between miR-221 and DNMT3b expression, we transfected T47D cells with a pre-miR-221 for 48 h and then analyzed DNMT3b levels by Western blot and qRT-PCR. We found that DNMT3b protein and mRNA levels were downregulated after miR-221 overexpression (Figure 4B). Similar results were obtained when we transfected miR-222, which shares a similar seed

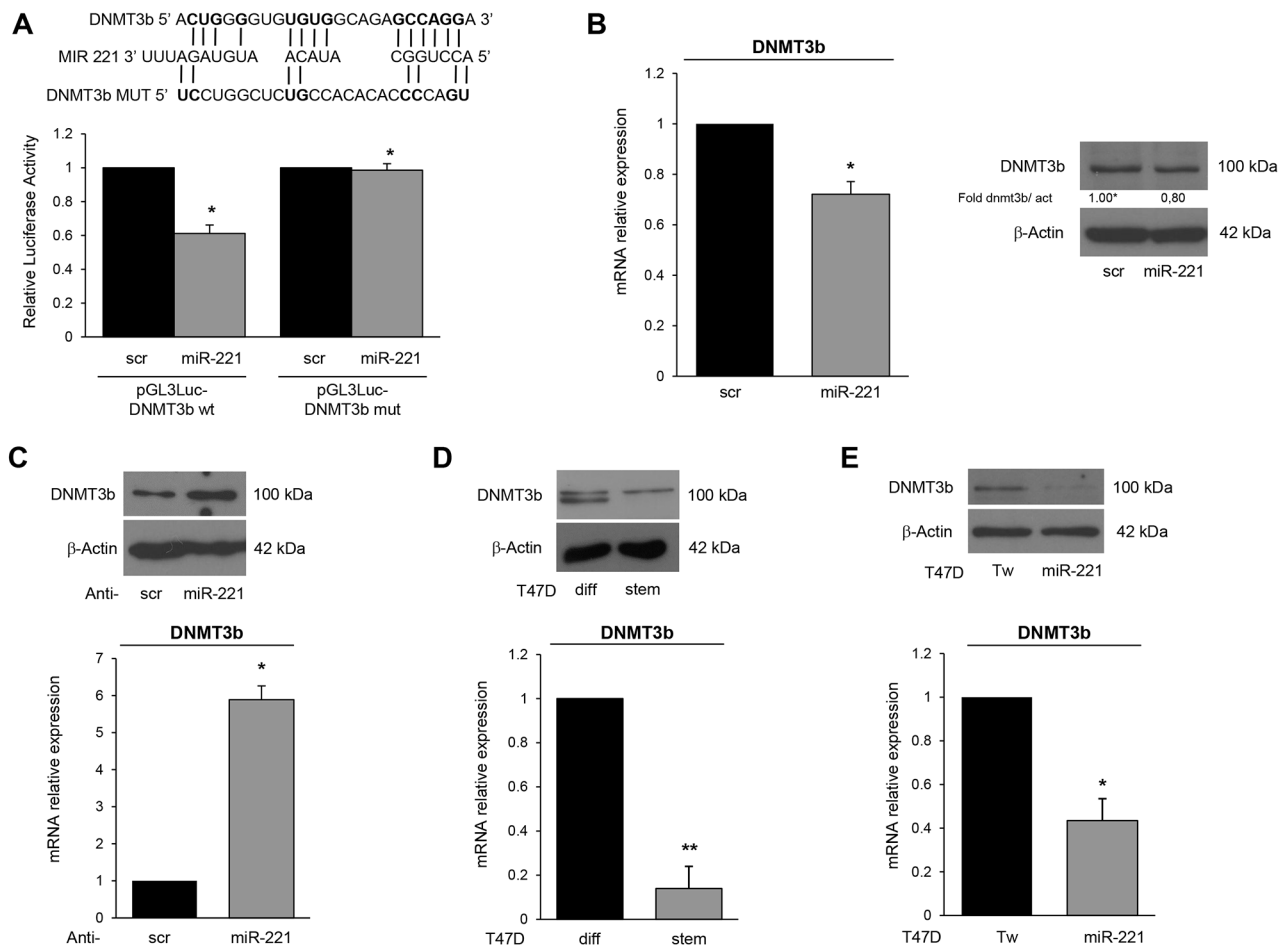


**Figure 4: DNMT3b is a direct target of miR-221.** **A.** Predicted alignment between the miR-221 sequence and the 3'UTR of *DNMT3b*. Luciferase assay showed that reporter activity was inhibited in T47D cells only in the presence of wild type *DNMT3b* and not with a mutated 3'UTR. The data represent the results of two independent experiments. **B.** MiR-221 transfection downregulated DNMT3b mRNA and protein levels, as assessed by qRT-PCR and Western blotting. **C.** Anti-miR-221 transfection upregulated the levels of DNMT3b. **D.** DNMT3b mRNA and protein were downregulated in T47D stem cells compared to differentiated cells. **E.** DNMT3b mRNA and protein were downregulated in T47D cells stably infected with a miR-221 lentivirus. In B, C, D, E data are mean values  $\pm$  SD from three independent experiments. Significance was calculated using Student's *t*-test. \*,  $p < 0.05$ ; \*\*,  $p < 0.01$ . Western blot analyses are from representative experiments.

sequence with miR-221 (Supplementary Figure S5). In contrast, anti-miR-221 induced an increase of DNMT3b levels (Figure 4C). Then, we verified DNMT3b expression in stem and differentiated T47D cells. As shown in Figure 4D, DNMT3b expression was lower in stem cells and inversely correlated with miR-221 levels. Furthermore, DNMT3b expression was reduced in T47D cells transfected with miR-221 lentiviral vectors (Figure 4E). We also observed a reduction of DNMT3b levels by qRT-PCR and immunofluorescence in stem cells compared to differentiated primary cells (Figure 5A, 5C), as well as in MCF7 cells and MDA-MB-231 cells (Figure 5B).

### miR-221 controls stemness by inhibiting DNMT3b expression

DNMT3b is a master regulator of Nanog and Oct 3/4 expression and, through its methylation activity, represses

their expression during embryogenesis [25]. Therefore, we wondered whether the stemness features observed upon expression of miR-221 were related to DNMT3b downregulation and, consequently, to a reduced methylation activity. We transfected T47D cells with a DNMT3b cDNA and investigated the effect on stem marker expression and mammosphere formation. As shown in Figure 6A–6B DNMT3b inhibited mammosphere formation (63 versus 80) and Nanog, and Oct 3/4 expression. In contrast, treatment with a specific si-DNMT3b-mRNA induced an increase in mammosphere number (Figure 6D) and upregulated Nanog and Oct 3/4 protein levels (Figure 6E). Furthermore, to establish a causal link between miR-221-mediated DNMT3b downregulation and stem cell phenotype, we performed a rescue experiment by transfecting T47D cells simultaneously with pre-miR-221 and a DNMT3b cDNA lacking the 3'UTR. We found that the effect of miR-221 on Nanog and Oct 3/4 expression was abolished by DNMT3b cDNA overexpression

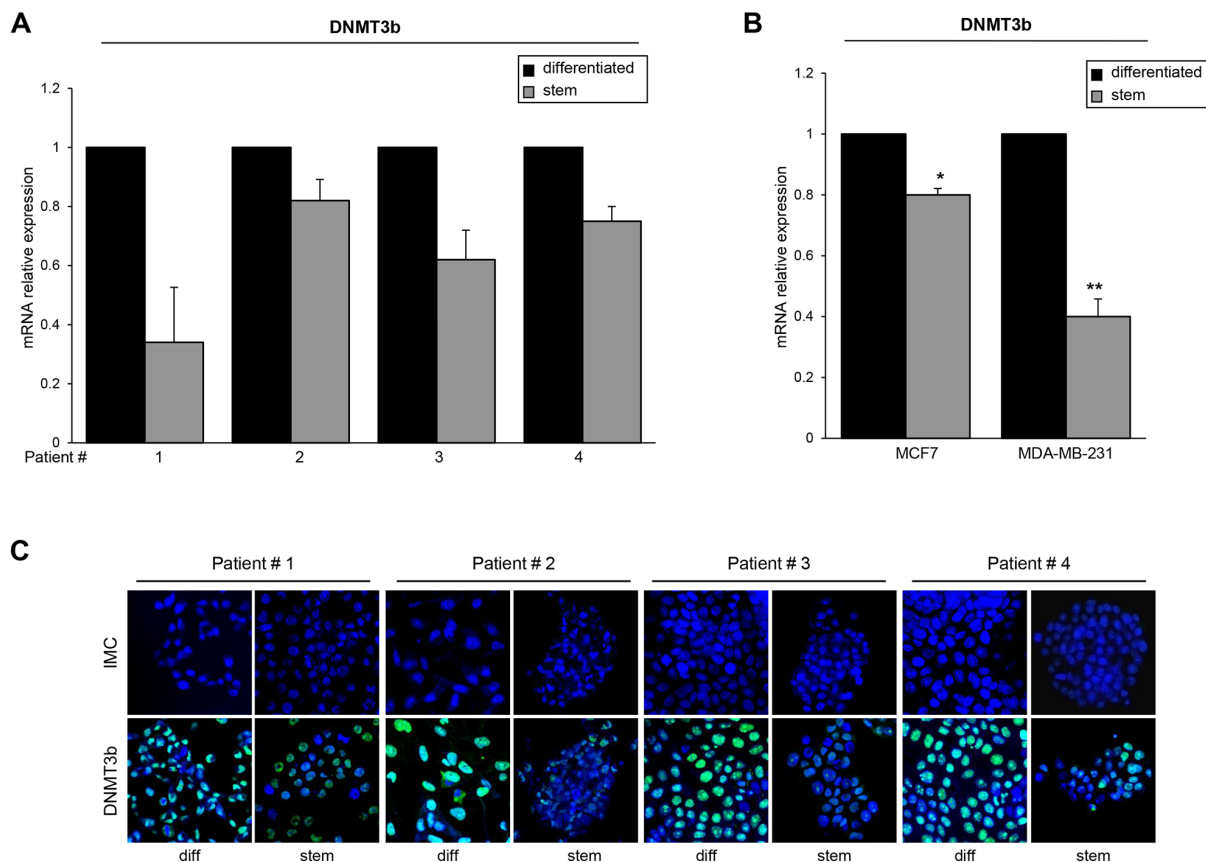


**Figure 5: DNMT3b expression in stem and differentiated breast cancer cells.** A. DNMT3b levels were analyzed by qRT-PCR in stem and differentiated breast cancer primary cells or B. in MCF7 cells and MDA-231 cells. C. Immunofluorescence analysis of DNMT3b expression in stem and differentiated breast cancer primary cells from 4 patients. In B, data are mean values  $\pm$  SD from three independent experiments. Significance was calculated using Student's *t*-test. \*,  $p < 0.05$ ; \*\*,  $p < 0.01$ .

(Figure 6B). Its effect on the number of mammospheres (114 versus 93) (Figure 6A) and on growth in soft agar was also partially reverted (Figure 6C). To further assess the role of DNMT3b, we evaluated mammosphere number in T47D cells stably transfected with a shRNA targeting DNMT3b. The expression of a DNMT3b short hairpin increased the number of mammospheres in DNMT3b-silenced T47D cells, an effect enhanced after the first replating (Figure 6F).

We then hypothesized that DNMT3b affects the methylation pattern of *Nanog* and *Oct 3/4* promoter regions, influencing their expression. Pyrosequencing analysis revealed that cells transfected with a DNMT3b siRNA showed a significant decrease (23% and 11%, respectively) in methylation levels at CpGs analyzed on *Nanog* and *Oct 3/4* promoters compared to the scrambled control cells (Figure 6G). Similar results were obtained in additional CpGs analyzed of both promoter regions (20% and 5% respectively) (Supplementary Figure S4B).

## DISCUSSION

Breast cancer is the leading cause of death in woman and is characterized by an elevated heterogeneity, different

responses to therapy, and metastatic variability among patients [26]. It represents the first human carcinoma for which a putative cancer stem cell subpopulation has been isolated on the basis of its  $CD44^+/CD24^-/low$  antigenic phenotype [2]. However, little is known on the mechanisms regulating the ability of BCSCs for self-renewal and to initiate tumors.

Recently, miRs have been found to be critical regulators of several cellular events [27]. By their ability to target hundreds of mRNAs, they can induce a rapid switch in cell fate and a fine exchange in genome expression; they are now accepted as major post-transcriptional regulators. The importance of miRs in gene expression regulation is emphasized by the finding that they are often deregulated in cancer [28]. MiRs may affect cancer development, progression, and response to therapy. Interestingly, some miRs have been reported to regulate CSC phenotype, since their modulation has been shown to contribute to the maintenance or triggering of the phenotype in different cancer models. For instance, it was found that miR-22 induces an expansion of the breast CSC compartment and induces metastasis by downregulating a member of the TET family [29]. Different members of the

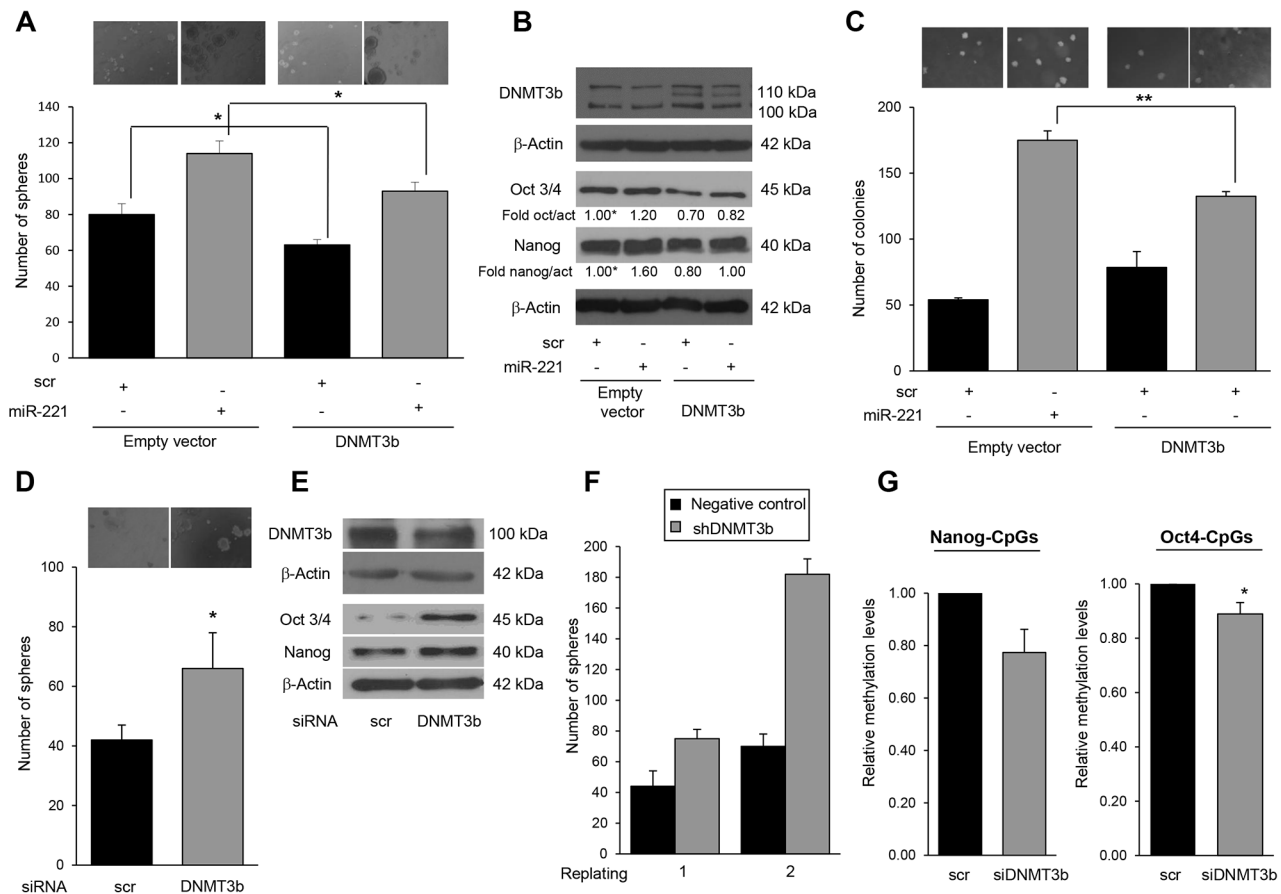


**Figure 6: MiR-221 regulates stemness by targeting DNMT3b.** **A.** DNMT3b represses mammosphere formation, as assessed with a mammosphere counting assay. Data are mean values  $\pm$  SD from three independent experiments. Significance was calculated using Student's *t*-test. \*,  $p < 0.05$ . **B.** Stem cell markers assessed by Western blotting. **C.** MiR-221 transfection in T47 stem cells induced an increase in the number of colonies, as assessed by a soft agar assay. Co-transfection of DNMT3b and miR-221 rescued this effect. Data are mean values  $\pm$  SD from two independent experiments. Significance was calculated using Student's *t*-test. \*\*,  $p < 0.01$ ; Transient DNMT3 silencing mimicked the effect of miR-221 on **D.** sphere formation and **E.** stem markers, whereas stable silencing mimicked miR-221 behavior **F.** on sphere number in a replating assay. In **D.**, data are mean values  $\pm$  SD of three independent experiments. Significance was calculated using Student's *t*-test. \*,  $p < 0.05$ . In **G.** Pyrosequencing analysis of cells transfected with a DNMT3b siRNA showed a significant decrease in methylation levels at CpGs analyzed on *Nanog* and *Oct 3/4* promoters compared to the scrambled control cells (23% and 11% respectively). Significance was calculated using *U*-Mann Whitney test. \*,  $p < 0.05$ . Western blot analyses are representative experiments.

miR-200 family were found downregulated in CSCs isolated from colorectal, head and neck, prostate, and breast cancer compared to their non-CSC counterparts [30–33]. Expression of miR-200 represses EMT, contributing thus to the progression of cancer by promoting invasion, metastasis [34], and stemness phenotype.

In the present study, we identify miR-221 as an important player in the control of the CSC homeostasis. We provide evidence that miR-221 is expressed at higher levels in the stem cell population of primary and T47D cells compared to differentiated cells. MiR-221 has been found overexpressed in a number of human tumors by us and others [14, 35–38]. The relevance of this miR as an oncogene in breast cancer is reported by several papers, demonstrating the broad spectrum of action miR-221 and its regulation of several features of tumorigenesis [35, 39]. MiR-221 is found often abnormally expressed in breast

cancer [40] and recent studies have found that it may be responsible for resistance to tamoxifene [41]. MiR-221 promotes tumorigenesis of triple negative breast cancer through the alteration of key genes of the EMT process, such as E-cadherin, Slug, and Snail [42]; its expression is under the direct control of Slug, suggesting the existence of a miR-221–EMT regulatory loop [43]. In addition, it was reported that miR-221 is upregulated in prolonged mammosphere cultures of MCF7 cells undergoing EMT and with downregulated ER- $\alpha$  [44], and that it is able to sustain breast cell hierarchy in normal and malignant breast cells, probably via EMT [45].

Here we demonstrate that miR-221 induces expression of pluripotency-associated genes, such as Nanog, Oct 3/4, and  $\beta$ -Catenin, enforcing stemness and mammosphere formation. miR-221 downregulates DNMT3b expression, modifying BCSC phenotype.

DNMT3a, DNMT3b, and DNMT1 are members of the DNA methylation machinery. During DNA replication, DNMT1 recognizes the CpGs present on the parent strand and methylates the corresponding CpG sites of the newly synthesized strand [46, 47]. In contrast, DNMT3a and DNMT3b are responsible for de novo DNA methylation predominantly during early development [48, 49]; in addition, they are important for stable inheritance of some DNA methylation, and the silencing of both enzymes in embryonic stem cells (ESCs) determines a progressive loss of DNA methylation at critical sites of the genome, such as repetitive and single copy elements [50]. Moreover, ESCs lacking both *DNMT3a* and *DNMT3b* progressively lose differentiation potential after several cell passages, but are able to maintain self-renewal [25, 50, 51]. Interestingly, it has been demonstrated that DNMT3a and DNMT3b ablation induces aberrant expression of Nanog and Oct 3/4 in ESCs [52]. The role of DNMT3b in cancer development is not still clear. Although DNMT3b was classically considered an oncogene, due to its role in the hypermethylation of tumor suppressor genes during tumor progression in lung, breast, colon, and bladder cancers [53, 54], several reports also indicate a tumor suppressor behavior at an advanced tumor stage [55, 56]. Therefore, DNMT3b may act as a tumor suppressor or an oncogene depending on tumor stage or on the type of tumor cell population. In the present study, we demonstrate that DNMT3b represses the expression of Nanog and Oct 3/4 and increases the number of breast cancer cell spheres. Thus, DNMT3b downregulation may represent an advantage for cancer development, driving the expansion of the stem cell compartment. Further experiments are necessary to elucidate the mechanism through which DNMT3b regulates stemness, other than acting directly on *Nanog* and *Oct 3/4* promoters.

In conclusion, we have identified a new mechanism by which miR-221 affects the tumor stemness phenotype of breast cancer cells, providing more information on the oncogenic role of miR-221 in breast cancer.

## MATERIALS AND METHODS

### Cell and mammosphere culture

Differentiated breast tumor cells from three patients (#1, #2, #3) and BTSCs (breast tumor stem cells) were obtained as previously described [57] and were used for microRNA array. T47D cells were grown in RPMI 1640 supplemented with 10% heat-inactivated fetal bovine serum (FBS), 2 mM L-glutamine, and 100 U/ml penicillin/streptomycin. For mammosphere culture, single cells were plated at a density of 1,000 cells/ml. Cells were grown in serum-free DMEM-F12 (Sigma, Milan, Italy) supplemented with B27 (Life technologies Milan Italy), 10 ng/ml EGF (Sigma, Milan, Italy), 20 ng/ml  $\beta$ FGF (BD Biosciences, Milan, Italy), and 1X antibiotic-antimycotics

(Life technologies, Milan, Italy). After 5–7 days, mammospheres, which appeared as spheres of floating viable cells, were collected by gentle centrifugation (800 rpm) and dissociated with 0.25% trypsin for 5 min. HEK-293 cells were grown in DMEM supplemented with 10% heat-inactivated FBS and 100 U/ml penicillin/streptomycin.

### Cell and sphere transfection

For transient transfection with miRs, cells at 50% confluence were transfected using Oligofectamine (Life Technologies Milan Italy) with 100 nM of pre-miR-221, scrambled, or anti miR-221 (Ambion, Life Technologies Milan Italy). In order to overexpress DNMT3b, cells were transfected with Lipofectamine 2000 and 3  $\mu$ g of DNMT3b cDNA, a kind gift of Ana Portela (IDIBELL, Barcelona, Spain). To transiently knockdown DNMT3b gene expression, a pool of DNMT3b siRNAs is transfected using Lipofectamine 2000 at a final concentration of 100 nM (Santa Cruz Biotechnology, MA, USA). To stably knockdown DNMT3b, cells were infected with a shDNMT3b (Santa Cruz Biotechnology, MA, USA) and the expression of DNMT3b studied by qRT-PCR in pooled cell populations (data not shown).

### Transduction with viral vectors

T47D cells and a primary breast cell line obtained from patient #5 were infected using Tween miR-221 or Tween control vector, as already described by Quintavalle et al. [14]. Briefly, on the day of infection, the medium was removed and replaced with viral supernatant with the addition of 4 mg/ml of polybrene (Sigma Aldrich, Milan Italy). Cells were then centrifuged in their plate for 45 min in a Beckman GS-6KR centrifuge, at 1800 rpm and 32°C. After centrifugation, cells were kept overnight in a 5% CO<sub>2</sub> incubator at 37°C. After exposure, cells were washed twice with cold PBS and fresh medium added. 48 h after the transduction, cells were washed with PBS, harvested with trypsin/EDTA, and analyzed by FACS for GFP expression.

### Protein isolation and western blotting

Cells were washed twice in ice-cold PBS, and lysed in JS buffer (50 mM HEPES pH 7.5 containing 150 mM NaCl, 1% Glycerol, 1% Triton X100, 1.5 mM MgCl<sub>2</sub>, 5 mM EGTA, 1 mM Na<sub>3</sub>VO<sub>4</sub>, and 1X protease inhibitor cocktail). Protein concentration was determined by the Bradford assay (BioRad, Milan, Italy) using bovine serum albumin as the standard, and equal amounts of proteins were analyzed by SDS-PAGE (12.5% acrylamide). Gels were electroblotted onto nitrocellulose membranes (G&E Healthcare, Milan, Italy). Membranes were blocked for 1 h with 5% non-fat dry milk in Tris Buffered Saline (TBS) containing 0.1% Tween-20, and incubated at

4°C overnight with the primary antibody. Detection was performed with peroxidase-conjugated secondary antibodies using an enhanced chemiluminescence system (ThermoEuroclone, Milan, Italy). Primary antibodies used were: anti-Zeb-1, -Oct 3/4, -Nanog, -cytokeratin 18, and -cytokeratin 8 (Santa Cruz Biotechnologies, MA, USA), anti-DNMT3b (Abcam, MA, USA), and anti-β-actin (Sigma Aldrich, Milan, Italy).

### miRNA microarray

5 µg of total RNA from each sample was reverse transcribed using biotin end-labeled random-Octamer oligonucleotide primer. Hybridization of biotin-labeled complementary DNA was performed on Ohio State University custom miRNA microarray chips (OSU\_CCC version 3.0), which contain 1150 miR probes, including 326 human and 249 mouse miR genes, spotted in duplicate. The hybridized chips were washed and processed to detect biotin-containing transcripts by streptavidin-Alexa647 conjugate and scanned on an Axon 4000B microarray scanner (Axon Instruments, Sunnyvale, California, USA).

Raw data were normalized and analyzed with GENESPRING 7.2 software (zcomSilicon Genetics, Redwood City, CA, USA). Expression data were median-centered with the GENESPRING normalization option and the global median normalization of the BIOCONDUCTOR package (<http://www.bioconductor.org>), which produced similar results. Statistical comparisons were done with the GENESPRING ANOVA tool, predictive analysis of microarray (PAM), and the Significance Analysis of Microarray (SAM) software (<http://www-stat.stanford.edu/~tibs/SAM/index.html>).

### Mammosphere forming assay

Mammospheres were resuspended in 0.5% agar (Bacto-Agar, Difco Laboratories) and layered on a preformed 0.8% agar layer using 60 mm Petri dishes (BD). Colonies were counted under an inverted microscope (Nikon, Milan, Italy) and then photographed.

### RNA extraction and real-time PCR

Total RNAs (miR and mRNA) were extracted using Trizol (LifeTechnologies, Milan, Italy) according to the manufacturer's protocol. Reverse transcription of total miRNA was performed using miScript reverse Transcription Kit (Qiagen, Milan Italy), for mRNA we used SuperScript® III Reverse Transcriptase (Life Technologies, Milan, Italy). Quantitative analysis of Nanog, Oct 3/4, Sox2, β-Actin (as an internal reference), miR-221, and *RNU6B* (as an internal reference) was performed by real time PCR using specific primers (Qiagen, Milan, Italy), miScript SYBR Green PCR Kit (Qiagen, Milan Italy), and iQ™ SYBR Green Supermix

(Bio-Rad, Milan, Italy), respectively. Experiments were carried out in triplicate for each data point, and data analysis was performed with software (Bio-Rad, Milan Italy).

### Luciferase assay

The 3' UTR of the human DNMT3b gene was PCR-amplified using the following primers: *DNMT3b*-Fw: 5'GCTCTAGACAGCCAGGCCCAAGCCC3'; *DNMT3b*-Rv: 5'GCTCTAGAACCTCAGGCTACCCCTGC3', and cloned downstream of the Renilla luciferase stop codon in pGL3 control vector (Promega, Milan, Italy). An inverted sequence of the miR-binding sites was used as negative control. HEK-293 cells were co-transfected with 1.2 µg of plasmid and 400 µg of a Renilla luciferase expression construct, pRL-TK (Promega, Milan, Italy), with Lipofectamine 2000 (Life Technologies, Milan, Italy). Cells were harvested 24 h post-transfection and assayed with Dual Luciferase Assay (Promega, Milan, Italy) according to the manufacturer's instructions. Three independent experiments were performed in triplicate.

### DNA methylation analysis by pyrosequencing

Bisulphite conversion of 500 ng of each DNA sample was performed with EZ DNA Methylation-Gold Kit (Zymo Research, Milan Italy) according to the manufacturer's recommendations. PCR for *Nanog* and *Oct 3/4* promoters was performed with 1 µl of bisulphite converted DNA under standard conditions with biotinylated primers using an annealing temperature of 60°C. Primer sequences are given in Supplementary Table S2 and were designed with PyroMark Assay Design 2.0. PCR products were observed on 2% agarose gels before pyrosequencing analysis. Reactions were performed in a PyroMark Q96 System version 2.0.6 (Qiagen, Milan, Italy) and the methylation values of the CpG dinucleotides were obtained using Pyro Q-CpG 1.0.9 (Qiagen, Milan, Italy). The 2 CpGs analyzed of *Nanog* promoter region were -83, -36, from to the Transcription Start Site (TSS); whereas the 3 CpGs analyzed of *Oct3/4* promoter region were +319, +346, +358 from the TSS. Additional GpGs analyzed of both promoter regions were -302, -300, -296 from TSS of *Nanog* and + 250, +253, +277 from TSS of *Oct 3/4*.

### Immunofluorescence

Immunofluorescence was performed on cultured BCSC cytoplasts fixed with 2% paraformaldehyde for 20 minutes at 37°C, washed and permeabilized with PBS plus 0.1% Triton X-100 for 10 min on ice. After washing, cells were stained overnight at 4°C using antibodies against DNMT3b (Abcam- ab13604) or isotype-matched controls at appropriate dilutions. Then cells were labeled with FITC-conjugated secondary antibodies for 1 h at 37°C.

Nucleus counterstaining was performed using Toto-3 iodide. Samples were analyzed by confocal microscope.

## Statistical analysis

All experiments were repeated at least twice. Continuous variables are given as mean  $\pm$  1 standard deviation (SD). For two-group comparison, Student's *t*-test was used to determine differences between mean values for normal distribution. All data were analyzed for significance using GraphPadPrism 6 software (San Diego, CA, USA); a probability level  $<0.05$  was considered significant throughout the analysis.

## ACKNOWLEDGMENTS AND FUNDING

This work was partially supported by funds from Associazione Italiana Ricerca sul Cancro, AIRC (grant no.10620 to G.C., and no. 10254 to M.T.).

MERIT (RBNE08E8CZ\_002) to G.C., and Fondazione Berlucci to G.C.

Angel Diaz-Lagares was supported by a R o Hortega (CM14/00067) from the "Instituto de Salud Carlos III". Manel Esteller is an ICREA Research Professor.

## CONFLICTS OF INTEREST

The authors declare to have no conflict of interests.

## REFERENCES

1. Reya T, Morrison SJ, Clarke MF, Weissman IL. Stem cells, cancer, and cancer stem cells. *Nature*. 2001; 414:685-9.
2. Al-Hajj M, Wicha MS, Benito-Hernandez A, Morrison SJ, Clarke MF. Prospective identification of tumorigenic breast cancer cells. *Proceedings of the National Academy of Sciences of the United States of America*. 2003; 100:3983-3988.
3. Visvader JE, Lindeman GJ. Cancer stem cells in solid tumours: accumulating evidence and unresolved questions. *Nature reviews Cancer*. 2008; 8:755-768.
4. Dontu G, Liu S, Wicha MS. Stem cells in mammary development and carcinogenesis: implications for prevention and treatment. *Stem cell reviews*. 2005; 13:207-213.
5. Pece S, Tosoni D, Confalonieri S, Mazzarol G, Vecchi M, Ronzoni S, Bernard L, Viale G, Pelicci PG, Di Fiore PP. Biological and molecular heterogeneity of breast cancers correlates with their cancer stem cell content. *Cell*. 2010; 140:62-73.
6. Iorio MV, Ferracin M, Liu CG, Veronese A, Spizzo R, Sabbioni S, Magri E, Pedriali M, Fabbri M, Campiglio M, Menard S, Palazzo JP, Rosenberg A, Musiani P, Volinia S, Nenci I, et al. MicroRNA gene expression deregulation in human breast cancer. *Cancer research*. 2005; 65:7065-7070.
7. Volinia S, Calin GA, Liu CG, Ambs S, Cimmino A, Petrocca F, Visone R, Iorio M, Roldo C, Ferracin M, Prueitt RL, Yanaihara N, Lanza G, Scarpa A, Vecchione A, Negrini M, et al. A microRNA expression signature of human solid tumors defines cancer gene targets. *Proceedings of the National Academy of Sciences of the United States of America*. 2006; 103:2257-2261.
8. Mattiske S, Suetani RJ, Neilsen PM, Callen DF. The oncogenic role of miR-155 in breast cancer. *Cancer epidemiology, biomarkers & prevention : a publication of the American Association for Cancer Research, cosponsored by the American Society of Preventive Oncology*. 2012; 21:1236-1243.
9. Li P, Sheng C, Huang L, Zhang H, Huang L, Cheng Z, Zhu Q. MiR-183/-96/-182 cluster is up-regulated in most breast cancers and increases cell proliferation and migration. *Breast cancer research*. 2014; 16:473.
10. Zhou M, Liu Z, Zhao Y, Ding Y, Liu H, Xi Y, Xiong W, Li G, Lu J, Fodstad O, Riker AI, Tan M. MicroRNA-125b confers the resistance of breast cancer cells to paclitaxel through suppression of pro-apoptotic Bcl-2 antagonist killer 1 (Bak1) expression. *The Journal of biological chemistry*. 2010; 285:21496-21507.
11. Piovani C, Palmieri D, Di Leva G, Braccioli L, Casalini P, Nuovo G, Tortoreto M, Sasso M, Plantamura I, Triulzi T, Taccioli C, Tagliabue E, Iorio MV, Croce CM. Oncosuppressive role of p53-induced miR-205 in triple negative breast cancer. *Molecular oncology*. 2012; 6:458-472.
12. Zhou J, Tian Y, Li J, Lu B, Sun M, Zou Y, Kong R, Luo Y, Shi Y, Wang K, Ji G. miR-206 is down-regulated in breast cancer and inhibits cell proliferation through the up-regulation of cyclinD2. *Biochemical and biophysical research communications*. 2013; 433:207-212.
13. Petrelli A, Carollo R, Cargnelutti M, Iovino F, Callari M, Cimino D, Todaro M, Mangiapane LR, Giammona A, Cordova A, Montemurro F, Taverna D, Daidone MG, Stassi G, Giordano S. By promoting cell differentiation, miR-100 sensitizes basal-like breast cancer stem cells to hormonal therapy. *Oncotarget*. 2015; 6:2315-2330.
14. Quintavalle C, Garofalo M, Zanca C, Romano G, Iaboni M, del Basso De Caro M, Martinez-Montero JC, Incoronato M, Nuovo G, Croce CM, Condorelli G. miR-221/222 overexpression in human glioblastoma increases invasiveness by targeting the protein phosphatase PTP[mu]. *Oncogene*. 2012; 31:858-868.
15. Fornari F, Gramantieri L, Ferracin M, Veronese A, Sabbioni S, Calin GA, Grazi GL, Giovannini C, Croce CM, Bolondi L, Negrini M. MiR-221 controls CDKN1C/p57 and CDKN1B/p27 expression in human hepatocellular carcinoma. *Oncogene*. 2008; 27:5651-5661.
16. Quintavalle C, Mangani D, Roscigno G, Romano G, Diaz-Lagares A, Iaboni M, Donnarumma E, Fiore D, De Marinis P, Soini Y, Esteller M, Condorelli G. miR-221/222 Target the DNA Methyltransferase MGMT in Glioma Cells. *PLoS ONE*. 2013; 8:e74466.

17. Cicalese A, Bonizzi G, Pasi CE, Faretta M, Ronzoni S, Giulini B, Brisken C, Minucci S, Di Fiore PP, Pelicci PG. The tumor suppressor p53 regulates polarity of self-renewing divisions in mammary stem cells. *Cell*. 2009; 1386:1083–1095.
18. Morrison SJ, Kimble J. Asymmetric and symmetric stem-cell divisions in development and cancer. *Nature*. 2006; 4417097:1068–1074.
19. Gaspar-Maia A, Alajem A, Meshorer E, Ramalho-Santos M. Open chromatin in pluripotency and reprogramming. *Nature reviews Molecular cell biology*. 2011; 121:36–47.
20. Deb-Rinker P, Ly D, Jezierski A, Sikorska M, Walker PR. Sequential DNA methylation of the Nanog and Oct-4 upstream regions in human NT2 cells during neuronal differentiation. *The Journal of biological chemistry*. 2005; 2808:6257–6260.
21. Zhang HJ, Siu MK, Wong ES, Wong KY, Li AS, Chan KY, Ngan HY, Cheung AN. Oct4 is epigenetically regulated by methylation in normal placenta and gestational trophoblastic disease. *Placenta*. 2008; 296:549–554.
22. Santi DV, Garrett CE, Barr PJ. On the mechanism of inhibition of DNA-cytosine methyltransferases by cytosine analogs. *Cell*. 1983; 331:9–10.
23. Jones PA, Liang G. Rethinking how DNA methylation patterns are maintained. *Nature reviews Genetics*. 2009; 1011:805–811.
24. Bachman KE, Rountree MR, Baylin SB. Dnmt3a and Dnmt3b are transcriptional repressors that exhibit unique localization properties to heterochromatin. *The Journal of biological chemistry*. 2001; 27634:32282–32287.
25. Meissner A, Gnirke A, Bell GW, Ramsahoye B, Lander ES, Jaenisch R. Reduced representation bisulfite sequencing for comparative high-resolution DNA methylation analysis. *Nucleic acids research*. 2005; 3318:5868–5877.
26. Bertos NR, Park M. Breast cancer - one term, many entities? *The Journal of clinical investigation*. 2011; 12110:3789–3796.
27. He L, Hannon GJ. MicroRNAs: small RNAs with a big role in gene regulation. *Nature reviews Genetics*. 2004; 57:522–531.
28. Sassen S, Miska EA, Caldas C. MicroRNA: implications for cancer. *Virchows Archiv : an international journal of pathology*. 2008; 4521:1–10.
29. Song SJ, Poliseno L, Song MS, Ala U, Webster K, Ng C, Beringer G, Brikbak NJ, Yuan X, Cantley LC, Richardson AL, Pandolfi PP. MicroRNA-antagonism regulates breast cancer stemness and metastasis via TET-family-dependent chromatin remodeling. *Cell*. 2013; 1542:311–324.
30. Lo WL, Yu CC, Chiou GY, Chen YW, Huang PI, Chien CS, Tseng LM, Chu PY, Lu KH, Chang KW, Kao SY, Chiou SH. MicroRNA-200c attenuates tumour growth and metastasis of presumptive head and neck squamous cell carcinoma stem cells. *The Journal of pathology*. 2011; 2234:482–495.
31. Williams LV, Veliceasa D, Vinokour E, Volpert OV. miR-200b inhibits prostate cancer EMT, growth and metastasis. *PLoS One*. 2013; 812:e83991.
32. Knezevic J, Pfefferle AD, Petrovic I, Greene SB, Perou CM, Rosen JM. Expression of miR-200c in claudin-low breast cancer alters stem cell functionality, enhances chemosensitivity and reduces metastatic potential. *Oncogene*. 2015 Mar 9. [Epub ahead of print] PMID: 25746005.
33. Lu YX, Yuan L, Xue XL, Zhou M, Liu Y, Zhang C, Li JP, Zheng L, Hong M, Li XN. Regulation of colorectal carcinoma stemness, growth, and metastasis by an miR-200c-Sox2-negative feedback loop mechanism. *Clinical cancer research : an official journal of the American Association for Cancer Research*. 2014; 2010:2631–2642.
34. Park SM, Gaur AB, Lengyel E, Peter ME. The miR-200 family determines the epithelial phenotype of cancer cells by targeting the E-cadherin repressors ZEB1 and ZEB2. *Genes & development*. 2008; 227:894–907.
35. Garofalo M, Quintavalle C, Romano G, Croce CM, Condorelli G. miR221/222 in cancer: their role in tumor progression and response to therapy. *Current molecular medicine*. 2012; 121:27–33.
36. Pineau P, Volinia S, McJunkin K, Marchio A, Battiston C, Terris B, Mazzaferro V, Lowe SW, Croce CM, Dejean A. miR-221 overexpression contributes to liver tumorigenesis. *Proceedings of the National Academy of Sciences of the United States of America*. 2010; 1071:264–269.
37. Garofalo M, Quintavalle C, Di Leva G, Zanca C, Romano G, Taccioli C, Liu CG, Croce CM, Condorelli G. MicroRNA signatures of TRAIL resistance in human non-small cell lung cancer. *Oncogene*. 2008; 2727:3845–3855.
38. Pallante P, Visone R, Ferracin M, Ferraro A, Berlingieri MT, Troncone G, Chiappetta G, Liu CG, Santoro M, Negrini M, Croce CM, Fusco A. MicroRNA deregulation in human thyroid papillary carcinomas. *Endocrine-related cancer*. 2006; 132:497–508.
39. Garofalo M, Di Leva G, Romano G, Nuovo G, Suh SS, Nanganke A, Taccioli C, Pichiorri F, Alder H, Secchiero P, Gasparini P, Gonelli A, Costinean S, Acunzo M, Condorelli G, Croce CM. miR-22&222 regulate TRAIL resistance and enhance tumorigenicity through PTEN and TIMP3 downregulation. *Cancer cell*. 2009; 166:498–509.
40. Wu X, Zeng R, Wu S, Zhong J, Yang L, Xu J. Comprehensive expression analysis of miRNA in breast cancer at the miRNA and isomiR levels. *Gene*. 2015; 5572:195–200.
41. Miller TE, Ghoshal K, Ramaswamy B, Roy S, Datta J, Shapiro CL, Jacob S, Majumder S. MicroRNA-221/222 confers tamoxifen resistance in breast cancer by targeting p27Kip1. *The Journal of biological chemistry*. 2008; 28344:29897–29903.

42. Nassirpour R, Mehta PP, Baxi SM, Yin MJ. miR-221 promotes tumorigenesis in human triple negative breast cancer cells. *PLoS One*. 2013; 84:e62170.
43. Lambertini E, Lolli A, Vezzali F, Penolazzi L, Gambari R, Piva R. Correlation between Slug transcription factor and miR-221 in MDA-MB-231 breast cancer cells. *BMC cancer*. 2012; 12:445.
44. Guttilla IK, Phoenix KN, Hong X, Tirnauer JS, Claffey KP, White BA. Prolonged mammosphere culture of MCF-7 cells induces an EMT and repression of the estrogen receptor by microRNAs. *Breast cancer research and treatment*. 2012; 1321:75–85.
45. Ke J, Zhao Z, Hong SH, Bai S, He Z, Malik F, Xu J, Zhou L, Chen W, Martin-Trevino R, Wu X, Lan P, Yi Y, Ginestier C, Ibarra I, Shang L, et al. Role of microRNA221 in regulating normal mammary epithelial hierarchy and breast cancer stem-like cells. *Oncotarget*. 2015; 66:3709–3721.
46. Bestor TH. Activation of mammalian DNA methyltransferase by cleavage of a Zn binding regulatory domain. *The EMBO journal*. 1992; 117:2611–2617.
47. Bestor TH, Gundersen G, Kolsto AB, Prydz H. CpG islands in mammalian gene promoters are inherently resistant to de novo methylation. *Genetic analysis, techniques and applications*. 1992; 92:48–53.
48. Hata K, Okano M, Lei H, Li E. Dnmt3L cooperates with the Dnmt3 family of de novo DNA methyltransferases to establish maternal imprints in mice. *Development*. 2002; 1298:1983–1993.
49. Okano M, Bell DW, Haber DA, Li E. DNA methyltransferases Dnmt3a and Dnmt3b are essential for de novo methylation and mammalian development. *Cell*. 1999; 993:247–257.
50. Chen T, Ueda Y, Dodge JE, Wang Z, Li E. Establishment and maintenance of genomic methylation patterns in mouse embryonic stem cells by Dnmt3a and Dnmt3b. *Molecular and cellular biology*. 2003; 2316:5594–5605.
51. Tsumura A, Hayakawa T, Kumaki Y, Takebayashi S, Sakaue M, Matsuoka C, Shimotohno K, Ishikawa F, Li E, Ueda HR, Nakayama J, Okano M. Maintenance of self-renewal ability of mouse embryonic stem cells in the absence of DNA methyltransferases Dnmt1, Dnmt3a and Dnmt3b. *Genes to cells : devoted to molecular & cellular mechanisms*. 2006; 117:805–814.
52. Li JY, Pu MT, Hirasawa R, Li BZ, Huang YN, Zeng R, Jing NH, Chen T, Li E, Sasaki H, Xu GL. Synergistic function of DNA methyltransferases Dnmt3a and Dnmt3b in the methylation of Oct4 and Nanog. *Molecular and cellular biology*. 2007; 2724:8748–8759.
53. Esteller M. Cancer epigenomics: DNA methylomes and histone-modification maps. *Nature reviews Genetics*. 2007; 84:286–298.
54. Issa JP. CpG island methylator phenotype in cancer. *Nature reviews Cancer*. 2004; 412:988–993.
55. Gao Q, Steine EJ, Barrasa MI, Hockemeyer D, Pawlak M, Fu D, Reddy S, Bell GW, Jaenisch R. Deletion of the de novo DNA methyltransferase Dnmt3a promotes lung tumor progression. *Proceedings of the National Academy of Sciences of the United States of America*. 2011; 10844:18061–18066.
56. Lin RK, Hsu HS, Chang JW, Chen CY, Chen JT, Wang YC. Alteration of DNA methyltransferases contributes to 5'CpG methylation and poor prognosis in lung cancer. *Lung cancer*. 2007; 552:205–213.
57. Ponti D, Costa A, Zaffaroni N, Pratesi G, Petrangolini G, Coradini D, Pilotti S, Pierotti MA, Daidone MG. Isolation and *in vitro* propagation of tumorigenic breast cancer cells with stem/progenitor cell properties. *Cancer research*. 2005; 6513:5506–5511.

## miR-340 predicts glioblastoma survival and modulates key cancer hallmarks through down-regulation of *NRAS*

Danilo Fiore<sup>1</sup>, Elvira Donnarumma<sup>2</sup>, Giuseppina Roscigno<sup>1,3</sup>, Margherita Iaboni<sup>1</sup>, Valentina Russo<sup>1</sup>, Alessandra Affinito<sup>1</sup>, Assunta Adamo<sup>1</sup>, Fabio De Martino<sup>1</sup>, Cristina Quintavalle<sup>4</sup>, Giulia Romano<sup>5</sup>, Adelaide Greco<sup>6,7</sup>, Soini Ylermi<sup>8</sup>, Arturo Brunetti<sup>6,7</sup>, Carlo M. Croce<sup>5</sup>, Gerolama Condorelli<sup>1,3</sup>

<sup>1</sup>Department of Molecular Medicine and Medical Biotechnology, "Federico II" University of Naples, Naples, Italy

<sup>2</sup>IRCCS-SDN, Naples, Italy

<sup>3</sup>IEOS, CNR, Naples, Italy

<sup>4</sup>Institute of Pathology, Molecular Pathology Division, University of Basel, Basel, Switzerland

<sup>5</sup>Department of Molecular Virology, Immunology and Medical Genetics, Human Cancer Genetics Program, Comprehensive Cancer Center, The Ohio State University, Columbus, OH, USA

<sup>6</sup>Department of Advanced Biomedical Science, University of Naples Federico II, Naples, Italy

<sup>7</sup>Ceinge, Biotecnologie Avanzate, Scarl, Naples, Italy

<sup>8</sup>Cancer Center of Eastern Finland, University of Eastern Finland, Kuopio, Finland

**Correspondence to:** Gerolama Condorelli, **e-mail:** gecondor@unina.it

**Keywords:** *microRNAs*, *glioblastoma*, *survival*, *NRAS*, *signal-transduction*

**Received:** August 10, 2015

**Accepted:** January 01, 2016

**Published:** January 21, 2016

### ABSTRACT

**Glioblastoma is the most common primary brain tumor in adults; with a survival rate of 12 months from diagnosis. However, a small subgroup of patients, termed long-term survivors (LTS), has a survival rate longer than 12–14 months. There is thus increasing interest in the identification of molecular signatures predicting glioblastoma prognosis and in how to improve the therapeutic approach. Here, we report miR-340 as prognostic tumor-suppressor microRNA for glioblastoma. We analyzed microRNA expression in > 500 glioblastoma patients and found that although miR-340 is strongly down-regulated in glioblastoma overall, it is up-regulated in LTS patients compared to short-term survivors (STS). Indeed, miR-340 expression predicted better prognosis in glioblastoma patients. Coherently, overexpression of miR-340 in glioblastoma cells was found to produce a tumor-suppressive activity. We identified *NRAS* mRNA as a critical, direct target of miR-340: in fact, miR-340 negatively influenced multiple aspects of glioblastoma tumorigenesis by down-regulating *NRAS* and downstream AKT and ERK pathways. Thus, we demonstrate that expression of miR-340 in glioblastoma is responsible for a strong tumor-suppressive effect in LTS patients by down-regulating *NRAS*. miR-340 may thus represent a novel marker for glioblastoma diagnosis and prognosis, and may be developed into a tool to improve treatment of glioblastoma.**

### INTRODUCTION

Malignant glioma (glioblastoma or GBM) is the most common and aggressive primary brain tumor [1, 2]. Despite continuous improvement in treatment approaches, with a combination of surgery, radiotherapy and chemotherapy, average survival of GBM patients has improved only slightly [3]. In fact, GBM patients tend to

have an extremely poor prognosis, with a median survival rate from diagnosis ranging from 12 to 14 months [4, 5]. Different factors are involved in GBM aggressiveness and poor prognosis, such as rapid cell proliferation, resistance to drug-induced apoptosis and enhanced invasiveness. Nevertheless, a small subset of patients presents a better outcome, surviving longer than 14 months: these patients are termed long-term survivors (LTS) [4]. The

molecular events associated with the LTS phenotype are not well elucidated. Better understanding of these events would be critical for the development of early detection methods, identification of new biomarkers, and improved therapeutic approaches.

MicroRNAs (miRNAs or miRs) are a class of evolutionary conserved small non-coding RNAs that have great impact on a wide spectrum of biological processes. miRNAs act by affecting gene expression at the post-transcriptional level [6]. Many studies have demonstrated a pivotal role for miRNAs in tumorigenesis, acting both as oncogenes or tumor suppressors [7–10]. During tumor initiation and progression, miRNAs may modulate proliferation, angiogenesis, invasion and survival [11]. Deregulation of miRNA expression has been found in many human cancers, including GBM [12–15].

*NRAS* is a member of the *RAS* oncogene family (which comprises *KRAS*, *HRAS* and *NRAS*); they encode small GTPases involved in cellular signal transduction. *RAS* is activated by a complex signal cascade and, in turn, triggers downstream signaling pathways such as the mitogen-activate protein kinases (MAPKs) pathway and the phosphatidylinositol 3-kinase (PI3K)/AKT pathway, to modulate cell growth and survival [16]. Various studies have demonstrated recurrent aberrant *NRAS* activation in GBM [17]. Recently, several miRNAs –such as miR-181d, let-7 and miR-143– have been reported to suppress *RAS* expression, and thus act as tumor suppressors; this suggests that the dysregulation of miRNAs targeting *NRAS* may have an important role in carcinogenesis [8, 18–20].

For the present study, we investigated differential miRNA expression in long- and short-term GBM survivors. We identified miR-340 as a novel tumor suppressor miRNA that is up-regulated in LTS patients and predictive of better prognosis. Furthermore, we describe the oncosuppressive mechanisms induced by this miRNA: its ability to directly target *NRAS*, and thus silence downstream pathways, contributed in the blunting of the tumorigenic behavior of GBM cells.

## RESULTS

### miR-340 expression correlates with survival in GBM patients

To identify miRNAs de-regulated in long- vs short-term GBM survivors, we profiled the miRNA signatures of primary GBM tissue harvested from 3 LTS and 3 STS patients. The analysis was performed with a microarray chip containing 1150 miRNA probes, including 326 human and 249 mouse miRNAs, spotted in duplicate. Data obtained indicated that seven miRNAs (namely miR-193b, -340, -19b, -20a-b, -219-5p, -137 and -129-3p) were significantly de-regulated (> 1.5-fold change) in LTS vs STS GBM patients (Supplementary Table 1). We

decided to focus our attention on miR-340, because we and others have already demonstrated the oncosuppressive role of this miRNA in different human tumors [21–27]. Accordingly with microarray data, qRT-PCR for miR-340 confirmed that it was up-regulated in LTS patients (Supplementary Figure 1A).

We then analyzed miR-340 expression in a larger cohort of glioblastoma patients ( $n = 61$ ), as well as in data collected from TCGA database (491 glioblastomas and 10 normal brain samples). As expected, miR-340 expression was significantly decreased in STS compared to LTS ( $p < 0.05$ ; Figure 1A, 1B), and in GBM compared to normal brain ( $p < 0.001$ ; Figure 1C). Furthermore, Log-Rank analysis of two different cohorts of GBM patients (43 GBM patients from our hospital and 327 from TCGA) indicated that patients with higher levels of miR-340 had longer overall survival, suggestive of a prognostic role of miR-340 ( $p < 0.05$ ;  $p < 0.01$ ). The Kaplan-Meier curves of the patient cohorts are given in Figure 1D–1E. Interestingly, higher levels of RNF130, the host gene of miR-340, was also predictive of a better prognosis in GBM patients ( $p < 0.05$ ; fig1f, data from R2.aml database). Finally, we found that miR-340 expression did not correlate with different glioma tumor stages (Supplementary Figure 1B) and with MGMT methylation status (Supplementary Figure 1C).

### *NRAS* mRNA is a direct target of miR-340

To identify possible miR-340 targets involved in the LTS phenotype, we parsed bioinformatics databases (TargetsCan, Miranda, Pictar). We found the presence of two distinct putative miR-340 binding sites on the 3'UTR of *NRAS* mRNA (Figure 2A). To assess if miR-340 directly bound to these two putative regions, we cloned them individually downstream of a luciferase reporter gene in the pGL3 vector. A549 NSCLC cells (expressing low endogenous level of miR-340) [25] were co-transfected with the reporter plasmids singularly or in combination, in the presence of either miR-340 or a control miRNA (scrambled). Luciferase activity of both reporters was repressed by the addition of miR-340 (Figure 2B); moreover, the effect was greater in cells co-transfected with both reporters, indicating that the two *NRAS* 3'UTR sites acted synergistically. Luciferase activity was not affected by miR-340 overexpression in the presence of mutant constructs, in which the seed sequences were cloned inversely (Figure 2A–2B).

To establish a causative effect between miR-340 and *NRAS*, we transfected different GBM cell lines (U251MG, U87MG and AM38 cells) with miR-340 and analyzed *NRAS* levels with qRT-PCR and Western blotting. We chose these three cell lines because they express low levels of miR-340, as assessed by qRT-PCR on a panel of 11 different GBM cell lines (Supplementary Figure 1D).

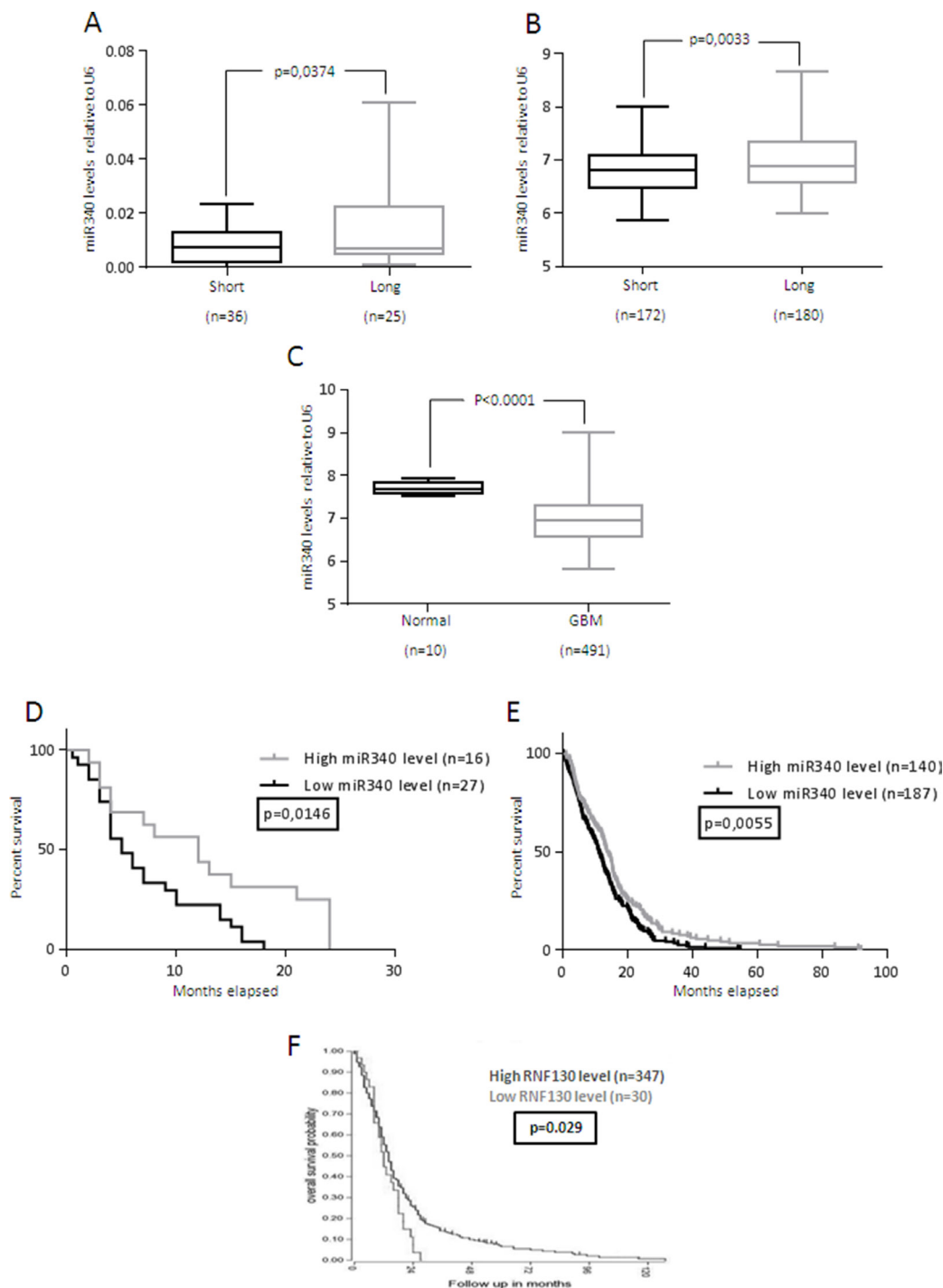


**Figure 1: miR-340 is down-regulated in GBM and correlates with GBM prognosis.** miR-340 expression was evaluated using three independent patient cohorts (A) FFPE tissue from 36 LTS and 25 STS GBM patients; (B) 180 LTS and 172 STS GBM patients from TCGA database; (C) 10 normal brain specimens and 491 GBM tissues from TCGA database. A significant increase in miR-340 expression was identified between LTS vs STS in both cohorts and in normal brain vs GBM tissue. miR-340 expression was assessed by Real-Time PCR and normalized against U6. An arbitrary cut-off of 12 months was used to divide LTS and STS patients. Statistical significance was calculated using Student's *t*-test.  $P < 0.05$  was considered significant. (D, E), Kaplan-Meier survival curve analysis of the correlation between miR-340 and overall survival of: (D) the FFPE tissues from 16 highly and 27 poorly miR-340-expressing glioblastoma patients; (E) 140 highly and 187 poorly miR-340-expressing glioblastoma patients collected from TCGA database. High miR-340 expression predicted a better prognosis in both cohorts. The patients were assigned to the high or low miR-340-expressing group using the media as a threshold.  $P$  was calculated using Log-Rank test.  $P < 0.05$  was considered significant. (F) Kaplan-Meier survival curve analysis of the correlation between RNF-130 and overall survival of 347 highly and 30 poorly *RNF-130*-expressing glioblastoma patients from the R2.a1l database. High RNF-130 expression predicted a better prognosis.  $P$  was calculated using Log-Rank test.  $P < 0.05$  was considered significant.

We found a consistent, strong decrease in *NRAS* mRNA and protein in all cell lines transfected (Figure 2C–2D). In contrast, anti-miR-340 induced an increase in *NRAS* levels in T98G cells (Figure 2C–2D). Interestingly, miR-340 overexpression was also able to decrease NRAS protein levels in three different breast cancer cell lines (BT-549, MDA-MB-231, MCF7; Figure 2E) and two NSCLC cell lines (A549, Calu-1; Figure 2F). Furthermore, to test the ability of miR-340 to specifically target *NRAS* mRNA, we verified that both sequences binding this miRNA were not conserved in *KRAS* or *HRAS* 3'UTRs (data not shown); coherently, miR-340 overexpression did not decrease *KRAS* or *HRAS* mRNA levels in GBM cells (Supplementary Figure 2A–2B).

### Effects of miR-340 in GBM cell lines

We investigated the tumor suppressive role of miR-340 in different GBM cell lines (U251MG, U87MG and AM38 cells) transfected with either miR-340 or a control miRNA. We analyzed the effects of miR-340 on cell cycle, cell proliferation and soft agar growth. miR-340 transfection induced a significant S-phase block, as assessed by FACS analysis after PI staining (Figure 3A, plots for qualitative data analysis are reported in Supplementary Figure 3A), and a significant decrease in cell proliferation, as assessed by BrdU incorporation (Figure 3B; plots for qualitative data analysis are reported in Supplementary Figure 4A) and MTT assay (Figure 3C–3E). In contrast, expression of anti-miR-340 in T98G cells increased cell proliferation 72 h after transfection (Figure 3E). We next investigated whether miR-340 expression had an impact on anchorage-independent cell growth with a soft agar assay. We found that miR-340 induced a reduction in colony formation in U251MG, U87MG and AM38 cells (Figure 3F). These results clearly demonstrate that miR-340 acts as tumor suppressor in GBM by blunting cell cycle, proliferation and anchorage-independent cell growth.

### miR-340 sensitizes GBM cells to TMZ

Because adjuvant chemotherapy with temozolomide is limited by the action of O-6-methylguanine-DNA methyltransferase (MGMT), a contributing factor for very poor survival in GBM patients [28], we investigated a possible role of miR-340 in TMZ sensitivity. MTT and Caspase 3/7 assays showed that miR-340 induced an increase in sensitivity to TMZ in all the cells analyzed (Figure 4A, 4B). Coherently, miR-340 overexpression determined an increase of apoptosis in GBM cells, as assessed by PARP cleavage (Figure 4C) as well as Annexin V assay (Figure 4D, plots for qualitative data analysis are reported in Supplementary Figure 5A). These results suggest that miR-340 expression contributes to the establishment of a LTS phenotype by enhancing the response of GBM patients to alkylating drugs.

### *NRAS*: a key target molecule of miR-340-mediated effects

*NRAS* is a key oncogene deregulated in many human cancers [16, 17, 29–31]. To demonstrate a causative link between miR-340 and *NRAS*, we performed rescue experiments, transfecting U251MG cells with miR-340 and with a construct expressing *NRAS* mRNA lacking the 3'UTR. Levels of transfected NRAS were detected by Western blotting (data not shown). Interestingly, expression of this *NRAS* counteracted the effects of miR-340 overexpression on proliferation (Figure 5A–5B; plots for qualitative data analysis are reported in Supplementary Figure 4B), cell cycle (Figure 5C; plots for qualitative data analysis are reported in Supplementary Figure 3B) and anchorage-independent cell growth (Figure 5D). Coherently, *NRAS* knock-down with a specific *NRAS* siRNA mimicked the effects of miR-340 overexpression, blocking cell cycle (Figure 5E; plots for qualitative data analysis are reported in Supplementary Figure 3C), decreasing the phosphorylation of ERK and AKT kinases (Figure 5F), and reducing proliferation (Figure 5G).

We then analyzed *NRAS* expression in a cohort of 39 GBM patients: we found that *NRAS* was down-regulated in LTS vs STS patients ( $p < 0.05$ , Supplementary Figure 6A). Moreover, *NRAS* expression was higher in 542 GBM samples compared to 10 normal brain specimens (data collected from the oncomine database;  $p < 0.001$ ; Supplementary Figure 6B). Furthermore, Log-Rank analysis of 28 GBM patients showed that those with higher levels of *NRAS* had shorter overall survival (Supplementary Figure 6C). This finding was confirmed by data from the R2.aml database (504 tissues;  $p < 0.05$ ; Supplementary Figure 6D). In conclusion, the anti-tumoral effects of miR-340 seem, at least in part, to be mediated by its targeting of *NRAS*.

Recently, miR-340 was reported to directly target two important oncogenes, *SKP2* and *ROCK1*, respectively in lung cancer and in osteosarcoma [22, 25, 26]. We found that miR-340 decreased the expression of both these oncogenes in three different GBM cell lines, suggesting that miR-340 may affect GBM tumorigenesis also by targeting other mRNAs (Supplementary Figure 7A).

### miR-340 blocks cell cycle and cell proliferation via inhibition of signaling pathways downstream from NRAS

AKT and ERK1/2 pathways act as major downstream signals of RAS, promoting multiple oncogenic features of RAS, such as cell proliferation and apoptosis resistance. We assessed the levels of phosphorylated (activated) forms of AKT and ERK1/2 (p-AKT and p-ERK1/2) by Western blotting in glioblastoma cells transfected with miR-340 or a control scrambled sequence. miR-340 drastically reduced p-AKT

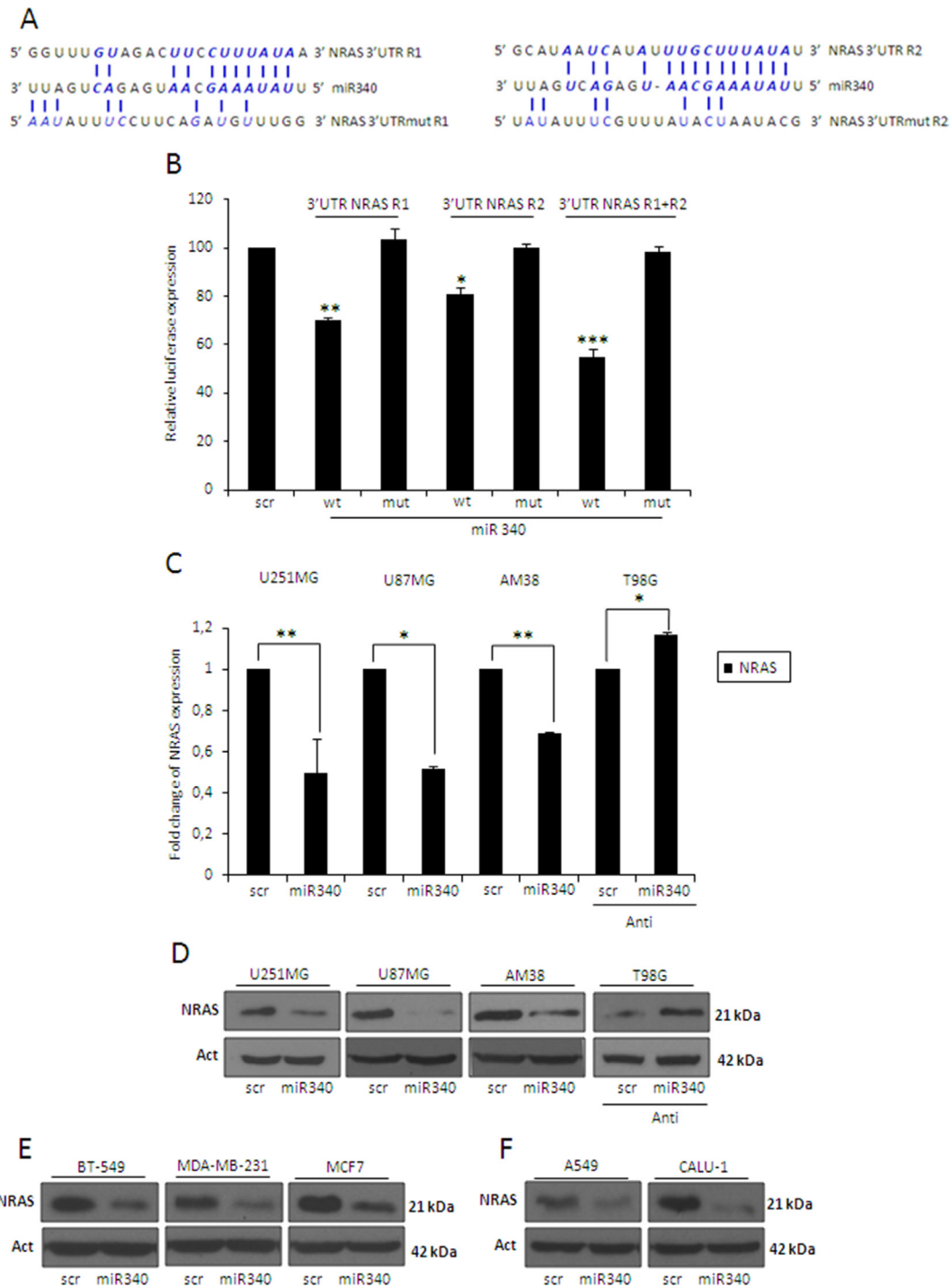


**Figure 2: miR-340 targets NRAS.** (A) Predicted miR-340 binding sites on 2 sites on *NRAS*-3'UTR (3'UTR *NRAS* R1 and 3'UTR *NRAS* R2) found with the MIRANDA algorithm ([www.microrna.org](http://www.microrna.org)) and the designed mutant sequences (3'UTR *NRAS* R1mut and 3'UTR *NRAS* R2mut). (B) *NRAS* luciferase constructs containing wild-type or mutated *NRAS*-3'UTR-R1 or -R2, were co-transfected alone or in combination with miR-340 or a scrambled miRNA in A549 cells. Luciferase activity was measured 24 h after transfection. Reporter activities of cells co-transfected with the scrambled miRNA sequence have been arbitrarily set as 100. The results were obtained from three independent experiments and are presented as mean  $\pm$  SD. In (B) *P* was calculated using ANOVA and adjusted for multiple comparisons with Bonferroni's *post hoc* testing. \**p* < 0.05; \*\**p* < 0.01; \*\*\**p* < 0.001 (over Scr). Glioblastoma cell lines (U251MG, U87MG and AM38), breast cancer cell lines (BT-549, MDA-MB-231 and MCF7), and NSCLC cell lines (A549 and Calu-1) were transfected with a scrambled miRNA sequence and miR-340, or with a scrambled anti-miR-340 sequence and anti-miR-340 in T98G cells for 72 h. Real-time PCR (C) and Western blotting (D–F) were performed to analyze *NRAS* mRNA and protein levels. Western blot analyses are from representative experiments. Actin was used as loading control. The experiments were repeated at least three times. In (C) the results are presented as mean  $\pm$  SD. *P* was calculated using Student's *t*-test. \**p* < 0.05; \*\**p* < 0.01.

and p-ERK1/2 levels in U251MG, U87MG and AM38 cells (Figure 6A). In contrast, transfection with anti-miR-340 induced an increase in p-AKT and p-ERK1/2 in T98G cells (Figure 6A). Interestingly, performing a more

comprehensive analysis of the AKT and ERK pathways, we found that miR-340 overexpression decreased the phosphorylation of other kinases of both AKT (mTOR, GSK3 $\beta$ ), and ERK pathway (ELK) (Figure 6B).

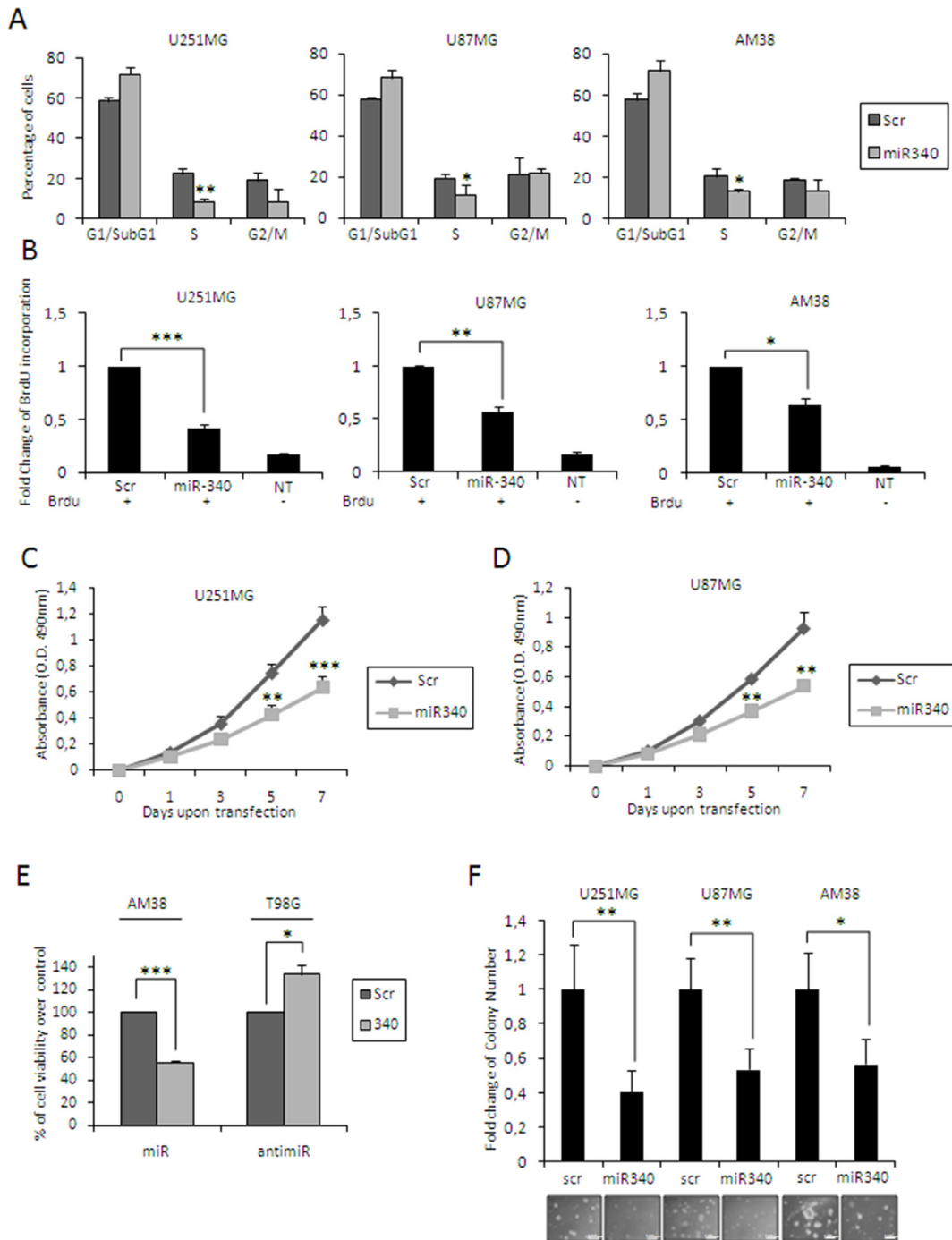


**Figure 3: miR-340's effects in glioblastoma cells.** Glioblastoma cell lines (U251MG, U87MG and AM38) were transfected with miR-340 or with a control scrambled miRNA sequence. We then analyzed: (A) cell cycle by flow cytometry after propidium iodide staining 72 h after transfection; (B) cell proliferation by BrdU incorporation assay, 3 days after transfection; (C–E) cell proliferation by MTT assay, 1, 3, 5 and 7 days after transfection (3 days for AM38); (F) anchorage-independent cell growth by Soft Agar assay, 14 days after transfection. (E) T98G cells were transfected with anti-miR-340 or a control with scrambled anti-miRNA sequence and cell proliferation analyzed with MTT 3 days after transfection. miR-340 overexpression blocked cell cycle and decreased cell proliferation and anchorage-independent cell growth. The data are representative of three independent experiments. Data are mean values  $\pm$  SD from three independent experiments.  $P$  was calculated using Student's  $t$ -test. \* $p < 0.05$ ; \*\* $p < 0.01$ ; \*\*\* $p < 0.001$ .

Next, we wondered whether miR-340-mediated blockade of cell cycle and cell proliferation was mediated by inhibition of AKT and ERK1/2 signaling pathways

downstream of NRAS. To this aim, we transfected U251MG cells with miR-340 and two constructs expressing constitutively active forms of AKT (AKT<sup>+</sup>) and

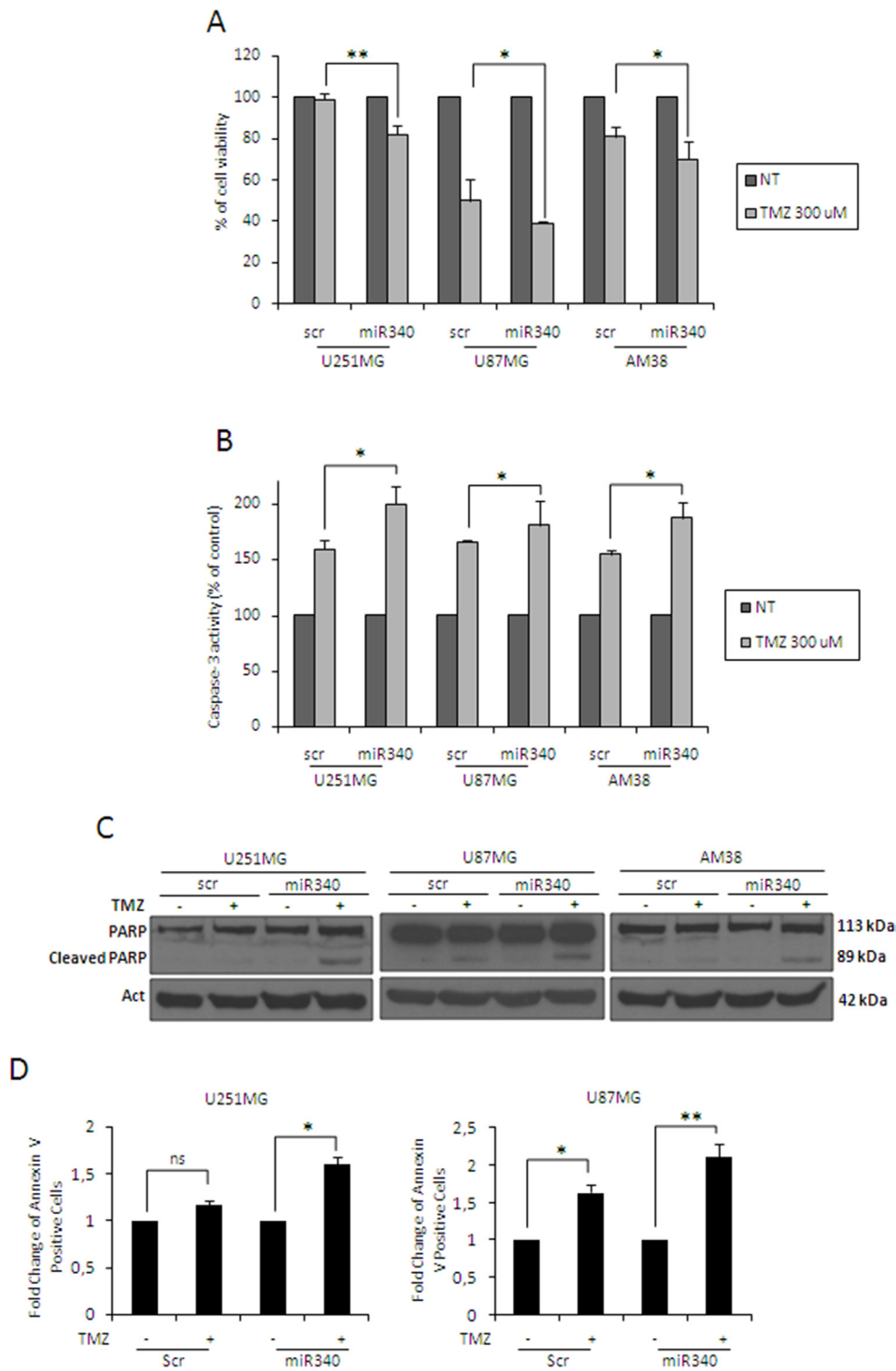


**Figure 4: miR-340 increases TMZ sensitivity in glioblastoma cells.** Glioblastoma cell lines (U251MG, U87MG and AM38) were transfected with a scrambled miRNA sequence or miR-340 for 24 h, and then treated with 300  $\mu$ M TMZ for 24 h. Cell death and apoptosis were analyzed respectively with the MTT assay (A) and caspase assay (B), western blot analysis for PARP (C), and Annexin V assay (D). miR-340 overexpression promoted TMZ-induced apoptosis. Data are mean values  $\pm$  SD of three independent experiments. *P* was calculated using Student's *t*-test. \**p* < 0.05; \*\**p* < 0.01.

ERK1 (ERK<sup>+</sup>) for 48 h, either alone or in combination. Levels of transfected AKT<sup>+</sup> and ERK<sup>+</sup> were assessed by Western blotting (data not shown). AKT<sup>+</sup> and ERK<sup>+</sup> were individually able to partially counter the effects of

miR-340 on cell cycle (Figure 7A; plots for qualitative data analysis are reported in Supplementary Figure 3D), proliferation (Figure 7B), and anchorage independent cell growth (Figure 7C); the effects were greater when AKT<sup>+</sup>

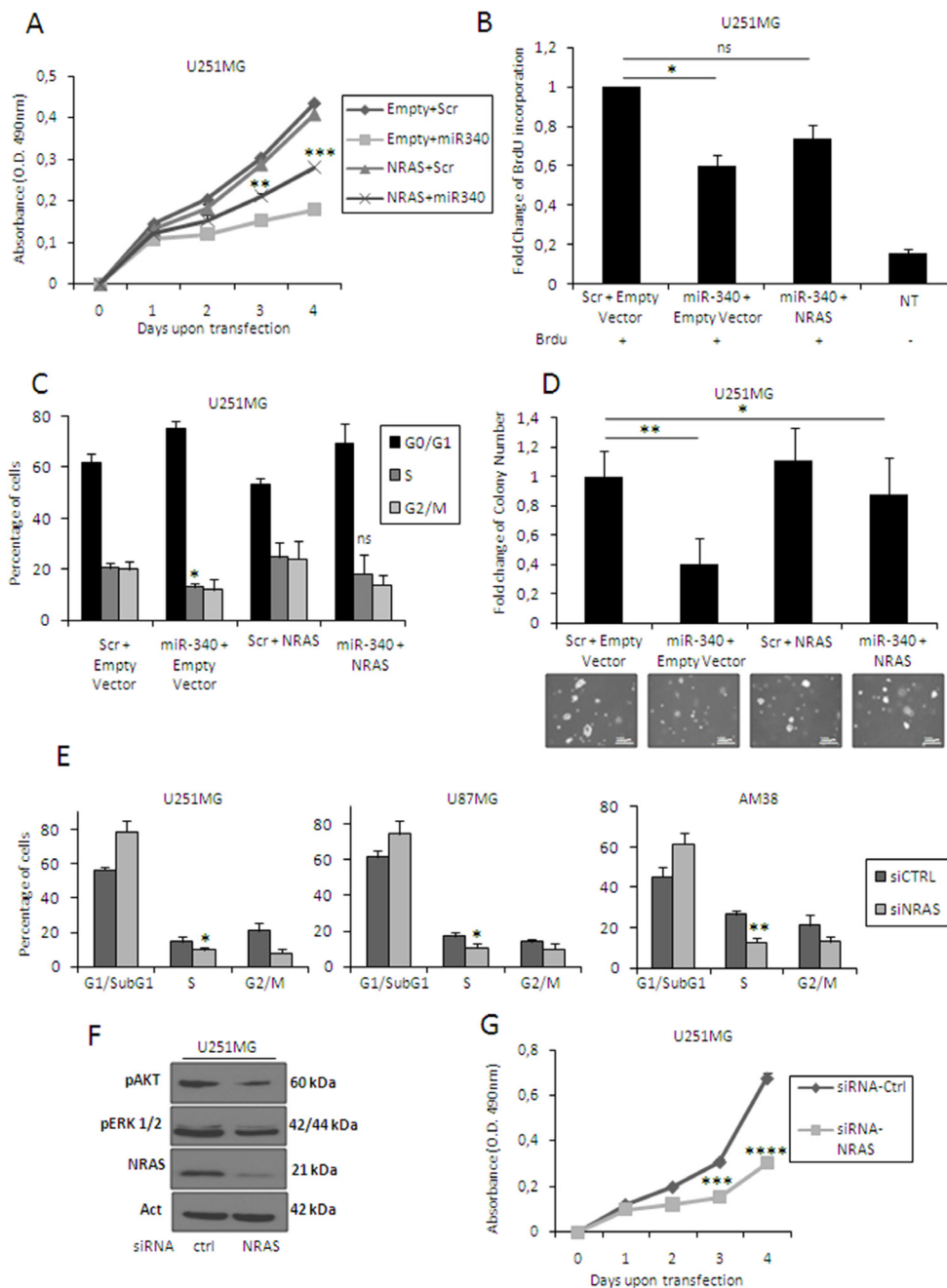


**Figure 5: NRAS mediates the effects of miR-340 on cell cycle, proliferation and anchorage-independent cell growth.** U251MG cells were co-transfected with miR-340 and either a vector carrying NRAS lacking 3'UTR or a control. Exogenous NRAS expression partially counteracted the effects of miR-340 on proliferation (A, B), cell cycle (C), and anchorage-independent growth (D). Moreover, NRAS knock-down reproduced the effects of miR-340 transfection in GBM cells. U251MG, U87MG, and AM38 cells were transfected with a control siRNA or with a specific siRNA targeting NRAS. NRAS silencing mimicked the effects of miR-340 on cell cycle (E) decreased the phosphorylation of AKT and ERK (F) and reproduced the block of proliferation induced by miR-340 transfection (G). The experiments were repeated at least three times. Presented data are mean values  $\pm$  SD of three independent experiments. Western blot analyses are representative experiments. Actin was used as the loading control. In (A–D) *P* was calculated using ANOVA and adjusted for multiple comparison with Bonferroni's *post hoc* testing (over Empty + Scr); in (E, G) *P* was calculated using Student's *t*-test. \**p* < 0.05; \*\**p* < 0.01; \*\*\**p* < 0.001; \*\*\*\**p* < 0.0001.

and ERK<sup>+</sup> were co-transfected (Figure 7A–7C). These results further support the notion that miR-340 acts as a tumor suppressor in GBM by targeting NRAS and, hence, blunting downstream AKT and ERK1/2 pathways.

### Overexpression of miR-340 inhibits GBM growth *in vivo*

To analyze the possible role of miR-340 in GBM tumorigenesis, we assessed the effects of miR-340 overexpression on tumor growth *in vivo*. To this end, we stably infected U251MG cells with a lentiviral construct expressing either miR-340 or control sequence (Supplementary Figure 8A–8B). In accordance with previous data, miR-340 stable infected cells showed a reduction of proliferation and a block of cell cycle (Supplementary Figure 8C–8D). These cells were

subcutaneously injected into the left flank ( $2 \times 10^6$  cells per flank) of CD1 nude mice ( $n = 6$  animals per group). Tumor volume and vessel formation were measured weekly by HFUS and color-doppler HFUS for 3 weeks. Tumor volume and vessel formation generated by miR-340-expressing U251MG xenografts were significantly less compared to those of control xenografts (Figure 8A, 8B). Coherently, Ki67 staining of tumor sections indicated a decrease of cell proliferation in miR-340-expressing U251MG xenografts (Figure 8C).

### DISCUSSION

GBM is one of the most aggressive types of human cancer and the most lethal form in the brain. It is characterized by extremely bad prognosis, with a median survival rate of only 12 months from diagnosis [2].

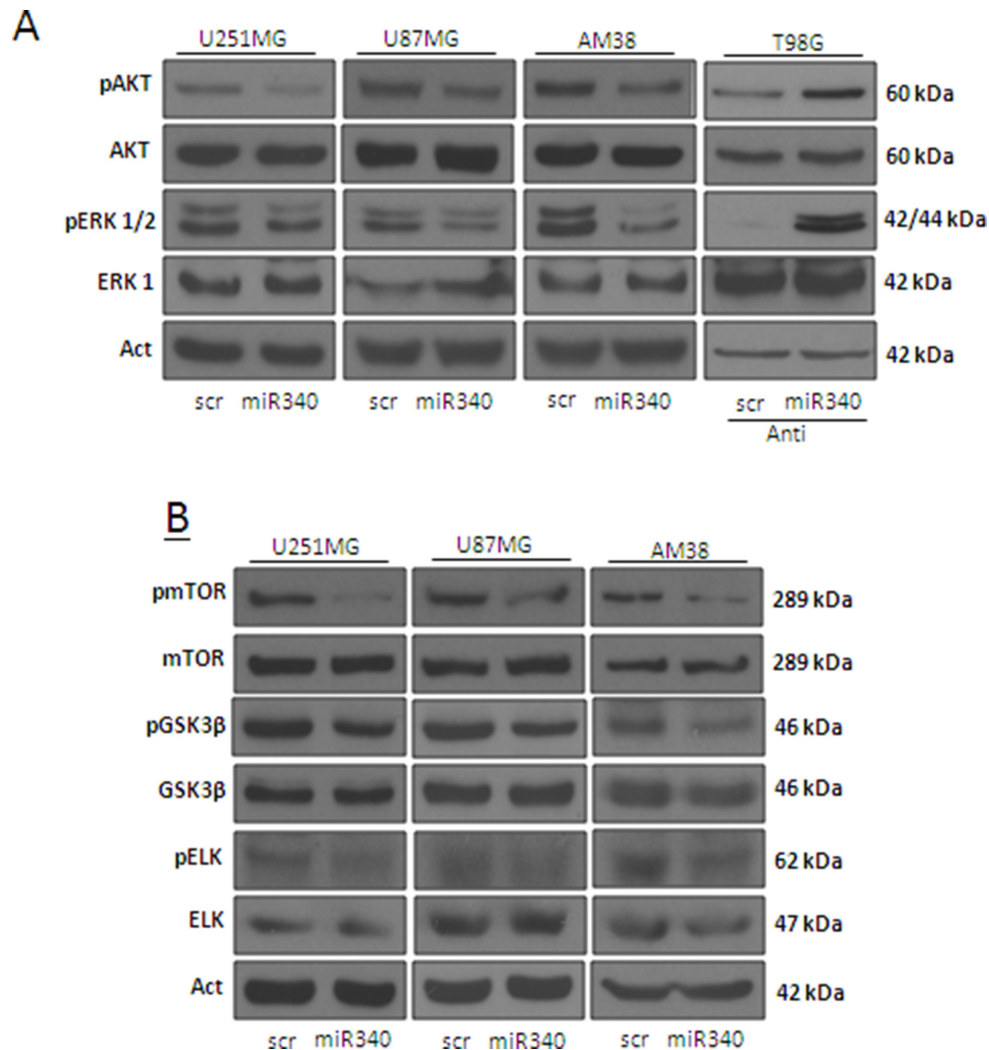


**Figure 6: miR-340 overexpression decrease the activation of molecular pathways downstream NRAS.** Glioblastoma cell lines (U251MG, U87MG and AM38) were transfected with a scrambled miRNA sequence or miR-340, or with a scrambled anti miRNA sequence or anti miR-340, in T98G cells, for 72 h. Western blotting was performed to analyze pAKT and pERK1/2 (A) and pmTOR, pGSK3β, and pELK protein levels (B) Western blot analyses are representative experiments. Actin was used as the loading control. The experiments were repeated at least three times.

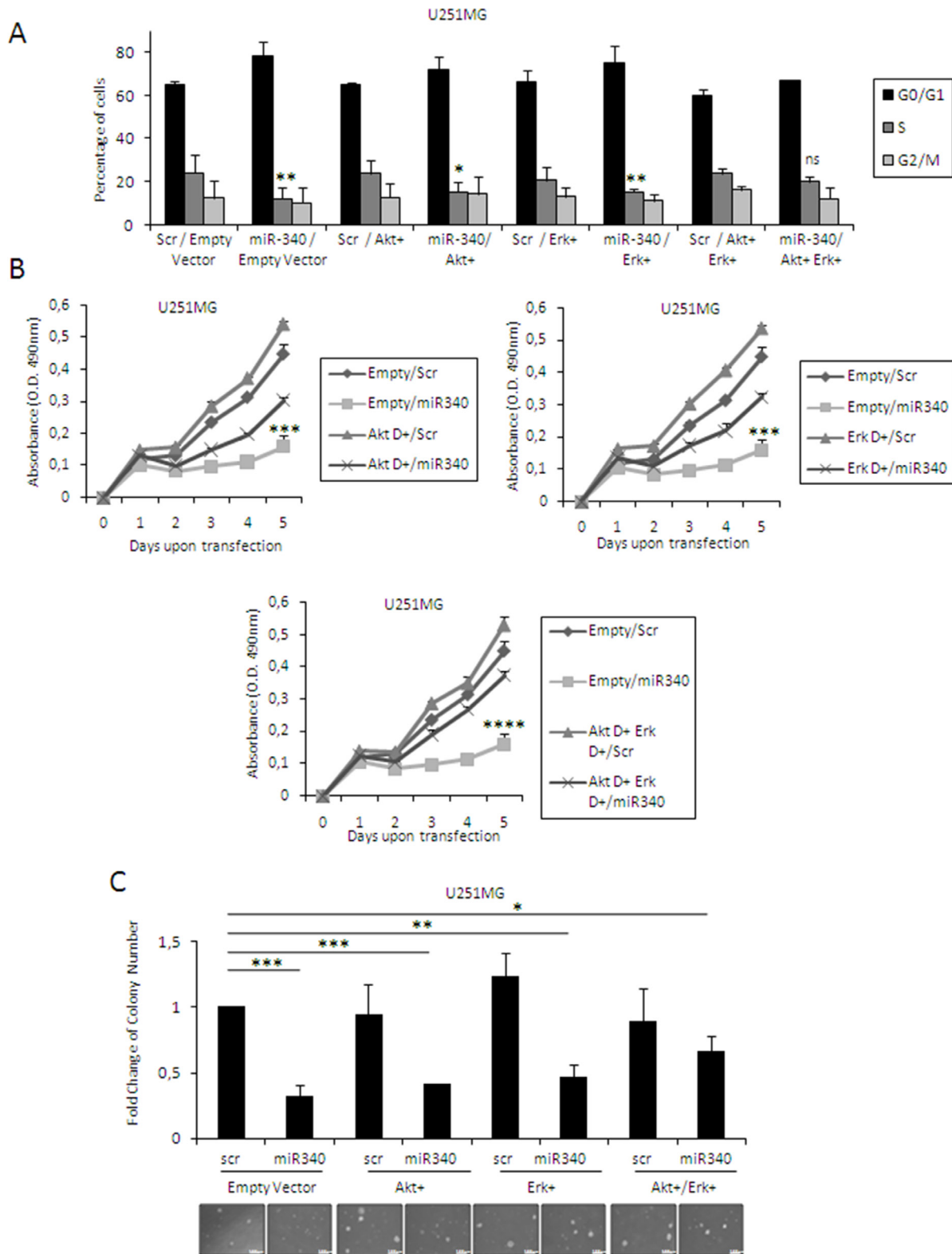


**Figure 7: Molecular pathways downstream from NRAS mediate the effects of miR-340 GBM cells.** U251MG glioblastoma cells were co-transfected with miR-340 and dominant active mutants constructs of ERK and AKT, alone or in combination, or with control vector. Exogenous dominant active expression of both ERKs and AKT was able to partially counteract the effects of miR-340 on cell cycle (A) proliferation (B) and anchorage independent cell growth (C) The experiments were repeated at least three times. Presented data are mean values  $\pm$  SD of three independent experiments. In (A)  $P$  was calculated using Student's  $t$ -test. In (B, C)  $P$  was calculated using ANOVA and adjusted for multiple comparisons with the Bonferroni's *post hoc* testing. \* $p < 0.05$ ; \*\* $p < 0.01$ ; \*\*\* $p < 0.001$ ; \*\*\*\* $p < 0.0001$  (over Empty + Scr).

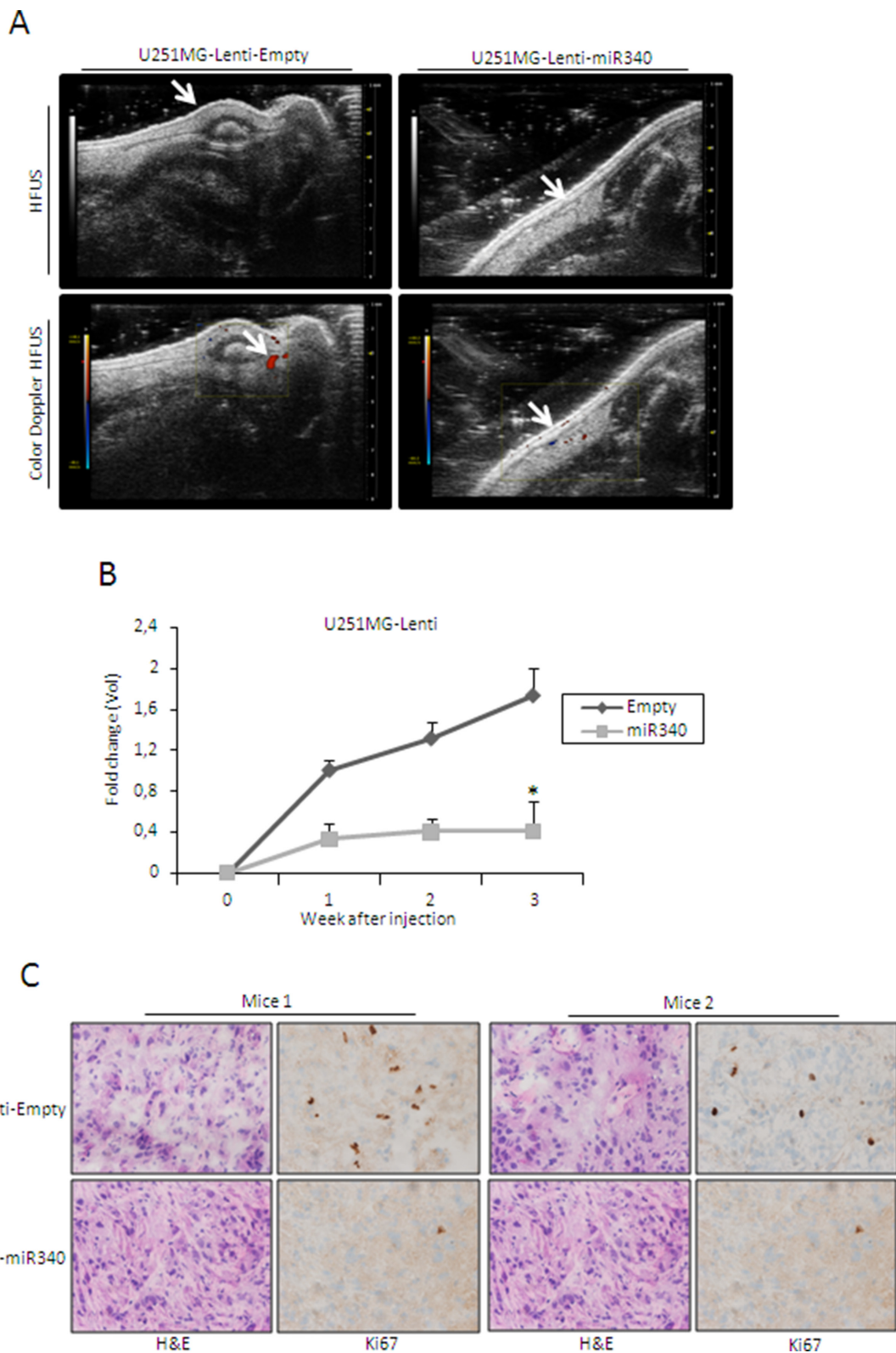


**Figure 8: miR-340 inhibits the growth of glioblastoma xenografts *in vivo*.** U251MG cells stably transduced with a lentiviral vector encoding miR-340 or with control particles were subcutaneously injected into the left flank of CD1 nude mice ( $n = 6$  per group). Tumor volume and vessel formation were measured weekly by HFUS and color-doppler HFUS (Vevo 2100 with a 40MHz probe) for three weeks. Data in (A) and (B) show that treatment with miR-340 reduced glioblastoma-derived xenograft growth and vessel formation. In (B)  $P$  was calculated using Student's  $t$ -test.  $*p < 0.05$ . (C) Nuclear localization of Ki67 staining and HE staining of xenograft mice injected with U251MG-Lenti-Empty expressing cells and U251MG-Lenti-miR340 overexpressing cells. A representative area of each tissue is represented. Two mice for each experimental point are represented. Magnification 40x (Figure 8C).

Interestingly, a small subgroup of patients survives longer. Better understanding of the specific molecular features underlying this LTS phenotype may lead to improved diagnosis, prognosis, treatment and, ultimately, survival of GBM patients [4]. At present, several molecular markers have been correlated to GBM prognosis, but they need further validation before they can be used in the clinical setting [28]. However, despite great effort over the last years, the cellular and molecular features of LTS have not been properly elucidated.

In the last decade, microRNAs have been frequently found deregulated in different human cancers, acting both as oncogenes or tumor suppressors. miRNAs are involved in basic cellular functions, including proliferation, cell death, differentiation, metabolism and, importantly, tumorigenesis [7–11, 13]. In addition, these noncoding RNAs have the capacity to target tens to hundreds of genes simultaneously [6]. Thus, they are attractive candidates as prognostic biomarkers and therapeutic tools/targets in cancer. Several studies have demonstrated that the expression of miRNAs is deregulated in gliomas [12, 14, 15, 18] and may affect GBM tumorigenesis [32–34]. More importantly, several reports have established a direct link between miRNA signatures and GBM prognosis [35–38]. In the present study, we identify miR-340 as a tumor-suppressive miRNA in GBM. Our experimental data, together with that obtained from TCGA database, show that miR-340 expression is significantly higher in LTS compared to STS patients, and in normal brain compared to GBM. Furthermore, statistical analysis revealed that patients with higher miR-340 expression had a longer survival rate and, thus, a better prognosis. Taken together, these data suggest that higher expression of miR-340 is a significant predictor of good prognosis in GBM.

Our functional studies show that overexpression of miR-340 in GBM cells determines a significant block of cell cycle, inhibition of cell proliferation, decrease of anchorage-independent cell growth, and an increase in sensitivity to TMZ. Furthermore, miR-340 directly binds to two different sites on the 3'UTR of *NRAS* mRNA to strongly inhibit *NRAS* protein expression. The *RAS* protein family consists of 4 highly homologous enzymes (*NRAS*, *HRAS*, *KRAS4A* and *KRAS4B*) that act as signaling molecules for the regulation of cell fate: they couple receptor activation to downstream effector pathways controlling different cellular responses, such as proliferation, resistance to therapy and survival [16]. Activating mutations of *RAS* proteins are common in human cancers, especially in hematopoietic cancers, colorectal cancer and melanoma [29–31]. In glioblastoma, *NRAS* activation could be caused by a direct mutation (5%) or by other alterations, such as amplification, overexpression of growth factor receptor or aberrations in other *RAS* pathway genes [17]. Recently, several miRNAs – including miR-181d, let-7 and miR-143– were reported to suppress *RAS* expression and function as tumor

suppressors, suggesting that miRNAs targeting *RAS* may have an important role in carcinogenesis [18–20]. Our findings indicate that miR-340's targeting of *NRAS* leads to a decrease in the activation of downstream pathways (namely *AKT* and *ERKs*). Experiments using dominant positive mutants of *AKT* and *ERKs* clearly show that both these pathways are down-regulated by a miR-340-mediated effect in GBM. Thus, we have identified a new link between miR-340 and *NRAS*, a novel player in GBM tumorigenesis.

miR-340 has been shown to have a tumor-suppressive activity also in other types of cancer. Wu et al. reported that miR-340 suppressed cell growth in breast cancer [21]; in osteosarcoma, miR-340 was found down-regulated compared to normal tissue, and *ROCK-1* was identified as a miR-340 target [22, 26]; Poenitzsch et al. demonstrated for the first time the pleiotropic regulation of the *RAS-RAF-MAPKs* pathway by miR-340 in melanoma, which resulted in a strong tumor-suppressive activity [24]; Fernandez et al. characterized the tumor-suppressive activity of miR-340 in lung cancer, where it mediated cell growth inhibition and apoptosis activation via the accumulation of p27 [25]; Yamashita et al. reported that miR-340 suppressed the stem-like cell function of glioma-initiating cells *in vitro* and in nude mouse brain – their findings indicated that miR-340 acted as a tumor suppressor in glioma-initiating cells, particularly affecting gliomagenesis and extensive tumor invasion [23]. Recently Huang et al. reported that miR-340 was able to inhibit glioblastoma tumorigenesis [27].

In the present study, we show that lentiviral vector-mediated overexpression of miR-340 in GBM cells inhibits cell growth in nude mice, suggestive of its possible therapeutic use.

In conclusion, we have observed for the first time a direct link between miR-340 expression and survival in GBM, demonstrating that miR-340 has a powerful oncosuppressive effect *in vitro* and *in vivo*. The mechanism is mediated, at least in part, by the targeting of *NRAS* and the consequential blunting of downstream *ERKs* and *AKT* pathways. We propose miR-340 as a novel biomarker for GBM prognosis, as well as a new therapeutic agent for the amelioration of GBM patient survival.

## MATERIALS AND METHODS

### Cells and tissue specimens

Glioblastoma cell lines T98G, U87MG, LN229 and LN18, breast cancer cell lines BT549, MDA-MB-231, MCF7, and NSCLC cell lines A549 and CALU-1 were obtained from American Type Culture Collection (ATCC), (LG Standards, Milan, Italy); U251MG, LN428, LN308, SF767 and A172 were kindly donated by Frank Furnari (La Jolla University, San Diego, CA, USA). U87MG, U251MG, T98G, AM38, A172, LN319, LN308, LN428,

SF767, MCF7 and Calu-1 were grown in Dulbecco's modified eagle's Medium, LN18 and LN229 in Advanced Dulbecco's modified eagle's Medium, and BT-549, MDA-MB-231 and A549 in RPMI Medium. Media were supplemented with 10% heat-inactivated fetal bovine serum (FBS) –5% FBS for LN229 and LN18– 2 mM L-glutamine and 100 U/ml penicillin/streptomycin. All media and supplements were from Sigma Aldrich (Milan, Italy).

A total of 61 formalin-fixed, paraffin-embedded (FFPE) tissue samples were collected from the archives of the Department of Pathology, University Hospital of Kuopio, Finland. Among the 61 samples, survival information for 43 cases was available. Permission to use the material was obtained from the National Supervisory Authority for Welfare and Health of Finland, and the study was accepted by the ethical committee of the Northern Savo Hospital District, Kuopio, Finland. Informed consent was obtained from each subject or subject's guardian.

### TCGA data analysis

The collection of data from The Cancer Genome Atlas (TCGA) platform was compliant with laws and regulations for the protection of human subjects, and necessary ethical approvals were obtained. Analysis of all data was done using GraphPad Prism 6 (San Diego, CA, USA). For differential expression analysis and determination of the effect of miR-340 and *NRAS* on patient's survival, we downloaded Agilent 8 × 15 miRNA expression (level 2) and HT\_HG-U133A (level 3) along with clinical information from the TCGA database in April 2014.

### Cell transfection

For transient overexpression of miRNAs and siRNAs, cells at 50% confluence were transfected using Oligofectamine (Invitrogen, Milan, Italy) and 100 nM of pre-miR-340, scrambled miRNA, anti-miR-340, scrambled anti-miRNA (Ambion®, Life Technologies), siNRAS or a siRNA control (Santa Cruz Biotechnologies, MA, USA). For transient overexpression of 4 µg of pcDNA3-NRAS, pcDNA3-AKT<sup>+</sup>, pcDNA3-ERK<sup>+</sup> or pcDNA3, cells were transfected using X-tremeGENE 9 DNA Transfection Reagent (Roche, Milan, Italy). Temozolomide (TMZ) was purchased from Sigma Aldrich (Milan, Italy).

### RNA extraction and real-time PCR

*Cell culture:* Total RNA (microRNA and mRNA) was extracted using Trizol (Invitrogen, Milan, Italy) according to the manufacturer's protocol. *Tissue specimens:* total RNA (miRNA and mRNA) from FFPE tissue specimens was extracted using RecoverAll Total Nucleic Acid isolation Kit (Ambion, Life Technologies,

Milan, Italy) according to the manufacturer's protocol. Reverse transcription of total RNA was performed starting from equal amounts of total RNA/sample (500 ng) using miScript reverse Transcription Kit (Qiagen, Milan, Italy) for miRNA analysis, and with SuperScript® III Reverse Transcriptase (Invitrogen, Milan, Italy) for mRNA analysis. Quantitative analysis of miR-340 and RNU6A (the latter as an internal reference) were performed by RT-PCR using specific primers (Qiagen, Milan, Italy) and miScript SYBR Green PCR Kit (Qiagen, Milan, Italy). RT-PCR was also used to assess the mRNAs of NRAS, KRAS, HRAS and β-actin (the latter as an internal reference), using iQTM SYBR Green Supermix (Bio-Rad, Milan, Italy). The primer sequences were: NRAS-Fw: 3'-CGCACTGACAATCCAGCTAA-5'; NRAS-Rv: 3'-TCGCTGTCCTCATGTATTG-5'; K-RAS-Fw: 3'-ACTGGGGAGGGCTTTCTTTG-5'; K-RAS-Rv: 3'-GGCATCATCAACACCCTGTCT-5'; H-RAS: Fw: 3'-TATAAGCTGGTGGTGGTGGG-5'; H-RAS-Rv: 3'-TGATGGCAAACACACACAGG-5'; Act-FW: 5'-TGCGTGACATTAAGGAGAAG-3'; Act-Rv: 5'-GCTCGTAGCTCTTCTCCA-3'.

The reaction for detection of mRNAs was performed in this manner: 95°C for 5 min, 40 cycles of 95°C for 30 s, 60°C for 30 s and 72°C for 30 s. The reaction for detection of miRNAs was performed in this manner: 95°C for 15 min, 40 cycles of 94°C for 15 s, 55°C for 30 s and 70°C for 30 s. All reactions were run in triplicate. The threshold cycle (CT) was defined as the fractional cycle number at which the fluorescence passed the fixed threshold. For relative quantization, the 2<sup>(-ΔΔCT)</sup> method was used. Experiments were carried out in triplicate for each data point, and data analysis was performed with Applied Biosystems' StepOnePlus™ Real-Time PCR System.

### miRNA expression microarray and data analysis

From each sample, 5 µg of total RNA (from 3 long- and 3 short-term GBM survivors) was reverse transcribed using biotin end-labeled random octamer oligonucleotide primer. Hybridization of biotin-labeled cDNA was performed on an Ohio State University custom miRNA microarray chip (OSU\_CCC version 3.0), which contained 1150 miRNA probes, including 326 human and 249 mouse miRNA genes, spotted in duplicates. The hybridized chips were washed and processed to detect biotin-containing transcripts with a streptavidin-Alexa647 conjugate and scanned on an Axon 4000B microarray scanner (Axon Instruments, Sunnyvale, CA, USA). Raw data were normalized and analyzed with GENESPRING 7.2 software (zcomSilicon Genetics, Redwood City, CA, USA). Expression data were median-centered with the GENESPRING normalization option and with the BIOCONDUCTOR package (www.bioconductor.org) global median normalization tool, with similar results. Statistical comparisons were done with the GENESPRING

ANOVA tool, predictive analysis of microarray and the significance analysis of microarray software (<http://www.stat.stanford.edu/Btibbs/SAM/index.html>).

### **Establishment of glioblastoma cells stably expressing miR-340**

Lentiviral vectors encoding an expression cassette containing a puromycin resistance gene, the green fluorescent protein (GFP) gene and the miR-340 sequence under the hCMV promoter were purchased from GE Healthcare Dharmacon (Milan, Italy). U251MG cells were infected with the miR-340 lentiviral vector or with an empty, control vector (which lacked the miR-340 sequence) at a final concentration of 20 MOI. After culturing in selection media supplemented with puromycin, GFP was detected by fluorescence microscopy (original magnification 10x; scale bar 100  $\mu$ m), and representative images were collected using the Leica Application Suite X (LAS X) software (Leica, Milan, Italy). Finally, puromycin-resistant, GFP-positive clones were picked.

### **Protein isolation and Western blotting**

Cells were lysed in JS buffer (50 mM HEPES, pH 7.5, containing 150 mM NaCl, 1% glycerol, 1% Triton X-100, 1.5 mM MgCl<sub>2</sub>, 5 mM EGTA, 1 mM Na<sub>3</sub>VO<sub>4</sub>, and 1X protease inhibitor cocktail). Protein concentration was determined with the Bradford assay (BioRad, Milan, Italy) using bovine serum albumin as the standard, and equal amounts of proteins were analyzed by SDS-PAGE (12% acrylamide). Gels were electroblotted into nitrocellulose membranes (G & E Healthcare, Milan, Italy). Membranes were blocked for 1 h with 5% non-fat dry milk in tris-buffered saline (TBS) containing 0.1% Tween-20, and incubated at 4°C overnight with the primary antibody. Detection was performed by peroxidase-conjugated secondary antibodies, using the enhanced chemiluminescence system (Thermo Euroclone, Milan, Italy). Primary antibodies used were: anti-NRAS, anti-ERK1, anti-SKP2, anti-ROCK1 (Santa Cruz Biotechnologies, MA, USA), anti-pP42/44, anti-pAKT, anti-AKT, anti-pmTOR, anti-mTOR, anti-pGSK3 $\beta$ , anti-GSK3 $\beta$ , anti-pELK, anti-ELK (Cell Signaling, Danvers, MA, USA), and anti- $\beta$ -actin (Sigma Aldrich, Milan, Italy).

### **MTT assay**

Cell vitality was evaluated with the CellTiter 96<sup>®</sup> AQueous One Solution Cell Proliferation Assay (Promega, Madison, WI, USA), according to the manufacturer's protocol. The assay is based on reduction of 3-(4,5-dimethylthiazol-2-yl)-5-(3-carboxymethoxyphenyl)-2-(4-sulfophenyl)-2H-tetrazolium, inner salt (MTS) to a colored product that is measured spectrophotometrically.

After 24 h from miRNA or siRNA transfection, cells ( $1 \times 10^3$ ) were plated in 96-well plates in triplicate and incubated at 37°C in a 5% CO<sub>2</sub> incubator. Metabolically active cells were detected by adding 20  $\mu$ l of MTS to each well; after 30 min of incubation, the plates were analyzed on a Multilabel Counter (Bio-Rad, Richmond, VA, USA).

### **BrdU incorporation assay**

Cell proliferation was evaluated with the *In Situ* Cell Proliferation Kit, FLUOS (Sigma Aldrich, Milan, Italy), according to the manufacturer's protocol. The assay is based on the incorporation of BrdU only in actively proliferating cells. Cells were plated in p100 plates and transfected with miR-340 or scrambled sequence. After 72 h, proliferating cells were detected by adding BrdU to each plate; after 4 h of incubation, the cells were fixed and labeled with anti-BrdU antibody conjugated with fluorescein for 45 min. Then, BrdU incorporation were detected with a Becton Dickinson FACScan flow cytometer.

### **Cell cycle analysis**

Cell cycle was analyzed via propidium iodide (PI) incorporation in permeabilized cells by flow cytometry. The cells ( $5 \times 10^4$ ) were washed in PBS and resuspended in 200  $\mu$ l of a solution containing 0.1% sodium citrate, 0.1% triton X-100 and 50  $\mu$ g/ml propidium 6 iodide (Sigma Aldrich, Milan, Italy). Following incubation at 4°C for 30 min in the dark, nuclei were analyzed with a Becton Dickinson FACScan flow cytometer. Cellular debris was excluded from analyses by raising the forward scatter threshold, and the DNA content of the nuclei was registered on a logarithmic scale. The percentage of elements in the hypodiploid region was calculated.

### **Soft-agar assay**

$1 \times 10^4$  cells were plated in 60mm dishes in a solution containing Dulbecco's modified Eagle's medium 2  $\times$  (Sigma, St Louis, MO, USA), TPB buffer (Difco, BD, Franklin Lakes, NJ, USA), and 1.25% Noble Agar (Difco, BD, Franklin Lakes, NJ, USA). Briefly, cells were harvested and counted, then a layer of 7 ml of Noble Agar solution was left to polymerize on the bottom of the dishes. Then cells were resuspended in 2 ml of same solution and plated. Cells were left to grow for 2 weeks in the incubator.

### **Cell death quantification and caspase assay**

Cells were transfected with miRNAs as described and were plated in 96-well plates in triplicate, treated, and incubated at 37°C in a 5% CO<sub>2</sub> incubator. Temozolomide was used at a final concentration of 300  $\mu$ M for 24 h. Cell viability was assessed using the CellTiter 96<sup>®</sup> AQueous

One Solution Cell Proliferation Assay (Promega, Madison, WI, USA), as described above. Apoptosis activation was analyzed with the Caspase-Glo® 3/7 Assay System (Promega, Madison, WI, USA), as reported in the instruction manual. Briefly, cells were incubated with medium supplemented with caspase 3/7 reagent; luminescence was measured following incubation for 30 min at room temperature.

### Apoptosis assessment by Annexin V staining

GBM cells were transfected with miR-340 or scrambled sequence. After 48 h, cells were treated with 300 µM of TMZ for 24 h, harvested, washed twice with cold PBS, and stained with Annexin V-FITC Apoptosis Detection Kit 1 (BD Pharmingen, Milan, Italy). Briefly, cells were resuspended in 100 µL of 1 × binding buffer and 5 µL of Annexin V and then incubated for 15 min at room temperature. Apoptotic cells were analyzed by flow cytometry.

### Rescue experiments

To determine whether *NRAS* mediated the effect of miR-340, rescue experiments were performed in which the effects of miR-340 were measured in the setting of overexpression of a deletion mutant of *NRAS*, i.e., one lacking the 3' untranslated region (UTR). Cells were transfected with miR-340 and with the mutant *NRAS* vector, using X-tremeGENE 9 DNA Transfection Reagent (Roche, Milan, Italy), as described. Growth and cell cycle were assessed as above.

### In vivo tumor formation

Five-week-old female CD1 nude mice (Charles River, Milan, Italy) were maintained in special pathogen free conditions for one week. The animal protocols used in this work were evaluated and approved by the Animal Use and Ethic Committee (OBA) of the Institute Ceinge, Biotecnologie Avanzate s.c.a.r.l. (Protocol 15/1/14\_n 4). The animals protocols were performed in accordance with FELASA guidelines and the guidelines defined by the European Communities Council directive (2010/63/EU). The investigators adhere to widely accepted national standards. U251MG cells stably expressing either miR-340 or miR-Empty were injected subcutaneously into the left flank of the nude mice ( $2 \times 10^6$  cells in 100 µl). Tumor size was assessed weekly with a Vevo 2100 equipment (FUJIFILM VisualSonics, Inc., Toronto, Ontario, Canada), an high-frequency ultrasound (HFUS) system mounting a 40 MHz probe, 1, 2, and 3 weeks after cells injection. The procedures were performed under general anesthesia with 2% isoflurane in 100% oxygen at 0.8 L/min. For each tumor, mediolateral, anteroposterior and craniocaudal diameters were measured. Tumor volume (TV) was

calculated according to the formula  $V = (\text{height} \times \text{width} \times \text{length} \times 3.14)/6$ .

### Immunohistochemical staining and evaluation

Xenograft fresh frozen tissue were embedded in OCT compound and were cut in sections of 5 µm thickness. Staining was performed with an automatic Benchmark XT staining machine (Ventana Medical Systems Inc., Tucson, AZ, USA) with an antihuman KI67 (Ventana) antibody according to manufacture procedure. KI67 nuclear staining intensity was evaluated by one expert pathologist. For H & E staining, 2.5 µm sections of all fixed samples were mounted on superfrost slides and performed using standard methodology.

### Luciferase assay

The two predicted regions on the 3'UTR of the human *NRAS* gene (R1 and R2) containing the putative miR-340 binding site were PCR amplified using the following primers: NRAS-R1-FW: 3'-GCTCTAGATGGCATCTGCTCTAGATTCATAAA-5'; NRAS-R1-Rv: 3'-GCTCTAGATGGCATCTGCTCTAGATTCATAAA-5'; NRAS-R2-FW: 3'-GCTCTAGACTATTTAGTGGGCCCATGTT-5'; NRAS-R2-Rv: 3'-GCTCTAGACAAGAAGCAGAACGCACC-5', and cloned downstream of the Renilla luciferase stop codon in a pGL3 control vector (Promega, Milan, Italy). An inverted sequence of the miRNA-binding sites was used as the negative control. A549 cells were transfected with miR-340 or a scrambled miRNA for 6 h. Then, the cells were co-transfected with 1.2 µg of 3'UTR NRAS-R1 or -R2 plasmids, or relative mutant constructs, plus 400 µg of a Renilla luciferase expression construct, pRL-TK (Promega, Milan, Italy), with Lipofectamine 2000 (Life Technologies, Milan, Italy). Cells were harvested 24 h post-transfection, and the luciferase activity assayed with Dual Luciferase Assay (Promega, Milan, Italy), according to the manufacturer's instructions. Three independent experiments were performed in triplicate.

### Statistical analysis

All experiments were repeated at least three times. Continuous variables are given as mean  $\pm$  1 standard deviation (SD). For two-groups comparison, Student's *t*-test was used to determine differences between mean values for normal distribution. Comparisons among more than two groups were determined by one-way ANOVA followed by Bonferroni's *post hoc* testing. Survival was illustrated by Kaplan-Meier curves; survival differences between groups were examined with log-rank test. All data were analyzed for significance using GraphPadPrism 6 software (San Diego, CA, USA); a probability level  $< 0.05$  was considered significant throughout the analysis.

## ACKNOWLEDGMENTS

We thank Micheal Latronico for critically reading the manuscript, Simona Romano for FACS Analysis, and Luigi Terracciano for his help with the histological analysis.

## FINANCIAL SUPPORT

This work was partially supported by funds from Associazione Italiana Ricerca sul Cancro (AIRC, grant no.10620) to G.C.; MERIT (RBNE08E8CZ\_002) to G.C.; POR Campania FSE 2007-2013, Project CREME to G.C.; and Fondazione Berlucci to G.C.

## CONFLICTS OF INTEREST

The authors disclose no potential conflicts of interest

## REFERENCES

- Porter KR, McCarthy BJ, Freels S, Kim Y, Davis FG. Prevalence estimates for primary brain tumors in the United States by age, gender, behavior, and histology. *Neuro Oncol*. 2010; 12:520–7.
- Tran B, Rosenthal MA. Survival comparison between glioblastoma multiforme and other incurable cancers. *J Clin Neurosci*. 2010; 17:417–21.
- Louis DN, Ohgaki H, Wiestler OD, Cavenee WK, Burger PC, Jouvet A, Scheithauer BW, Kleihues P. The 2007 WHO classification of tumours of the central nervous system. *Acta Neuropathol*. 2007; 114:97–109.
- Krex D, Klink B, Hartmann C, von Deimling A, Pietsch T, Simon M, Sabel M, Steinbach JP, Heese O, Reifenberger G, Weller M, Schackert G; German Glioma Network. Long-term survival with glioblastoma multiforme. *Brain*. 2007; 130:2596–606.
- Stupp R, Hegi ME, Mason WP, van den Bent MJ, Taphoorn MJ, Janzer RC, Ludwin SK, Allgeier A, Fisher B, Belanger K, Hau P, Brandes AA, Gijtenbeek J, et al. Effects of radiotherapy with concomitant and adjuvant temozolomide versus radiotherapy alone on survival in glioblastoma in a randomised phase III study: 5-year analysis of the EORTC-NCIC trial. *Lancet Oncol*. 2009; 10:459–66.
- Bartel DP. MicroRNAs: genomics, biogenesis, mechanism, and function. *Cell*. 2004; 116:281–97.
- Calin GA, Dumitru CD, Shimizu M, Bichi R, Zupo S, Noch E, Aldler H, Rattan S, Keating M, Rai K, Rassenti L, Kipps T, Negrini M, et al. Frequent deletions and down-regulation of micro- RNA genes miR15 and miR16 at 13q14 in chronic lymphocytic leukemia. *Proc Natl Acad Sci U S A*. 2002; 99:15524–9.
- Johnson SM, Grosshans H, Shingara J, Byrom M, Jarvis R, Cheng A, Labourier E, Reinert KL, Brown D, Slack FJ. RAS is regulated by the let-7 microRNA family. *Cell*. 2005; 120:635–47.
- Costinean S, Zanesi N, Pekarsky Y, Tili E, Volinia S, Heerema N, Croce CM. Pre-B cell proliferation and lymphoblastic leukemia/high-grade lymphoma in E(mu)-miR155 transgenic mice. *Proc Natl Acad Sci USA*. 2006; 103: 7024–9.
- Croce CM. Causes and consequences of microRNA dysregulation in cancer. *Nat Rev Genet*. 2009; 10:704–14.
- Tavazoie SF, Alarcon C, Oskarsson T, Padua D, Wang Q, Bos PD, Gerald WL, Massagué J. Endogenous human microRNAs that suppress breast cancer metastasis. *Nature*. 2008; 451:147–52.
- Ciafre SA, Galardi S, Mangiola A, Ferracin M, Liu CG, Sabatino G, Negrini M, Maira G, Croce CM, Farace MG. Extensive modulation of a set of microRNAs in primary glioblastoma. *Biochem Biophys Res Commun*. 2005; 334: 1351–8.
- Calin GA, Croce CM. MicroRNA signatures in human cancers. *Nat Rev Cancer*. 2006; 6:857–66.
- Chan JA, Krichevsky AM, Kosik KS. MicroRNA-21 is an antiapoptotic factor in human glioblastoma cells. *Cancer Res*. 2005. 65:6029–33.
- Hermansen SK, Kristensen BW. MicroRNA biomarkers in glioblastoma. *J Neurooncol*. 2013; 114:13–23.
- Schubbert S, Shannon K, Bollag G. Hyperactive Ras in developmental disorders and cancer. *Nat Rev Cancer*. 2007; 7:295–308.
- Knobbe CB, Reifenberger J, Reifenberger G. Mutation analysis of the Ras pathway genes NRAS, HRAS, KRAS and BRAF in glioblastomas. *Acta Neuropathol*. 2004; 108:467–70.
- Lee ST, Chu K, Oh HJ, Im WS, Lim JY, Kim SK, Park CK, Jung KH, Lee SK, Kim M, Roh JK. Let-7 microRNA inhibits the proliferation of human glioblastoma cells. *J Neurooncol*. 2011; 102:19–24.
- Wang XF, Shi ZM, Wang XR, Cao L, Wang YY, Zhang JX, Yin Y, Luo H, Kang CS, Liu N, Jiang T, You YP. MiR-181d acts as a tumor suppressor in glioma by targeting K-ras and Bcl-2. *J Cancer Res Clin Oncol*. 2011; 138:573–84.
- Wang L, Shi ZM, Jiang CF, Liu X, Chen QD, Qian X, Li DM, Ge X, Wang XF, Liu LZ, You YP, Liu N, Jiang BH. MiR-143 acts as a tumor suppressor by targeting NRAS and enhances temozolomide-induced apoptosis in glioma. *Oncotarget*. 2014; 5:5416–27. doi: 10.18632/oncotarget.2116.
- Wu ZS, Wu Q, Wang CQ, Wang XN, Huang J, Zhao JJ, Mao SS, Zhang GH, Xu XC, Zhang N. miR-340 inhibition of breast cancer cell migration and invasion through targeting of oncoprotein c-Met. *Cancer*. 2011; 117:2842–52.
- Zhou X, Wei M, Wang W. MicroRNA-340 suppresses osteosarcoma tumor growth and metastasis by directly targeting ROCK1. *Biochem Biophys Res Commun*. 2013; 437:653–8.
- Yamashita D, Kondo T, Ohue S, Takahashi H, Ishikawa M, Matoba R, Suehiro S, Kohno S, Harada H, Tanaka J,

- Ohnishi T. miR340 suppresses the stem-like cell function of glioma-initiating cells by targeting tissue plasminogen activator. *Cancer Res.* 2015; 75:1123–33.
24. Poenitzsch Strong AM, Setaluri V, Spiegelman VS. MicroRNA-340 as a modulator of RAS-RAF-MAPK signaling in melanoma. *Arch Biochem Biophys.* 2014; 563:118–24.
  25. Fernandez S, Risolino M, Mandia N, Talotta F, Soini Y, Incoronato M, Condorelli G, Banfi S, Verde P. miR-340 inhibits tumor cell proliferation and induces apoptosis by targeting multiple negative regulators of p27 in non-small cell lung cancer. *Oncogene.* 2014; 34:3240–50
  26. Cai H, Lin L, Cai H, Tang M, Wang Z. Combined microRNA-340 and ROCK1 mRNA profiling predicts tumor progression and prognosis in pediatric osteosarcoma. *Int J Mol Sci.* 2014; 15:560–73.
  27. Huang D, Qiu S, Ge R, He L, Li M, Li Y, Peng Y. miR-340 suppresses glioblastoma multiforme. *Oncotarget.* 2015; 6:9257–70. doi: 10.18632/oncotarget.3288.
  28. Hegi ME, Diserens AC, Gorlia T, Hamou MF, de Tribolet N, Weller M, Kros JM, Hainfellner JA, Mason W, Mariani L, Bromberg JE, Hau P, Mirimanoff RO, et al. MGMT gene silencing and benefit from temozolomide in glioblastoma. *The New England journal of medicine.* 2005; 352:997–1003.
  29. Wang J, Liu Y, Li Z, Tan LX, Ryu MJ, Meline B, Du J, Young KH, Ranheim E, Chang Q, Zhang J. Endogenous oncogenic Nras mutation initiates hematopoietic malignancies in a dose- and cell type-dependent manner. *Blood.* 2011; 118:368–79.
  30. Vaughn CP, Zobel SD, Furtado LV, Baker CL, Samowitz WS. Frequency of KRAS, BRAF, and NRAS mutations in colorectal cancer. *Genes Chromosomes Cancer.* 2011; 50:307–12.
  31. Tschandl P, Berghoff AS, Preusser M, Burgstaller-Muehlbacher S, Pehamberger H, Okamoto I, Kittler H. NRAS and BRAF mutations in melanoma-associated nevi and uninvolved nevi. *PLoS One.* 2013; 8:e69639.
  32. Quintavalle C, Donnarumma E, Iaboni M, Roscigno G, Garofalo M, Romano G, Fiore D, De Marinis P, Croce CM, Condorelli G. Effect of miR-21 and miR-30b/c on TRAIL-induced apoptosis in glioma cells. *Oncogene.* 2013; 32:4001–8.
  33. Quintavalle C, Garofalo M, Zanca C, Romano G, Iaboni M, del Basso De Caro M, Martinez-Montero JC, Incoronato M, Nuovo G, Croce CM, Condorelli G. miR-221/222 overexpression in human glioblastoma increases invasiveness by targeting the protein phosphatase PTPmu. *Oncogene.* 2012; 31:858–68.
  34. Quintavalle C, Mangani D, Roscigno G, Romano G, Diaz-Lagares A, Iaboni M, Donnarumma E, Fiore D, De Marinis P, Soini Y, Esteller M, Condorelli G. MiR-221/222 target the DNA methyltransferase MGMT in glioma cells. *PLoS One.* 2013; 8:e74466.
  35. Hayes J, Thygesen H, Tumilson C, Droop A, Boissinot M, Hughes TA, Westhead D, Alder JE, Shaw L, Short SC, Lawler SE. Prediction of clinical outcome in glioblastoma using a biologically relevant nine-microRNA signature. *Mol Oncol.* 2014; 9:704–14.
  36. Jiang L, Mao P, Song L, Wu J, Huang J, Lin C, Yuan J, Qu L, Cheng SY, Li J. miR-182 as a prognostic marker for glioma progression and patient survival. *Am J Pathol.* 2010; 177:29–38.
  37. Niyazi M, Zehentmayr F, Niemoller OM, Eigenbrod S, Kretzschmar H, Schulze-Osthoff K, Tonn JC, Atkinson M, Mörtl S, Belka C. MiRNA expression patterns predict survival in glioblastoma. *Radiat Oncol.* 2011; 6:153.
  38. Srinivasan S, Patric IR, Somasundaram K. A ten-microRNA expression signature predicts survival in glioblastoma. *PLoS One.* 2011; 6:e17438.

# Aptamer-miRNA-212 Conjugate Sensitizes NSCLC Cells to TRAIL

Margherita Iaboni<sup>1</sup>, Valentina Russo<sup>1</sup>, Raffaella Fontanella<sup>2</sup>, Giuseppina Roscigno<sup>3</sup>, Danilo Fiore<sup>1</sup>, Elvira Donnarumma<sup>4</sup>, Carla Lucia Esposito<sup>3</sup>, Cristina Quintavalle<sup>1</sup>, Paloma H Giangrande<sup>5</sup>, Vittorio de Franciscis<sup>3</sup> and Gerolama Condorelli<sup>1,3</sup>

TNF-related apoptosis-inducing ligand (TRAIL) is a promising antitumor agent for its remarkable ability to selectively induce apoptosis in cancer cells, without affecting the viability of healthy bystander cells. The TRAIL tumor suppressor pathway is deregulated in many human malignancies including lung cancer. In human non-small cell lung cancer (NSCLC) cells, sensitization to TRAIL therapy can be restored by increasing the expression levels of the tumor suppressor microRNA-212 (miR-212) leading to inhibition of the anti-apoptotic protein PED/PEA-15 implicated in treatment resistance. In this study, we exploited a previously described RNA aptamer inhibitor of the tyrosine kinase receptor Axl (GL21.T) expressed on lung cancer cells, as a means to deliver miR-212 into human NSCLC cells expressing Axl. We demonstrate efficient delivery of miR-212 following conjugation of the miR to GL21.T (GL21.T-miR212 chimera). We show that the chimera downregulates PED and restores TRAIL-mediated cytotoxicity in cancer cells. Importantly, treatment of Axl+ lung cancer cells with the chimera resulted in (i) an increase in caspase activation and (ii) a reduction of cell viability in combination with TRAIL therapy. In conclusion, we demonstrate that the GL21.T-miR212 chimera can be employed as an adjuvant to TRAIL therapy for the treatment of lung cancer.

*Molecular Therapy—Nucleic Acids* (2016) 5, e289 ; doi:10.1038/mtna.2016.5; published online 8 March 2016

## Introduction

Members of the tumor necrosis factor (TNF) superfamily of cytokines bind to cognate receptors, called death receptors, on the surface of cells. Since their first discovery, more than 20 human TNF ligands and more than 30 corresponding receptors have been identified.<sup>1</sup> Members of this superfamily have a wide tissue distribution and regulate broad physiological processes such as immune responses, hematopoiesis, morphogenesis, and cell death, thus playing a key role in homeostasis, up to their role in tumorigenesis.<sup>2</sup> Key members of this family include TNF, CD95L (FasL), and TNF-related apoptosis-inducing ligand (TRAIL).

The clinical application of TNF ligands as cytotoxic agents for cancer is limited due to their toxicity. For example, TNF induces systemic toxicity.<sup>3</sup> *In vivo* use of CD95L is also limited by its lethal hepatotoxicity resulting from massive hepatocyte apoptosis.<sup>4,5</sup> TRAIL, instead, has been developed as a promising antitumor agent because it induces apoptosis in several tumor-derived cell types, but not in normal cells.<sup>6,7</sup> However, tumors often develop resistance to TRAIL monotherapy. Resistance to drug treatment is mainly due to deregulation of apoptosis-related proteins such as PED, a death effector domain (DED) family member of 15 kDa having a variety of effects on cell growth and metabolism.<sup>8</sup> PED has a broad anti-apoptotic function, being able to inhibit both the intrinsic and the extrinsic apoptotic pathways. In the extrinsic pathway, its interaction with Fas-associated protein with death domain (FADD) and pro-caspase-8 acts as competitive inhibitor of these pro-apoptotic molecules during the assembly of the

death-inducing signaling complex (DISC).<sup>9–13</sup> PED has been shown to be overexpressed in TRAIL-resistant human non-small cell lung cancer (NSCLC) cells.<sup>14</sup> An important mechanism of protein expression regulation involves microRNAs (miRNAs).<sup>15,16</sup> Toward this end, we found that miR-212 negatively modulates PED expression and sensitizes NSCLC cells to TRAIL-induced apoptosis. In fact, miR-212 levels in resistant cell lines of NSCLC were downregulated and inversely correlated with PED levels.<sup>17</sup> Consistently, transfection of a miR-212 mimic resulted in sensitization of resistant cancer cells to TRAIL-induced apoptosis. This occurred, at least in part, through PED downregulation.<sup>17</sup>

A major obstacle to the translation of RNAi drugs (e.g., miRNA mimics) into the clinic is the absence of an effective targeted delivery system. In addition to their ability to inhibit the function of their targets, in the past decade much attention has been focused on aptamers as delivery vehicles for targeted therapy.<sup>18–20</sup> Aptamers are highly structured single-stranded RNA molecules that bind to their cognate molecular targets (including transmembrane receptors) with high affinity and selectivity.<sup>21,22</sup> Aptamers have been successfully adapted for the targeted delivery of active molecules both *in vitro* and *in vivo*, including anticancer drugs, toxins, radionuclides, siRNAs, and, more recently, miRNAs.<sup>23–25</sup> Aptamer-siRNA or aptamer-miRNA chimeras are characterized by low immunogenicity, easy chemical synthesis and modification, and superior target selectivity.<sup>23,26–28</sup>

In previous studies, an internalizing RNA aptamer (GL21.T)<sup>29</sup> has been identified, through a cell-SELEX (systematic evolution of ligands by exponential enrichment)

<sup>1</sup>Department of Molecular Medicine and Medical Biotechnology, “Federico II” University of Naples, Naples, Italy; <sup>2</sup>IBB, CNR, Naples, Italy; <sup>3</sup>IEOS, CNR, Naples, Italy; <sup>4</sup>IRCCS-SDN, Naples, Italy; <sup>5</sup>Department of Internal Medicine, University of Iowa, Iowa City, Iowa, USA. Correspondence: Gerolama Condorelli, Department of Molecular Medicine and Medical Biotechnology, “Federico II” University of Naples, Via Pansini, 5-80131 Naples, Italy. E-mail: [gecondor@unina.it](mailto:gecondor@unina.it)

**Keywords:** aptamer; microRNA; non-small cell lung cancer; TNF-related apoptosis-inducing ligand

Received 1 September 2015; accepted 29 December 2015; published online 8 March 2016. doi:10.1038/mtna.2016.5

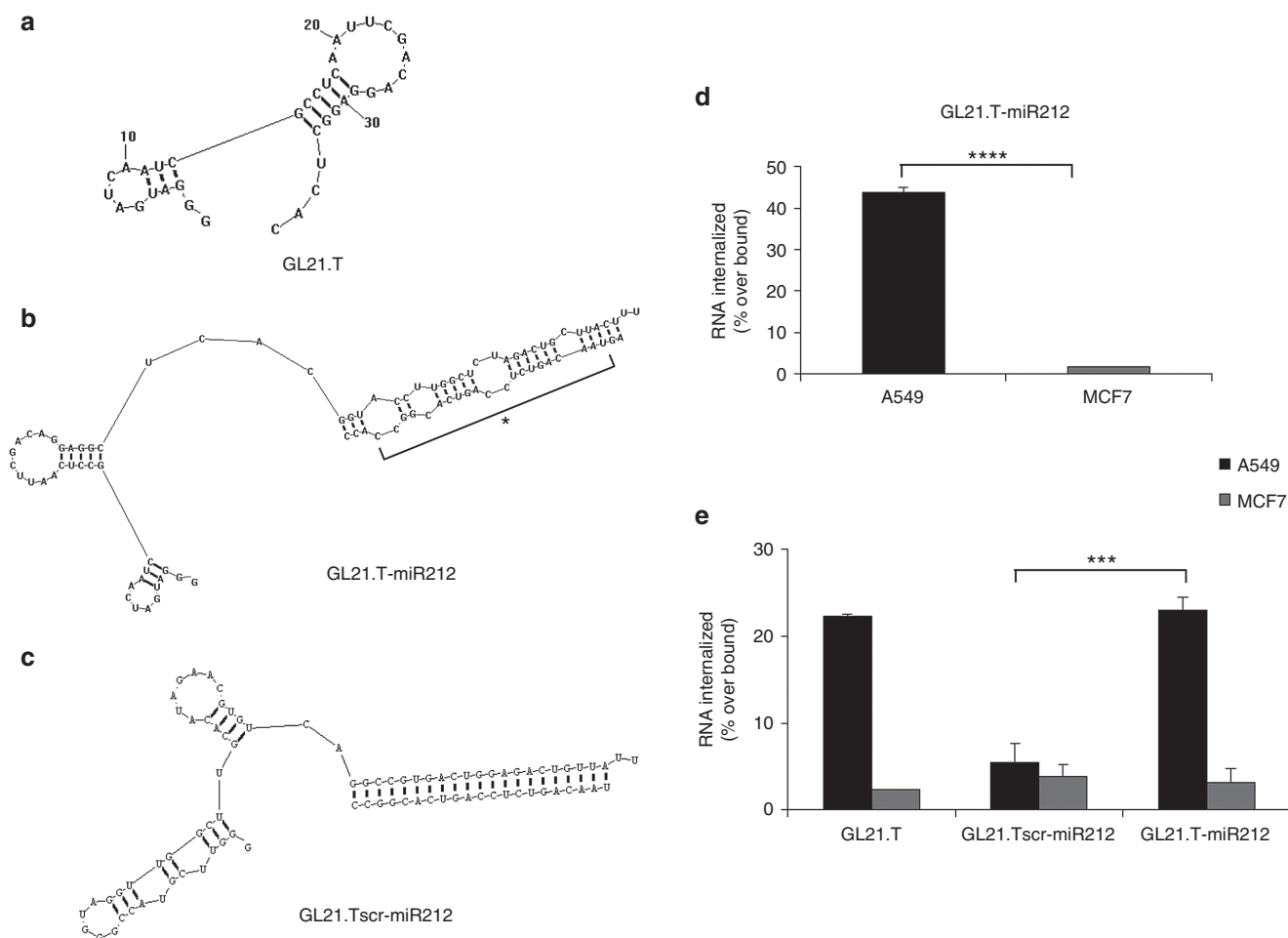


**Figure 1 Chimeras structure prediction and binding and internalization analysis.** Secondary structure prediction of chimeras using RNA structure 5.3 program. (a) GL21.T aptamer; (b) GL21.T-miR212; (c) GL21.Tscr-miR212. MiR mature sequence is indicated with an asterisk. (d) Internalization assay for the 5'-[<sup>32</sup>P]-labeled GL21.Tscr-miR212 and GL21.T-miR212 chimeras performed on A549 (Axl+) and MCF7 (Axl-) cells. The percentage of the RNA internalized over bound was obtained subtracting the counts relative to the scrambled chimera GL21.Tscr-miR212 used as negative control. Each bar shows the mean  $\pm$  SD values from three wells. (e) Internalization analysis of GL21.T, GL21.Tscr-miR212, and GL21.T-miR212 was monitored using quantitative RT-PCR (qRT-PCR) and normalizing to an internal RNA reference control for the PCR. The percentage of internalization has been expressed as the amount of internalized RNA relative to total bound RNA. Statistics were calculated using Student's *t*-test, \*\*\*\* $p < 0.0001$ ; \*\*\* $p < 0.001$ . Each bar shows the mean  $\pm$  SEM values from three wells.

methodology.<sup>30</sup> GL21.T aptamer is able to bind and inhibit the signaling of Axl receptor, belonging to the TAM family of tyrosine kinase receptors. Axl family members are activated by growth-arrest-specific gene 6 (GAS6), a member of the vitamin K-dependent protein family, that resembles blood coagulation factors rather than typical growth factors.<sup>31</sup> Axl overexpression has been reported in many human cancers and is associated with invasiveness and/or metastasis in lung,<sup>32</sup> prostate,<sup>33</sup> breast,<sup>34</sup> gastric,<sup>35</sup> and pancreatic cancers,<sup>36</sup> renal cell carcinoma,<sup>37</sup> as well as glioblastoma.<sup>38</sup> Importantly, we have recently described the combinatorial potential of a chimera composed of GL21.T aptamer and a miRNA combining the clinical benefits of both moieties.<sup>24</sup> Here, we demonstrate selective delivery of miR-212 to Axl+ lung cancer cells with GL21.T resulting in restoration of TRAIL-mediated sensitivity in NSCLC cells. Treatment of Axl+ cells with the GL21.T-miR212 chimera resulted in caspase activation and in a concomitant reduction of cancer cell viability. In conclusion,

we describe a novel aptamer-miRNA chimera as a means to sensitize lung cancers to TRAIL therapy.

## Results

### Chimera design

To conjugate GL21.T aptamer and miR-212, a molecular chimera (termed GL21.T-miR212) was designed using the RNA structure 5.3 program. GL21.T is a 34-mer truncated version of the original GL21 aptamer, corresponding to the functional portion of the aptamer able to bind to and to antagonize Axl receptor.<sup>29</sup> GL21.T was used as a delivery carrier of human miR-212. For this purpose, the GL21.T sequence was elongated at its 3' end, by a covalent bond, with the sequence of the passenger strand of miR-212, and annealed to the guide strand. Even if full complementary miRNA sequences have been shown to be sufficient for targeted gene silencing,<sup>27,28</sup> several recent reports on the use of molecular

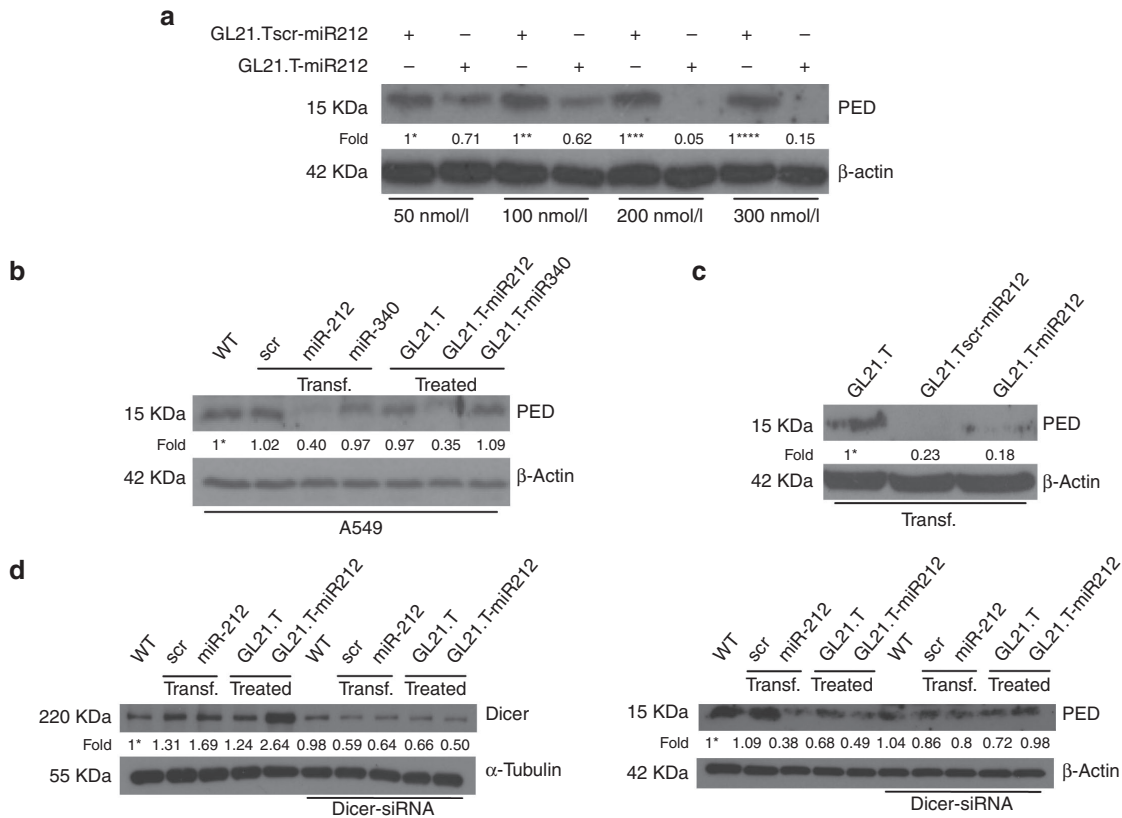


**Figure 2** MiR-212 effect, aptamer-mediated specific delivery, and Dicer processing of GL21.T-miR212 chimera. (a) A549 cells were treated with different final concentrations (50, 100, 200, and 300 nM) of chimera and scrambled chimera for 48 hours. (b) A549 cells were incubated with GL21.T-miR340, GL21.T, and GL21.T-miR212 or alternatively were transfected with pre-miR-212 and pre-miR-340. (c) A549 cells were transfected with the aptamer alone, GL21.T-scr-miR212 and GL21.T-miR212. (d) A549 cells were transfected with control scrambled or pre-miR-212 or treated with the aptamer alone or GL21.T-miR212 in presence or absence of Dicer-siRNA. After 48 hours, the efficiency of si-Dicer transfection (left panel) was controlled by immunoblotting using anti-Dicer and anti- $\alpha$ -tubulin antibodies. The effect on the downregulation of target protein (right panel) was analyzed by immunoblotting with anti-PED and anti- $\beta$  actin antibodies. Values below the blots indicate signal levels relative to (a) scrambled chimera-treated cells, arbitrarily set to 1 (with a different number of asterisks for each dose), or (b,d) to untreated cells (indicated as “WT”), and (c) to GL21.T-treated cells arbitrarily set to 1 (with asterisk). Intensity of bands was calculated using ImageJ (v1.46r). For a, b, and c, cell lysates were immunoblotted with anti-PED and anti- $\beta$  actin antibodies.

aptamer-siRNA chimeras have shown that silencing efficacy and specificity can be improved by introducing internal partial complementarities and increased length extension with respect to the mature sequence in order to obtain a more effective Dicer substrate.<sup>26,39,40</sup> Therefore, in order to encourage correct strand selection and thereby encourage target specificity, passenger and guide strands presented an imperfect pairing, consisting in a portion of stem-loop structure making the double strand similar to the pre-miR. A scrambled chimera, GL21.T-scr-miR212, was also designed, with the GL21.T sequence substituted by an unrelated sequence of the same length elongated with the miR-212 mimic passenger strand and annealed to the full complementary miR-212 guide strand. In both types of chimera, the antisense strand presented two overhanging bases (UU) at 3' end necessary for Dicer processing (Figure 1). Since, based on its predicted structure, the folding of GL21.T appears to be preserved also in the context of the chimera, we experimentally assessed the selective binding and the internalization potential of GL21.T-miR212 on Axl-expressing cells. Binding and internalization assays were performed using A549 (Axl+) cells, while MCF7 cells were used as negative control since they

do not express Axl. As shown in Figure 1, GL21.T-miR212 was able to bind to and internalize into A549 respect to the scrambled chimera used as control, but not in MCF7 cells, as assessed by two different methods (Figure 1d,e). Noteworthy, a similar percentage of internalization was obtained comparing GL21.T-miR212 and GL21.T alone (Figure 1e). These results indicate that, as previously reported for the GL21.T aptamer,<sup>29</sup> in the GL21.T-miR212 conjugate, the binding specificity of the GL21.T aptamer moiety is preserved and the conjugate is internalized into target cells in a receptor-dependent manner.

#### Dose-response effects and dicer processing of GL21.T-miR212 chimera

In order to characterize the effects of the chimera treatment on the miR-212 target, PED protein, A549 cells were treated with increasing amounts of GL21.T-miR212 and of control, GL21.T-scr-miR212, for 48 hours (Figure 2a). By western blot, we observed that PED levels were reduced in a dose-response manner by a concentration of 200 nM.

To test the specificity of the GL21.T-miR212 chimera and simultaneously evaluate the broad applicability of our delivery

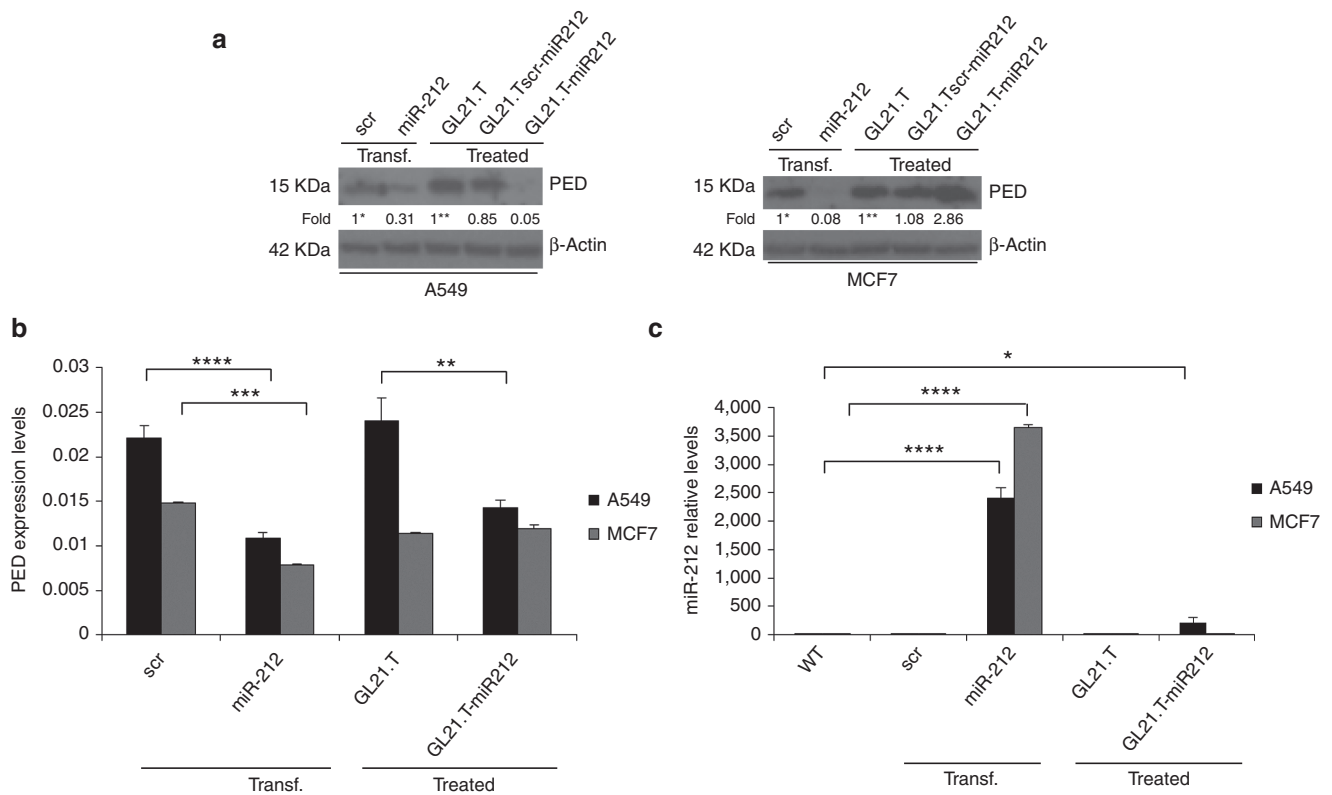


**Figure 3 Cell-type specificity of chimera treatment.** (a) A549 and MCF7 cells were treated with 300 nM of GL21.T-miR212 for 48 hours. GL21.T-scr-miR212 and GL21.T aptamer were used as negative controls, whereas transfection with 100 nM of pre-miR-212 was used as positive control. Control scrambled was used to assure transfection efficiency. Cell lysates were immunoblotted with anti-PED and anti- $\beta$  actin antibodies for PED protein levels while (b) PED expression levels were analyzed by qRT-PCR. (c) The same samples were subjected to qRT-PCR for miR-212 expression levels analysis. Bands' intensity has been calculated as in Figure 2. In b and c each bar shows the mean  $\pm$  SD values from three wells. Statistics were calculated using Student's *t*-test, \*\*\*\* $p$  < 0.0001; \*\*\* $p$  < 0.001; \*\* $p$  < 0.01; \* $p$  < 0.05.

platform, we conjugated the Axl aptamer to a different miR, miR-340. We have recently described that miR-340 has an onco-suppressive role in NSCLC by targeting *PUM1*, *PUM2*, and *SKP2*. The downregulation of these three genes was inversely correlated to *p27* expression.<sup>41</sup> Treatment of A549 cells with GL21.T-miR340 resulted in an increase in miR-340 expression levels suggesting the proper internalization of the chimera. The effect on *SKP2* downregulation, as well as on the increase of *p27* levels, confirmed the effectiveness of the conjugate (Supplementary Figure S1). This effect was similar to that observed with transfection of A549 cells with miR-340 (used as positive control). In contrast, as anticipated, the aptamer alone and the aptamer conjugated to miR-340 (GL21.T-miR340) did not reduce PED protein levels under the same experimental conditions. By western blot, results showed that GL21.T-miR340 was not able to modify PED levels, thus indicating that PED downregulation was merely dependent on miR-212 moiety (Figure 2b).

To demonstrate that GL21.T-scr-miR212 was not functional due to the aptamer portion and not to inactivation of the miR sequence, A549 cells were transfected with the aptamer alone, GL21.T-scr-miR212 and GL21.T-miR212. As shown, following transfection, the scrambled chimera was as effective as the GL21.T-miR212 at downregulating PED protein levels (Figure 2c).

In order to investigate the mechanism by which the chimera was functional, A549 cells were transfected with a Dicer-specific siRNA and, then, treated with GL21.T-miR212. The co-transfection of pre-miR-212 was used as positive control. The efficiency of si-Dicer transfection and the effect on the downregulation of target protein were determined by immunoblotting (Figure 2d). As shown, in the presence of a Dicer-specific siRNA, GL21.T-miR212 was not able to reduce PED protein level, suggesting that Dicer was necessary for chimera processing.

### Cell-type specificity of chimera treatment

To test whether PED downregulation was cell-type specific, A549 (Axl+) and MCF7 (Axl-) cells were treated with GL21.T-miR212 and GL21.T-scr-miR212. Transfection of pre-miR-212 and treatment with GL21.T aptamer were used as positive and negative controls, respectively. In A549 cells, GL21.T-miR212 downregulated PED both at mRNA level (measured using qRT-PCR) and protein level (assessed by immunoblotting with specific antibodies). As expected, no effect of the chimeras on PED expression was observed in MCF7 (Axl-negative) cells (Figure 3a,b). To confirm that the effects on PED protein levels were mediated by miR-212 upregulation, the same samples were evaluated by qRT-PCR to analyze miR-212 expression (Figure 3c). GL21.T delivered miR-212 inside the target cells, resulting in miR-212

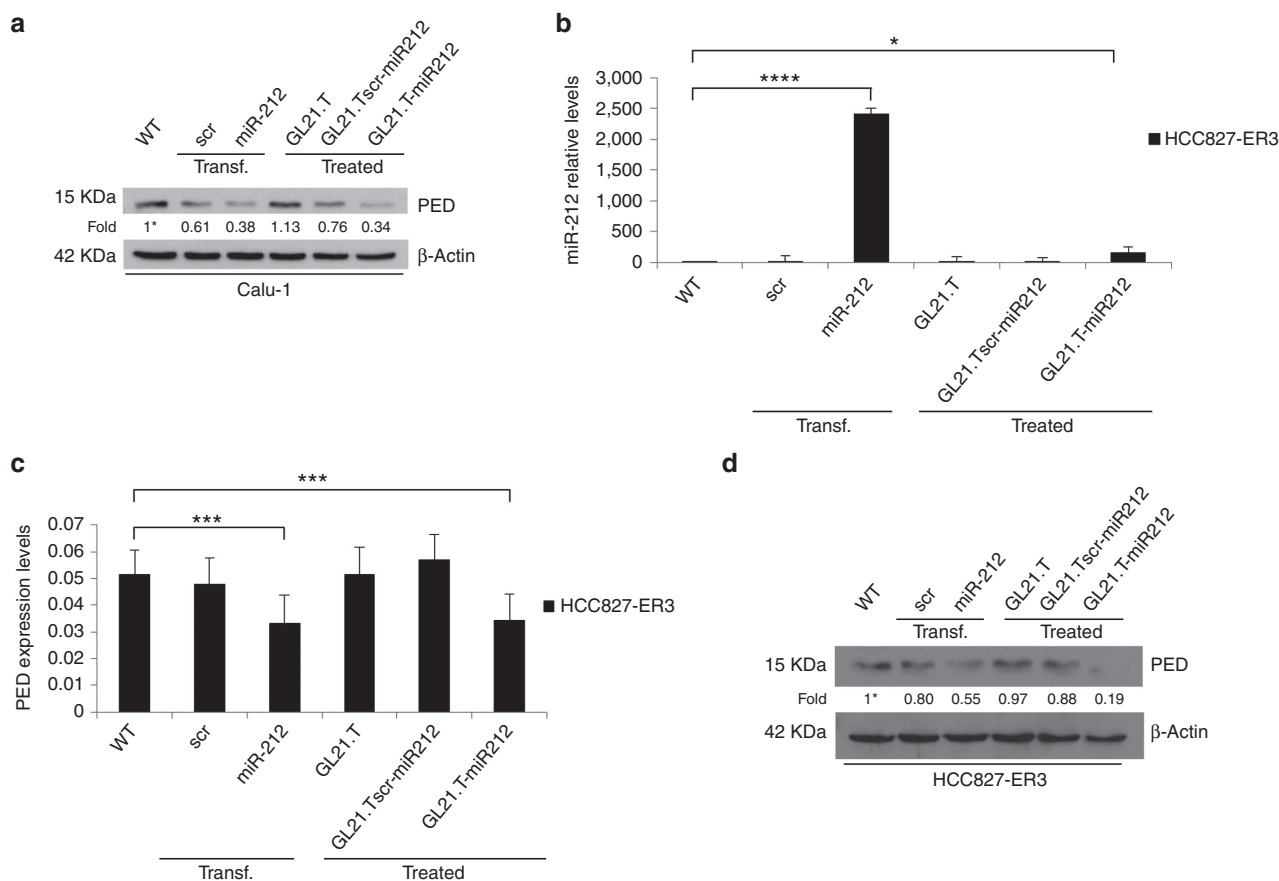


**Figure 4** Effects of GL21.T-miR212 on additional Axl+ non-small cell lung cancer (NSCLC) cell lines. (a,d) Calu-1 and HCC827-ER3 cells were treated with 300 nM of GL21.T-miR212, GL21.T.Tscr-miR212, and GL21.T aptamer or, alternatively, transfected with 100 nM of pre-miR-212. After 72 hours for Calu-1 or 48 hours for HCC827-ER3, cells were collected and cell lysates were immunoblotted with anti-PED and anti- $\beta$  actin antibodies for PED protein levels. (b) The same samples of HCC827-ER3 were subjected to qRT-PCR for miR-212 and (c) for PED expression levels analysis. In a,d values below the blots indicate signal levels relative to untreated cells (indicated as “WT”), arbitrarily set to 1 (with asterisk). Bands’ intensity has been calculated as in Figure 2. In b and c each bar shows the mean  $\pm$  SD values from three wells. Statistics were calculated using Student’s *t*-test, \*\*\*\* $p < 0.0001$ ; \*\*\* $p < 0.001$ ; \* $p < 0.05$ .

upregulation. Furthermore, despite the fact that the intracellular levels of miR-212 were lower in cells treated (no transfection reagent used) with GL21.T-miR212 compared with cells transfected with the pre-miR, the effects on PED downregulation were comparable. Results indicate that the efficiency of the conjugate to deliver functional miR-212 and thus modulate the expression of miRNA target genes is similar to that observed with transfection. We also validated the effect of GL21.T-miR212 on PED downregulation in other NSCLC Axl+ cell lines, Calu-1 and HCC827-ER3 (Figure 4).

### Receptor-dependent internalization of GL21.T-miR212 chimera

To confirm receptor-dependent internalization of GL21.T-miR212 chimera, we silenced Axl levels in A549 cells with RNAi. Following 48 hours of si-Axl transfection, we tested the binding and internalization potential of GL21.T-miR212. As expected, we observed a statistically significant decrease in bound/internalized GL21.T aptamer and chimera in A549 (siAxl)-treated cells. In contrast, no differences in binding/internalization were observed for the

scrambled chimera (Figure 5a). The efficiency of si-Axl transfection and the effect on the downregulation of target protein were determined by immunoblotting (Figure 5b). Alternatively, Axl levels were transiently upregulated transfecting Axl cDNA. Following Axl overexpression, the treatment with GL21.T-miR212 increased miR-212 levels by twofold compared with parental A549. Simultaneously, the conjugate decreased PED levels to the same extent in parental and transfected A549 cells (Figure 5c). Thus, we conclude that the functional delivery of miR-212 is dependent on the amount of Axl on the cell surface and that the additional miR-212 delivered is not necessary to increase the effect on PED downregulation. We next assessed whether internalization of the conjugate was Axl mediated. MCF7 cells were transiently transfected with Axl cDNA and levels of miR-212 evaluated following treatment with the conjugate. As predicted, miR-212 levels were higher in cells treated with GL21.T-miR212, compared with the treatment with GL21.Tscr-miR212 or the aptamer alone, thus indicating that internalization of GL21.T-miR212 chimera is receptor dependent (Supplementary Figure S2).

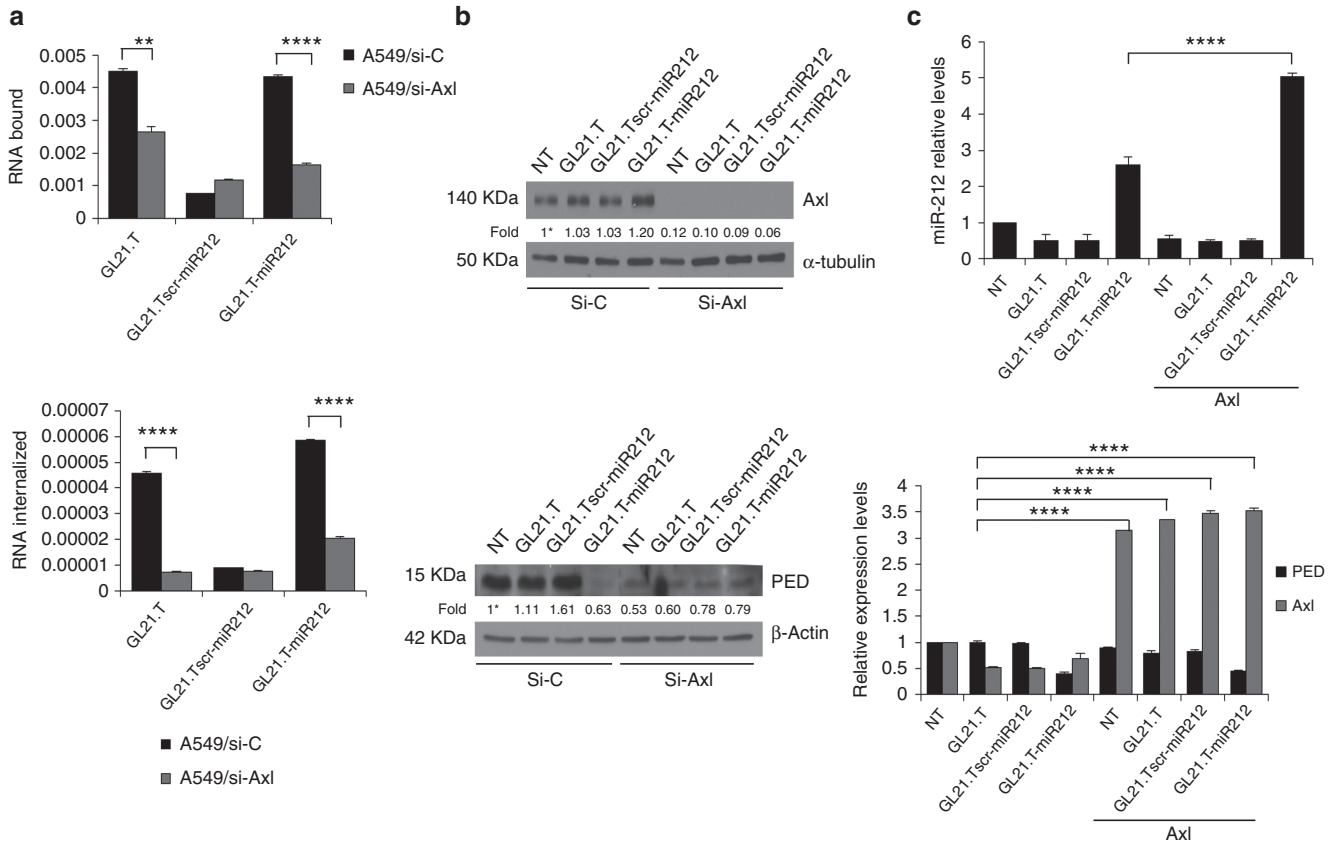


**Figure 5 Receptor-dependent internalization of GL21.T-miR212 chimera.** (a) A549 cells were transfected with si-Axl or siRNA control for 24 hours and, then, treated with GL21.T-miR212, the scrambled chimera or with the aptamer alone to perform the binding (upper panel) and internalization (lower panel) assays. Each bar shows the mean  $\pm$  SEM values from three wells. (b) The efficiency of si-Axl transfection and the effect on the downregulation of target protein were evaluated after 48 hours of treatment by immunoblotting with anti-Axl and anti-tubulin, in the upper panel, and with anti-PED and anti- $\beta$  actin antibodies, in the lower panel. Values below the blots indicate signal levels relative to untreated cells (indicated as “WT”), arbitrarily set to 1 (with asterisk). Bands’ intensity has been calculated as in Figure 2. (c) A549 (Axl+) cells, following 24-hour transfection with Axl TruClone (Axl), were treated with 300 nM of GL21.T-miR212, GL21.T:sc-miR212, or GL21.T for additional 48 hours. miR-212 (upper panel), PED and Axl (lower panel) levels were quantified by RT-qPCR. Each bar shows the mean  $\pm$  SD values from three wells. Statistics were calculated using Student’s *t*-test, \*\*\*\* $p$  < 0.0001; \*\* $p$  < 0.01.

### GL21.T-miR212 regulates TRAIL-induced cell death

We have previously shown that the TRAIL-resistant phenotype in NSCLC is related to aberrant elevated levels of PED. Furthermore, we showed that ectopic expression of miR-212 (achieved with a miR mimic) downregulates PED and re-establishes sensitivity to TRAIL.<sup>14,17</sup> To investigate whether treatment with the chimera induced sensitivity to TRAIL, we treated A549 cells with GL21.T-miR212. GL21.T:sc-miR212 and transfected pre-miR-212 were included as negative and positive controls, respectively. Caspase-8 activation was evaluated following treatment with TRAIL for 3 hours by western blot (Figure 6a). As shown, cleavage of caspase-8 was evident in cells treated with GL21.T-miR212 or, alternatively, transfected with pre-miR-212, but not with the GL21.T:sc-miR212, and accompanied by the activation of caspase 3/7, assessed by Caspase-Glo® 3/7 Assay (Figure 6b). Thus, sensitization to TRAIL upon treatment with the chimera was selective for Axl-expressing cells as demonstrated by the activation of caspase 3/7. To further confirm that the chimera sensitizes cancer cells to TRAIL-induced apoptosis, we evaluated the percentage of apoptotic cells after TRAIL treatment (Figure 7a). Transfected or treated cells were labeled with

Annexin V-FITC and propidium iodide and analyzed using flow cytometry. GL21.T-miR212 increased the percentage of apoptotic (Annexin V—positive, PI—negative) cells following TRAIL treatment, as miR-212 was used as positive control. In addition, we measured cell viability using an MTT assay that showed the same results (Figure 7b). GL21.T-miR340 treatment did not produce any gain in TRAIL sensitivity (Figure 7c). In summary, the GL21.T-miR212 chimera was able to increase the activation of caspase3/7 and, consequently, TRAIL-induced cell death in A549 cells, but not in MCF7 cells. TRAIL sensitization mediated by GL21.T-miR212 treatment was also confirmed on additional NSCLC cell lines, Calu-1 and HCC827-ER3, which display a TRAIL-resistant phenotype (Figure 8).

### Discussion

NSCLC represents about 80% of all lung cancers and is mostly diagnosed at an advanced stage (either locally advanced or metastatic disease). Because of resistance to therapeutic drugs, standard treatment of this tumor has

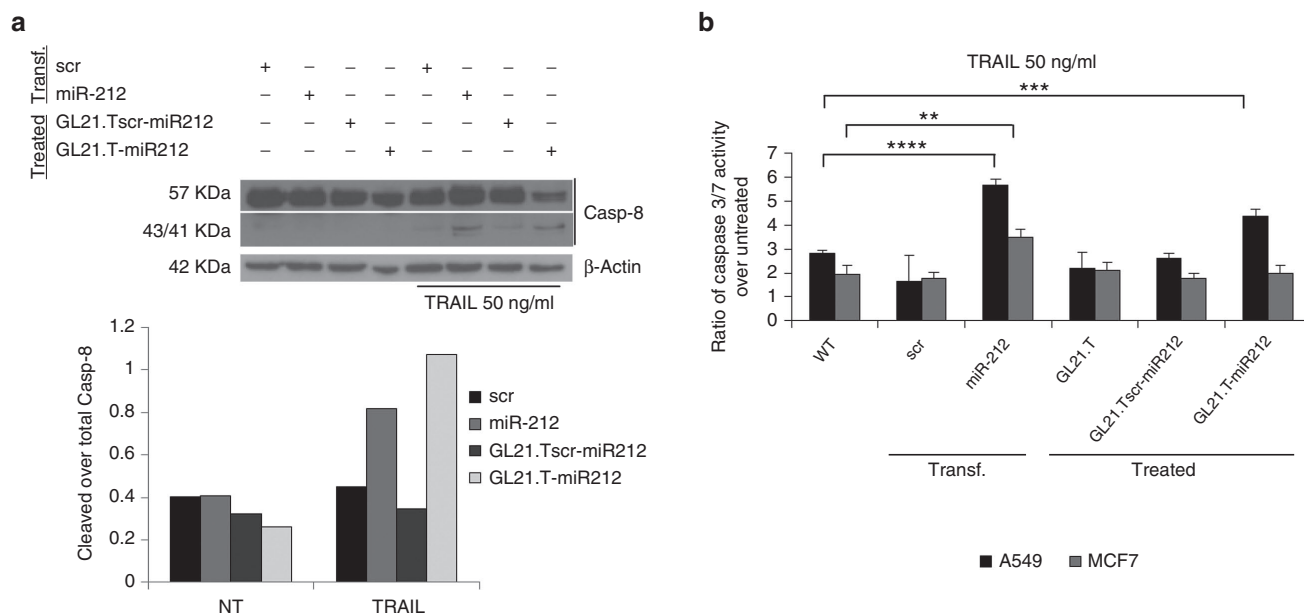


**Figure 6 Caspases activation induced by GL21.T-miR212.** (a) A549 cells were transfected with 100 nM of pre-miR-212 or alternatively treated with 300 nM of GL21.T-miR212 for 48 hours. Scrambled miR and scrambled chimera were used as negative controls. Cells were, then, treated for 3 hours with TNF-related apoptosis-inducing ligand (TRAIL) 50 ng/ml, and cell lysates were immunoblotted with anti-caspase-8 antibody (upper panel). Band intensity is represented in the diagram of the lower panel as a ratio of cleaved over total caspase-8, both quantization normalized over  $\beta$ -actin. (b) A549 and MCF7 cells were transfected with pre-miR-212 or treated with the unconjugated aptamer, the scrambled chimera and GL21.T-miR212 for 48 hours and then incubated with 50 ng/ml of TRAIL for 6 hours. The activation of caspase 3/7 was measured by Caspase-Glo® 3/7 Assay. Each bar shows the mean  $\pm$  SD values from three wells. Statistics were calculated using Student's *t*-test, \*\*\*\**p* < 0.0001; \*\*\**p* < 0.001; \*\**p* < 0.01.

only a 20% to 30% positive clinical response. Over the last years, the discovery of the pivotal of epidermal growth factor receptor (EGFR) in tumorigenesis has opened the way to a new class of targeted therapeutic agents: the EGFR tyrosine kinase inhibitors (EGFR TKIs). Since their introduction in therapy, in advanced NSCLC patients harboring EGFR mutations, the use of EGFR TKIs in first-line treatment has provided an unusually large progression-free survival benefit with a negligible toxicity when compared with cytotoxic chemotherapy. Nevertheless, resistance invariably occurs.<sup>42</sup> In this setting, TRAIL emerged as a novel therapeutic agent. TRAIL (ApoL/TNF-related apoptosis-inducing ligand) is a relatively new member of the tumor necrosis factor (TNF) ligand family, which induces apoptosis in a variety of cancers.

Initial promising studies demonstrated its remarkable specificity in inducing apoptosis in tumor cell lines, but not in normal cells both *in vitro* and *in vivo*.<sup>7</sup> This unique property makes TRAIL an attractive candidate for targeted cancer therapy.<sup>43,44</sup> However, resistance to TRAIL-induced apoptosis poses a challenge for effective anticancer strategies. To overcome this problem, drug cocktails in combination with TRAIL therapy have been proposed in order to induce synergism or sensitize resistant cancer cells. Toward this end, a number of combinatorial treatments with chemotherapeutic agents are in phase 1/2 of clinical studies.<sup>45–47</sup> More recently, aptamer-siRNA/miRNA chimeras have been proposed as novel adjuvants to standard chemotherapy.<sup>48,49</sup> Unlike nontargeted drugs, the advantage of these new class of biodrugs is that they are specifically delivered into target cells where they release their therapeutic cargo, thus limiting toxicity to normal cells.

In this study, we designed a chimera composed of a RNA aptamer to Axl (GL21.T) and miR-212 as a means to deliver functional miR-212 into TRAIL-resistant Axl+ A549 cells, but not into Axl- MCF7 cells. Indeed, GL21.T-miR212 selectively sensitizes the A549 cells to TRAIL-induced apoptosis, proving to be a unique tool to synergize with TRAIL in mediating cell death.

To increase specificity and facilitate large-scale chemical synthesis,<sup>24,26,50</sup> we conjugated a truncated version of the GL21 aptamer (GL21.T) to the tumor suppressor miR-212 duplex sequence. We demonstrated that in the context of the chimera, the active sequence (sequence required for binding to Axl) of GL21 is preserved, thus providing high binding affinity and the subsequent selective internalization of the conjugate into Axl+ cells. The miRNA moiety is a 25/27mer duplex having two overhanging bases (UU) at the 3' end of the passenger strand, thus adopting the conformation described as Dicer substrate for duplex siRNAs.<sup>51</sup> By using a similar approach with miRNAs, we have recently shown that nonperfect duplex miRNAs are correctly processed by Dicer, increasing the gene target specificity of the miRNA moiety.<sup>24</sup> Indeed, the optimal loading of the guide strand into RNA-induced silencing complex (RISC) is thought to reduce off-target effects that result from inappropriate incorporation of both miRNA strands into the silencing complex.<sup>52</sup>

A major limitation to the use of RNA-based drugs *in vivo* is the rapid degradation (within few minutes) of natural RNAs in serum or blood. As previously described, in order to protect the GL21.T aptamer from degradation, it was generated as a 2'-F-Py containing RNA.<sup>29</sup> Therefore, in order to increase the stability of the entire GL21.T-miR212 molecule, we substituted the

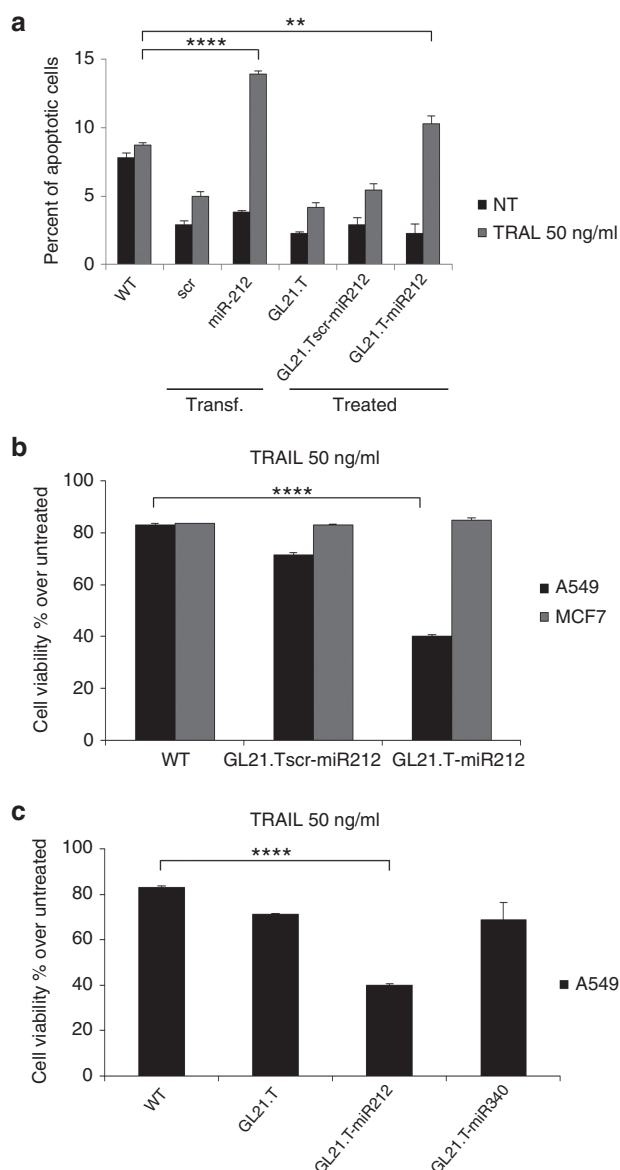


**Figure 7** TNF-related apoptosis-inducing ligand (TRAIL) sensitization induced by GL21.T-miR212. (a) A549 cells were transfected with pre-miR-212 and control scrambled or treated with the chimera, the scrambled chimera and the unconjugated aptamer for 48 hours. Cells were, then, incubated with TRAIL for 24 hours, and the percentage of apoptotic cells was evaluated by flow cytometry. (b) A549 and MCF7 cells were treated with 300nM of GL21.T-miR212 and GL21.T:scr-miR for 48 hours and were exposed to TRAIL for 24 hours at 50 ng/ml as final concentration. (c) A549 cells were treated with the unconjugated aptamer, GL21.T-miR212 or GL21.T-miR340 for 48 hours and were exposed to TRAIL for 24 hours at 50 ng/ml as final concentration. For **b** and **c** cell viability was evaluated with MTT assay. In **a**, **b** and **c** each bar shows the mean  $\pm$  SD values from three wells. Statistics were calculated using Student's *t*-test, \*\*\*\* $p < 0.0001$ ; \*\* $p < 0.01$ .

pyrimidines with 2'-F-Py at all positions. This modification is well characterized in humans and is reported to be well tolerated with little toxicity.<sup>53</sup> RNA aptamers with this modification have already been approved for their use in humans (Macugen), with many more quickly moving through the clinical pipeline.<sup>54</sup>

Although we cannot completely rule out potential intracellular toxicity of 2'-F-Py-modified RNAs leading to nonspecific immunostimulation, experiments *in vivo* demonstrated that problematic toxicity in humans is not expected.<sup>24,26</sup>

The silencing moiety of the chimera is constituted by the miR-212, a tumor suppressor miRNA that acts by negatively modulating PED expression, an onco-protein with a broad anti-apoptotic action. Indeed, the presence of elevated cellular levels of PED has been shown to contribute to resistance to TRAIL-induced cell death in several human tumors, including breast and lung cancer.<sup>17,55</sup> The DED domain of PED acts as a competitive inhibitor for pro-apoptotic molecules during the assembly of a functional DISC and inhibiting the activation of caspase-8, which take place following treatment with different apoptotic cytokines (CD95/FasL, TNF- $\alpha$ , and TRAIL). These data demonstrate that GL21.T-miR212 is a functional molecule that upon internalization, downregulates PED in a dose-dependent manner, reaching a plateau at around 200nM. In turn, target cells become sensitive to TRAIL and upon treatment undergo apoptosis following caspase-8 and caspase-3 activation.

Based on the suppressive action of miR-212 on PED expression as a means to sensitize cancer cells to TRAIL, here we demonstrated that GL21.T-miR212 chimera can sensitize target cells in a high selective manner. Specifically, exogenous miR-212 delivered by GL21.T aptamer led to TRAIL sensitization via activation of the apoptotic cascade selectively in A549, NSCLC Axl+ cells. In conclusion, the approach presented in this work indicates an innovative tool for a combined therapy that makes use of an aptamer-based molecular chimera to selectively sensitize TRAIL-resistant target tumor cells.

## Materials and methods

**Cell lines and transfection.** A549 and HCC827-ER3 cells were grown in RPMI 1640 while MCF7 and Calu-1 cells were grown in Dulbecco's modified Eagle's medium. A549, MCF7, and Calu cells were from American Type Culture Collection, while HCC827-ER3 were kindly provided by Dr. Balazs Halmos (Columbia University Medical Center, New York, NY). Their media were supplemented with 10% heat-inactivated fetal bovine serum, 2mM of glutamine, and 100U/ml of penicillin/streptomycin. For miRNAs transient transfection, cells were transfected with 100nM (final concentration) of miRNA stem-loop precursor hsa-miR212, hsa-miR340, or negative control 1 (Ambion, Foster City, CA) using Oligofectamine (Invitrogen, Carlsbad, CA). Also si-control and si-Axl (Santa Cruz Biotechnology, Santa Cruz, CA) were transfected using Oligofectamine (Invitrogen), according to the manufacturer's protocol. For aptamer and chimeras transient transfection, cells were transfected with 100nM (final concentration) of RNAs, using Lipofectamine 2000 (Invitrogen). Also Axl TruClone (Origene, Rockville, MD) and si-Dicer (Cell Signaling Technology, Beverly, MA) were transfected with Lipofectamine 2000, according to the manufacturer's protocol.

**Aptamer-miRNA chimeras.** The following sequences were used for the chimera production: GL21.T-miR212 passenger strand:

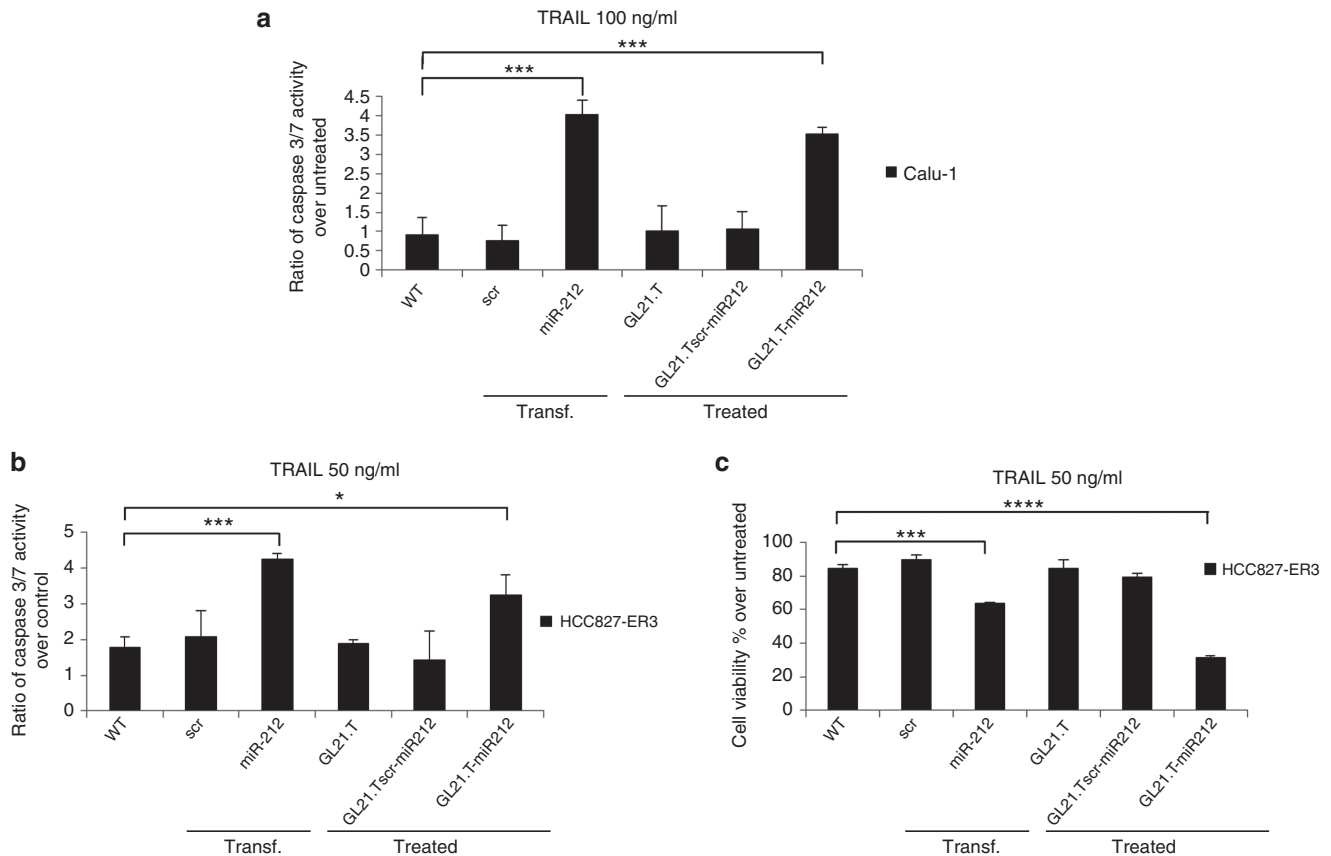


**Figure 8.** TNF-related apoptosis-inducing ligand (TRAIL) sensitization induced by GL21.T-miR212 in additional Axl+ non-small cell lung cancer (NSCLC) cell lines. Calu-1 and HCC827-ER3 cells were transfected with pre-miR-212 or treated with the unconjugated aptamer, the scrambled chimera and GL21.T-miR212. (a,b) After 72 hours for Calu-1 or 48 hours for HCC827-ER3 of treatment or transfection, cells were incubated with TRAIL (100 ng/ml in Calu-1 and 50 ng/ml in HCC827-ER3) for 6 hours. The activation of caspase 3/7 was measured by Caspase-Glo® 3/7 Assay. (c) The same samples of HCC827-ER3 were exposed to TRAIL for 24 hours, and cell viability was evaluated with MTT assay. Each bar shows the mean  $\pm$  SD values from three wells. Statistics were calculated using Student's *t*-test, \*\*\*\* $p < 0.0001$ ; \*\*\* $p < 0.001$ ; \* $p < 0.05$ .

5'GGGAUGAUCAAUCGCCUCAAUUCGACAGGAGG CUCACGGUACCUUGGCUCUAGACUGCUUACUUU. miR-212 guide strand: 5' AGUACAGUCUCCAGUCACGGCC ACC. GL21.T:scr-miR212 passenger strand: 5'GGGUUCGU ACCGGUAGGUUGGCUUGCACAUAGAACGUGUCAGG CCGUGACUGGAGACUGUUAUU. miR-212 (1g) guide strand: 5' UACAGUCUCCAGUCACGGCC. GL21.T: 5' GGG AUGAUCAAUCGCCUCAAUUCGACAGGAGGCUCAC. GL21.T-miR340 passenger strand: 5'GGAUGAUCAAUCG CCUCAAUUCGACAGGAGGCUCACAAUCAGUCUCA UUGC UUUUAAUU. miR-340 guide strand: 5' UUAUAAA GCAAUGAGACUGAUU.

All RNAs were custom synthesized by TriLink Biotechnologies (San Diego, CA) as 2'-fluoropyrimidine RNAs. UU in bold are 3'-overhang. The control conjugate is composed of an unrelated aptamer sequence linked to the fully complementary miR-212 duplex. In the context of the control conjugate, it was necessary to use a fully complementary miR-212 to stabilize the functional miR duplex and prevent unwanted intramolecular interactions with the scrambled aptamer sequence.

To prepare GL21.T-miR212, GL21.T:scr-miR212, and GL21.T-miR340, 5  $\mu$ M of aptamer-passenger RNA strand

was denatured at 98  $^{\circ}$ C for 20 minutes, combined with 5  $\mu$ M of the appropriate guide strand at 55  $^{\circ}$ C for 10 minutes in binding buffer 10 $\times$  (200 mM N-2-Hydroxyethylpiperazine-N'-2-Ethanesulfonic Acid, pH 7.4, 1.5 M NaCl, 20 mM CaCl<sub>2</sub>) and then warmed up to 37  $^{\circ}$ C for 20 minutes.

**Cell binding and internalization assays.** Aptamer binding and internalization have been assessed by two different methods, by radioactivity labeling or by quantitative reverse transcription-PCR (qRT-PCR)

**Radioactivity labeling.** A549 and MCF7 cells were plated in 24 multiwell plates in triplicate. RNAs were 5'-[<sup>32</sup>P]-labeled and incubated at 200 nM as final concentration on cells at 37  $^{\circ}$ C for 15 minutes. After several washings, the amount of <sup>32</sup>P-labeled RNA recovered in SDS 1% was determined by scintillation counting. In contrast, to check the endocytosis rate, after the incubation with radiolabeled chimeras, the cells were subjected to a stringent high-salt wash, with High Salt phosphate-buffered saline (PBS; 0.5M NaCl), to remove any unbound RNAs or RNAs bound to the cell surface. Following 5-minute treatment at 4  $^{\circ}$ C, the amount of <sup>32</sup>P-labeled RNA internalized was recovered in Sodium Dodecyl Sulfate 1% and determined by scintillation counting. In both assays, results were normalized for cell

number. The background values obtained with the scrambled chimera were subtracted from the values obtained with GL21.T-miR212. Finally, the resulting recovered RNAs were plotted as percent of RNA internalized over RNA bound.

**qRT-PCR method.** Target (A549) and nontarget (MCF7) cells were incubated with 100 nM of aptamer or chimeras for 15 minutes at 37 °C with 5% CO<sub>2</sub>. Cells were washed with ice-cold PBS or incubated with High Salt PBS (0.5M NaCl) at 4 °C for 5 minutes, and RNA was recovered using TRIzol reagent (Invitrogen). Samples were normalized to an internal RNA reference control. Specifically, 0.5 pmol per sample CL4 aptamer<sup>56</sup> was added to each sample along with TRIzol as a reference control. Recovered RNAs were quantitated using Reverse Transcriptase M-MuLV (Roche Life Science, Basel, Switzerland) with SYBR Green (BioRad) with a Biorad iCycler. All reactions were done in a 25-ml volume in triplicate with specific primers (GL21.T 5': TAATACGACTCATATAGGGATGATC; 3': GTGAGCCTCCTGTcGAAT; GL21.Tscr 5': TTCGTACCGGGTAGGTT; 3': TGACACGTTCTATGTGCA) and CL4 reference control (CL4 5': TAATACGACTCACTATAGGGGCCTTA; 3': GCCTCCTGTGCAATCG).

For each cell line, the percentage of internalization has been expressed as the amount of internalized RNA relative to total bound RNA without normalizing for background. The same protocol was used for the experiment on A549 cells upon transfection with si-control and si-AXL.

**Protein isolation and immunoblotting.** Cells were treated with chimeras for 48 hours, or alternatively Calu-1 for 72 hours, and then were washed twice in ice-cold PBS and lysed in Lysis buffer (50 mM N-2-Hydroxyethylpiperazine-N'-2-Ethanesulfonic Acid pH 7.5 containing 150 mM NaCl, 1% GLYCEROL, 1% Triton 100x, 1.5 mM MgCl<sub>2</sub>, 5 mM ethylene glycol tetraacetic acid, 1 mM Na<sub>3</sub>VO<sub>4</sub> and 1X protease inhibitor cocktail). Protein concentration was determined by the Bradford assay (BioRad, Hercules, CA) using bovine serum albumin as the standard, and equal amounts of protein were analyzed by Sodium Dodecyl Sulfate Polyacrylamide Gel Electrophoresis (15% acrylamide). Gels were electroblotted onto nitrocellulose membrane (Merck Millipore, Billerica, MA). For immunoblot experiments, membranes were blocked for 1 hour with 5% non-fat dry milk in tris-buffered saline containing 0.1% Tween-20 and incubated at 4 °C overnight with primary antibody. Detection was performed by peroxidase-conjugated secondary antibodies using the enhanced chemiluminescence system (GE Healthcare Life Sciences, Pittsburgh, PA). Primary antibodies used were anti-PED,<sup>57</sup> anti-Caspase-8, anti-p27, and anti-Dicer from Cell Signaling Technology, anti- $\alpha$  tubulin from Santa Cruz Biotechnology, anti- $\beta$  actin from Sigma-Aldrich (St. Louis, MO), and anti-Axl from R&D Systems (Minneapolis, MN).

**RNA extraction and Real-time PCR.** Cells were treated with 300 nM of chimeras for 48 hours, and then total RNAs (miRNA and mRNA) were extracted using TRIzol (Invitrogen) according to the manufacturer's protocol. Reverse transcription of total miRNA was performed starting from equal amounts of total RNA/sample (1  $\mu$ g) using miScript reverse Transcription Kit (Qiagen, Hilden, Germany). Quantitative analysis of miRNAs and RNU6B (as an internal reference) was performed by real-time PCR using specific primers (Qiagen) and miScript

SYBR Green PCR Kit (Qiagen). The reaction for detection of miRNAs was performed as follows: 95 °C for 15 minutes, 40 cycles of 94 °C for 15 seconds, 55 °C for 30 seconds, and 70 °C for 30 seconds. All reactions were run in triplicate. For reverse transcription of mRNA, we used SuperScript® III Reverse Transcriptase (Life Technologies). Quantitative analysis of *PED*, *AXL*, and *actin* (as an internal reference) was performed by real-time PCR using specific primers and iQ™ SYBR Green Supermix (BioRad). The threshold cycle (CT) is defined as the fractional cycle number at which the fluorescence passes the fixed threshold. For quantization has been used the 2<sup>(- $\Delta$ CT)</sup> method, where  $\Delta$ Ct is the difference between the amplification fluorescent thresholds of the miRNA of interest and the miRNA of U6 used as an internal reference. Instead, fold changes were calculated with 2<sup>(- $\Delta\Delta$ CT)</sup> method as previously described.<sup>58</sup> Experiments were carried out in triplicate for each data point, and data analysis was performed by using software (Bio-Rad).

**Cell death quantification.** A549, MCF7, and HCC827-ER3 cells were treated with GL21.T-miR212 and GL21.Tscr-miR212 300 nM for 3 hours. Then, cells were plated in 96 multiwell plates in triplicate for 48 hours and incubated with TRAIL (Vinci-Biochem, Firenze, Italy) at a final concentration of 50 ng/ml for 24 hours. Cell viability was assessed with CellTiter 96 Aqueous One Solution Cell Proliferation Assay (Promega, Madison, WI). Metabolically active cells were detected by adding 20  $\mu$ l of 3-(4,5-dimethylthiazol-2-yl)-5-(3-carboxymethoxyphenyl)-2-(4-sulfophenyl)-2H-tetrazolium to each well, and plates were analyzed in a Multilabel Counter (BioTek, Winooski, VT).

**Caspase 3/7 assay.** The assay was performed with the use of Caspase-Glo® 3/7 Assay (Promega) according to the manufacturer's protocol. Briefly, A549, MCF7, and HCC827-ER3 cells were before transfected with pre-miR-212 or treated with GL21.T, GL21.Tscr-miR212, GL21.T-miR212 for 48 hours, or alternatively Calu-1 for 72 hours, and, then, incubated for 6 hours with TRAIL. An equal volume of Caspase-Glo 3/7 reagent was added to each well for 30 minutes in the dark, and luminescence was measured by luminometer (Turner BioSystems-Promega). The ratio of caspase 3/7 activity over control was calculated normalizing treated samples over untreated ones.

**Flow cytometry.** Apoptosis was analyzed via Annexin V-FITC Apoptosis Detection kit I (BD Biosciences, San Diego, CA). A549 cells were transfected with pre-miR-212 or treated with GL21.T, GL21.Tscr-miR212, GL21.T-miR212 for 48 hours and, then, incubated for 24 hours with TRAIL. The cells were washed in PBS, resuspended in binding buffer 10x, and labeled with Annexin V-FITC and propidium iodide according to the manufacturer's protocol. After incubation at room temperature for 15 minutes in the dark, cells were analyzed with a BD Accuri™ C6 Flow cytometry (BD Biosciences). To calculate the percent of apoptotic cells, the gate was placed on annexin V-positive, PI-negative cells, and thus double positive cells were excluded from the analysis.

### Supplementary material

**Figure S1.** GL21.T-miR340 characterization.

**Figure S2.** Internalization of the GL21.T-miR212 conjugate in MCF7 exogenously expressing Axl.

**Acknowledgments** This work was partially supported by funds from Associazione Italiana Ricerca sul Cancro, AIRC (grant n.ro 10620) to G.C. and AIRC (grant n.ro 13345) to V.d.F.; MERIT (RBNE08E8CZ\_002) to G.C., POR Campania FSE 2007–2013, Project CREME to G.C., Fondazione Ber-lucchi to G.C. This work was partially supported by grants to P.H.G. from the National Institutes of Health (R01CA138503 and R21DE019953), Mary Kay Foundation (9033-12 and 001-09), Elsa U Pardee Foundation (E2766) and the Roy J Carver Charitable Trust (RJCCT 01-224). M.I. was supported by the ‘Federazione Italiana Ricerca sul Cancro’ (FIRC) Post-Doctoral Research Fellowship. G.R. was supported by a MERIT project Fellowship. The authors declare no conflict of interest.

- Aggarwal, BB, Gupta, SC and Kim, JH (2012). Historical perspectives on tumor necrosis factor and its superfamily: 25 years later, a golden journey. *Blood* **119**: 651–665.
- Grewal, IS (2009). Overview of TNF superfamily: a chest full of potential therapeutic targets. *Adv Exp Med Biol* **647**: 1–7.
- Wielockx, B, Lannoy, K, Shapiro, SD, Itoh, T, Itohara, S, Vandekerckhove, J et al. (2001). Inhibition of matrix metalloproteinases blocks lethal hepatitis and apoptosis induced by tumor necrosis factor and allows safe antitumor therapy. *Nat Med* **7**: 1202–1208.
- Ni, R, Tomita, Y, Matsuda, K, Ichihara, A, Ishimura, K, Ogasawara, J et al. (1994). Fas-mediated apoptosis in primary cultured mouse hepatocytes. *Exp Cell Res* **215**: 332–337.
- Galle, PR, Hofmann, WJ, Walczak, H, Schaller, H, Otto, G, Stremmel, W et al. (1995). Involvement of the CD95 (APO-1/Fas) receptor and ligand in liver damage. *J Exp Med* **182**: 1223–1230.
- Ashkenazi, A, Pai, RC, Fong, S, Leung, S, Lawrence, DA, Marsters, SA et al. (1999). Safety and antitumor activity of recombinant soluble Apo2 ligand. *J Clin Invest* **104**: 155–162.
- Walczak, H, Miller, RE, Ariail, K, Gliniak, B, Griffith, TS, Kubin, M et al. (1999). Tumoricidal activity of tumor necrosis factor-related apoptosis-inducing ligand *in vivo*. *Nat Med* **5**: 157–163.
- Fiory, F, Formisano, P, Perruolo, G and Beguinot, F (2009). Frontiers: PED/PEA-15, a multifunctional protein controlling cell survival and glucose metabolism. *Am J Physiol Endocrinol Metab* **297**: E592–E601.
- Zanca, C, Cozzolino, F, Quintavalle, C, Di Costanzo, S, Ricci-Vitiani, L, Santoriello, M et al. (2010). PED interacts with Rac1 and regulates cell migration/invasion processes in human non-small cell lung cancer cells. *J Cell Physiol* **225**: 63–72.
- Quintavalle, C, Di Costanzo, S, Zanca, C, Tasset, I, Fraldi, A, Incoronato, M et al. (2014). Phosphorylation-regulated degradation of the tumor-suppressor form of PED by chaperone-mediated autophagy in lung cancer cells. *J Cell Physiol* **229**: 1359–1368.
- Garofalo, M, Romano, G, Quintavalle, C, Romano, MF, Chiurazzi, F, Zanca, C et al. (2007). Selective inhibition of PED protein expression sensitizes B-cell chronic lymphocytic leukaemia cells to TRAIL-induced apoptosis. *Int J Cancer* **120**: 1215–1222.
- Garofalo, M, Quintavalle, C, Di Leva, G, Zanca, C, Romano, G, Taccioli, C et al. (2008). MicroRNA signatures of TRAIL resistance in human non-small cell lung cancer. *Oncogene* **27**: 3845–3855.
- Ricci-Vitiani, L, Pedini, F, Mollinari, C, Condorelli, G, Bonci, D, Bez, A et al. (2004). Absence of caspase 8 and high expression of PED protect primitive neural cells from cell death. *J Exp Med* **200**: 1257–1266.
- Zanca, C, Garofalo, M, Quintavalle, C, Romano, G, Acunzo, M, Ragno, P et al. (2008). PED is overexpressed and mediates TRAIL resistance in human non-small cell lung cancer. *J Cell Mol Med* **12**(6A): 2416–2426.
- Garofalo, M, Leva, GD and Croce, CM (2014). MicroRNAs as anti-cancer therapy. *Curr Pharm Des* **20**: 5328–5335.
- Garofalo, M, Condorelli, GL, Croce, CM and Condorelli, G (2010). MicroRNAs as regulators of death receptors signaling. *Cell Death Differ* **17**: 200–208.
- Incoronato, M, Garofalo, M, Urso, L, Romano, G, Quintavalle, C, Zanca, C et al. (2010). miR-212 increases tumor necrosis factor-related apoptosis-inducing ligand sensitivity in non-small cell lung cancer by targeting the antiapoptotic protein PED. *Cancer Res* **70**: 3638–3646.
- Yan, AC and Levy, M (2009). Aptamers and aptamer targeted delivery. *RNA Biol* **6**: 316–320.
- Farokhzad, OC, Karp, JM and Langer, R (2006). Nanoparticle-aptamer bioconjugates for cancer targeting. *Expert Opin Drug Deliv* **3**: 311–324.
- Zhou, J and Rossi, JJ (2014). Cell-type-specific, aptamer-functionalized agents for targeted disease therapy. *Mol Ther Nucleic Acids* **3**: e169.
- Wang, J and Li, G (2011). Aptamers against cell surface receptors: selection, modification and application. *Curr Med Chem* **18**: 4107–4116.
- Catuogno, S, Esposito, CL, de Franciscis, V (2016). Developing Aptamers by Cell-Based SELEX. *Methods Mol Biol* **1380**: 33–46.
- Zhou, J and Rossi, JJ (2010). Aptamer-targeted cell-specific RNA interference. *Silence* **1**: 4.
- Esposito, CL, Cerchia, L, Catuogno, S, De Vita, G, Dassi, JP, Santamaria, G et al. (2014). Multifunctional aptamer-miRNA conjugates for targeted cancer therapy. *Mol Ther* **22**: 1151–1163.
- Dai, F, Zhang, Y, Zhu, X, Shan, N and Chen, Y (2012). Anticancer role of MUC1 aptamer-miR-29b chimera in epithelial ovarian carcinoma cells through regulation of PTEN methylation. *Target Oncol* **7**: 217–225.
- Dassi, JP, Liu, XY, Thomas, GS, Whitaker, RM, Thiel, KW, Stockdale, KR et al. (2009). Systemic administration of optimized aptamer-siRNA chimeras promotes regression of PSMA-expressing tumors. *Nat Biotechnol* **27**: 839–849.
- McNamara, JO 2nd, Andrechek, ER, Wang, Y, Viles, KD, Rempel, RE, Gilboa, E et al. (2006). Cell type-specific delivery of siRNAs with aptamer-siRNA chimeras. *Nat Biotechnol* **24**: 1005–1015.
- Dai, F, Zhang, Y, Zhu, X, Shan, N and Chen, Y (2013). The anti-chemoresistant effect and mechanism of MUC1 aptamer-miR-29b chimera in ovarian cancer. *Gynecol Oncol* **131**: 451–459.
- Cerchia, L, Esposito, CL, Camorani, S, Rienzo, A, Stasio, L, Insabato, L et al. (2012). Targeting Axl with an high-affinity inhibitory aptamer. *Mol Ther* **20**: 2291–2303.
- Ellington, AD and Szostak, JW (1990). *In vitro* selection of RNA molecules that bind specific ligands. *Nature* **346**: 818–822.
- Stitt, TN, Conn, G, Gore, M, Lai, C, Bruno, J, Radziejewski, C et al. (1995). The anticarcinogenic factor protein S and its relative, Gas6, are ligands for the Tyro 3/Axl family of receptor tyrosine kinases. *Cell* **80**: 661–670.
- Shieh, YS, Lai, CY, Kao, YR, Shieh, SG, Chu, YW, Lee, HS et al. (2005). Expression of axl in lung adenocarcinoma and correlation with tumor progression. *Neoplasia* **7**: 1058–1064.
- Sainaghi, PP, Castello, L, Bergamasco, L, Galletti, M, Bellosta, P and Avanzi, GC (2005). Gas6 induces proliferation in prostate carcinoma cell lines expressing the Axl receptor. *J Cell Physiol* **204**: 36–44.
- Zhang, YX, Knyazev, PG, Cheburkin, YV, Sharma, K, Knyazev, YP, Orfi, L et al. (2008). AXL is a potential target for therapeutic intervention in breast cancer progression. *Cancer Res* **68**: 1905–1915.
- Wu, CW, Li, AF, Chi, CW, Lai, CH, Huang, CL, Lo, SS et al. (2002). Clinical significance of AXL kinase family in gastric cancer. *Anticancer Res* **22**(2B): 1071–1078.
- Koorstra, JB, Karikari, CA, Feldmann, G, Bisht, S, Rojas, PL, Offerhaus, GJ et al. (2009). The Axl receptor tyrosine kinase confers an adverse prognostic influence in pancreatic cancer and represents a new therapeutic target. *Cancer Biol Ther* **8**: 618–626.
- Chung, BI, Malkowicz, SB, Nguyen, TB, Libertino, JA and McGarvey, TW (2003). Expression of the proto-oncogene Axl in renal cell carcinoma. *DNA Cell Biol* **22**: 533–540.
- Hutterer, M, Knyazev, P, Abate, A, Reschke, M, Maier, H, Stefanova, N et al. (2008). Axl and growth arrest-specific gene 6 are frequently overexpressed in human gliomas and predict poor prognosis in patients with glioblastoma multiforme. *Clin Cancer Res* **14**: 130–138.
- Wu, X, Ding, B, Gao, J, Wang, H, Fan, W, Wang, X et al. (2011). Second-generation aptamer-conjugated PSMA-targeted delivery system for prostate cancer therapy. *Int J Nanomedicine* **6**: 1747–1756.
- Amarzguioi, M, Lundberg, P, Cantin, E, Hagstrom, J, Behlke, MA and Rossi, JJ (2006). Rational design and *in vitro* and *in vivo* delivery of Dicer substrate siRNA. *Nat Protoc* **1**: 508–517.
- Fernandez, S, Risolino, M, Mandia, N, Talotta, F, Soini, Y, Incoronato, M et al. (2014). miR-340 inhibits tumor cell proliferation and induces apoptosis by targeting multiple negative regulators of p27 in non-small cell lung cancer. *Oncogene* **34**: 3240–3250.
- Sgambato, A, Casaluze, F, Maione, P, Rossi, A, Rossi, E, Napolitano, A et al. (2012). The role of EGFR tyrosine kinase inhibitors in the first-line treatment of advanced non small cell lung cancer patients harboring EGFR mutation. *Curr Med Chem* **19**: 3337–3352.
- Stuckey, DW and Shah, K (2013). TRAIL on trial: preclinical advances in cancer therapy. *Trends Mol Med* **19**: 685–694.
- Herbst, RS, Eckhardt, SG, Kurzrock, R, Ebbinghaus, S, O’Dwyer, PJ, Gordon, MS et al. (2010). Phase I dose-escalation study of recombinant human Apo2L/TRAIL, a dual proapoptotic receptor agonist, in patients with advanced cancer. *J Clin Oncol* **28**: 2839–2846.
- Falschlehner, C, Ganten, TM, Koschny, R, Schaefer, U and Walczak, H (2009). TRAIL and other TRAIL receptor agonists as novel cancer therapeutics. *Adv Exp Med Biol* **647**: 195–206.
- Soria, JC, Smit, E, Khayat, D, Besse, B, Yang, X, Hsu, CP et al. (2010). Phase 1b study of dulanerin (recombinant human Apo2L/TRAIL) in combination with paclitaxel, carboplatin, and bevacizumab in patients with advanced non-squamous non-small-cell lung cancer. *J Clin Oncol* **28**: 1527–1533.
- Hotte, SJ, Hirte, HW, Chen, EX, Siu, LL, Le, LH, Corey, A et al. (2008). A phase 1 study of mapatumumab (fully human monoclonal antibody to TRAIL-R1) in patients with advanced solid malignancies. *Clin Cancer Res* **14**: 3450–3455.
- Thiel, KW, Hernandez, LI, Dassi, JP, Thiel, WH, Liu, X, Stockdale, KR et al. (2012). Delivery of chemo-sensitizing siRNAs to HER2+ breast cancer cells using RNA aptamers. *Nucleic Acids Res* **40**: 6319–6337.
- Liu, N, Zhou, C, Zhao, J and Chen, Y (2012). Reversal of paclitaxel resistance in epithelial ovarian carcinoma cells by a MUC1 aptamer-let-7i chimera. *Cancer Invest* **30**: 577–582.

50. Esposito, CL, Catuogno, S and de Franciscis, V (2014). Aptamer-mediated selective delivery of short RNA therapeutics in cancer cells. *J RNAi Gene Silencing* **10**: 500–506.
51. Ma, JB, Ye, K and Patel, DJ (2004). Structural basis for overhang-specific small interfering RNA recognition by the PAZ domain. *Nature* **429**: 318–322.
52. Sledz, CA, Holko, M, de Veer, MJ, Silverman, RH and Williams, BR (2003). Activation of the interferon system by short-interfering RNAs. *Nat Cell Biol* **5**: 834–839.
53. Behlke, MA (2008). Chemical modification of siRNAs for *in vivo* use. *Oligonucleotides* **18**: 305–319.
54. Keefe, AD, Pai, S and Ellington, A (2010). Aptamers as therapeutics. *Nat Rev Drug Discov* **9**: 537–550.
55. Stassi, G, Garofalo, M, Zerilli, M, Ricci-Vitiani, L, Zanca, C, Todaro, M et al. (2005). PED mediates AKT-dependent chemoresistance in human breast cancer cells. *Cancer Res* **65**: 6668–6675.
56. Esposito, CL, Passaro, D, Longobardo, I, Condorelli, G, Marotta, P, Affuso, A et al. (2011). A neutralizing RNA aptamer against EGFR causes selective apoptotic cell death. *PLoS One* **6**: e24071.
57. Condorelli, G, Vigiotta, G, Iavarone, C, Caruso, M, Tocchetti, CG, Androzzzi, F et al. (1998). PED/PEA-15 gene controls glucose transport and is overexpressed in type 2 diabetes mellitus. *EMBO J* **17**: 3858–3866.
58. Livak, KJ and Schmittgen, TD (2001). Analysis of relative gene expression data using real-time quantitative PCR and the 2(-Delta Delta C(T)) Method. *Methods* **25**: 402–408.



**This work is licensed under a Creative Commons Attribution-NonCommercial-NoDerivs 4.0 International License. The images or other third party material in this article are included in the article's Creative Commons license, unless indicated otherwise in the credit line; if the material is not included under the Creative Commons license, users will need to obtain permission from the license holder to reproduce the material. To view a copy of this license, visit <http://creativecommons.org/licenses/by-nc-nd/4.0/>**